

ACTA UNIVERSITATIS AGRICULTURAE SUECIAE

DOCTORAL THESIS NO. 2022:58

Trees assimilate atmospheric carbon to form wood and non-structural carbohydrates, including sucrose and starch, which are used for growth when assimilation is limiting. This PhD thesis work investigates the transcriptional mechanisms underlying wood formation and the pathways and mechanisms dividing carbon between growth and storage.

Sonja Viljamaa received her graduate education at the Department of Forest Genetics and Plant Physiology at the Swedish University of Agricultural Sciences. She completed a Master of Science in Genetics and Plant Physiology at University of Oulu, Finland.

Acta Universitatis Agriculturae Suecicae presents doctoral theses from the Swedish University of Agricultural Sciences (SLU).

SLU generates knowledge for the sustainable use of biological natural resources. Research, education, extension, as well as environmental monitoring and assessment are used to achieve this goal.

Online publication of thesis summary: <http://pub.epsilon.slu.se/>

ISSN 1652-6880

ISBN (print version) 978-91-7760-991-9

ISBN (electronic version) 978-91-7760-992-6

DOCTORAL THESIS NO. 2022:58 • Carbon allocation in aspen trees • Sonja Viljamaa

DOCTORAL THESIS NO 2022:58
FACULTY OF FOREST SCIENCES

Carbon allocation in aspen trees

SONJA VILJAMAA



Carbon allocation in aspen trees

Sonja Viljamaa

Faculty of Forest Science

Department of Forest Genetics and Plant Physiology

Umeå



SWEDISH UNIVERSITY
OF AGRICULTURAL
SCIENCES

DOCTORAL THESIS

Umeå 2022

Acta Universitatis Agriculturae Sueciae
2022:58

Cover: Aspen leaves in autumn colours.
(photo: S. Viljamaa)

ISSN 1652-6880

ISBN (print version) 978-91-7760-991-9

ISBN (electronic version) 978-91-7760-992-6

© 2022 Sonja Viljamaa, Swedish University of Agricultural Sciences

Umeå

Print: Original Tryckeri Umeå 2022

Carbon allocation in aspen trees

Abstract

Trees allocate assimilated carbon between growth and storage. In this PhD thesis, I investigated the regulation of carbon allocation during tree growth both at transcriptional as well as whole-tree level, and with a focus on wood formation.

I performed a large-scale DNA affinity purification sequencing (DAP-seq) screen on transcription factor proteins that regulate gene expression in developing wood of aspen (*Populus tremula*). Together with bioinformaticians, I identified both novel and previously reported interactions. The results were integrated into a publicly available database, providing a novel resource for wood biology. We also present a practical guide for the analysis of DAP-seq data to facilitate similar studies.

Next, I investigated carbon partitioning between growth and storage in aspen, focusing on the role of starch as the major storage compound. We report that aspen growth is not limited by starch reserves and suggest a passive starch storage mechanism where sink tissues are the growth-limiting factor.

In a study on *Arabidopsis* (*Arabidopsis thaliana*), I address the debate on whether sucrose synthase (SUS) enzymes are required in the biosynthesis of cellulose, the most abundant component of wood. As mutants lacking all SUS isoforms grew normally and their cellulose content was comparable to that of wild-type, I conclude that SUS activity is not required for cellulose biosynthesis in *Arabidopsis*.

Taken together, the results of this PhD study fill key knowledge gaps in the field and provide new starting points for future research projects on carbon allocation in trees.

Keywords: Wood formation, Secondary cell wall (SCW), Non-structural carbohydrates (NSC), Carbon allocation, Source-sink dynamics, Transcriptional regulation, *Arabidopsis*, *Populus*, DAP-seq

Author's address: Sonja Viljamaa, Swedish University of Agricultural Sciences, Department of Forest Genetics and Plant Physiology, 90187 Umeå, Sweden

Kolfördelning i aspträd

Sammanfattning

Träd fördelar upptaget kol mellan tillväxt och lagring. I denna doktorsavhandling har jag studerat regleringen av kolfördelning under träd tillväxt både på transkriptionell- och helträdsnivå, med ett speciellt fokus på vedbildning.

Jag utförde en storskalig ”DNA affinity purification sequencing” (DAP-seq) - studie av transkriptionsfaktorsproteiner som reglerar genuttrycket i aspträdets (*Populus tremula*) ved under dess tillväxt och utveckling. Tillsammans med bioinformatiker identifierade jag både nya och tidigare rapporterade interaktioner. Resultaten publicerades i en offentlig databas som erbjuder en ny resurs för studier inom vedbiologin. Vi har också utvecklat en praktisk guide för analys av DAP-seqdata för att underlätta liknande forskningsprojekt.

Även kolfördelningen mellan tillväxt och lagring i aspträdet granskades, med fokus på stärkelse som det viktigaste lagringsämnet. Jag rapporterar att aspträdets tillväxt inte är begränsad av stärkelseserverna och föreslår att trädet använder en passiv stärkelselagringsmekanism där vävnaderna som är kolsänkor begränsar tillväxten.

I en studie av *Arabidopsis* (backtrav, *Arabidopsis thaliana*) tar jag itu med debatten om sukrossyntasenzym (SUS) är nödvändiga för biosyntesen av cellulosa, den vanligast förekommande komponenten i ved. Då mutanterna utan alla SUS-isoformerna hade normal tillväxt och likadan celluloshalt som vildtypsväxterna, drar jag slutsatsen att SUS-aktivitet inte behövs för cellulosasyntes i *Arabidopsis*.

Sammantaget fyller resultaten viktiga kunskapsluckor inom fältet och erbjuder nya utgångspunkter för framtida forskningsprojekt kring kolfördelning i träd.

Nyckelord: Vedbildning, Sekundär cellvägg, Icke-strukturella kolhydrater, Kolfördelning, Källa-sänka -dynamik, Transkriptionell reglering, *Arabidopsis*, *Populus* (poppel/asp), DAP-seq

Contents

List of publications.....	7
List of figures.....	9
Abbreviations	11
1. Introduction.....	13
1.1 Photosynthesis is the source of carbon for wood formation	14
1.2 Source and sink tissues in plants: the concept and terminology	15
1.3 Source-sink relationships in trees.....	16
1.3.1 Regulation of carbon allocation in trees – who decides: the source or the sink?.....	16
1.3.2 Tree source-sink dynamics in space and time	20
1.3.3 Seasonal variation of non-structural carbon resources in trees	21
1.3.4 Diel patterns of non-structural carbon during growth of trees	23
1.3.5 Availability and mixing of NSC resources in trees	24
1.4 NSC storage in trees: active, passive or something in between?	26
1.5 Starch as the storage polymer	28
1.6 Studying starchless mutants helps in understanding NSC dynamics.....	30
1.7 Sucrose cleavage pathways as key determinants of sink strength in trees	32
1.7.1 Sucrose cleavage by invertases.....	32
1.7.2 Sucrose cleavage by sucrose synthases	35
1.7.3 Sucrose metabolism is tightly connected to other important metabolic pathways	38
1.8 Wood formation is the main carbon sink during growth of trees.	41
1.9 Carbon allocation to the main wood polymers	43

1.10	Primary metabolism is a key component in defining sink strength in developing wood	45
1.11	Transcription factor proteins as regulators of sink strength and carbon allocation to wood	47
1.11.1	TFs in wood formation: Hierarchy and master regulations	50
1.11.2	From a strictly hierarchical pyramid towards a complex transcriptional network.....	56
2.	Research aims and objectives	59
3.	Material and methods	61
3.1	Arabidopsis and aspen as model organisms	61
3.2	DNA affinity purification sequencing (DAP-seq)	62
4.	Results and discussion	67
4.1	Genome-wide map of transcriptional regulation in developing aspen wood (paper I).....	67
4.2	A practical guide for DAP-seq data analysis in plant genomes (paper II)	71
4.3	Aspen growth is not limited by starch reserves (paper III)	74
4.4	Sucrose synthase activity is not required for cellulose biosynthesis in Arabidopsis (paper IV)	78
5.	Conclusions and future perspectives.....	81
	References.....	85
	Popular science summary	111
	Populärvetenskaplig sammanfattning	113
	Suomenkielinen tiivistelmä	115
	Acknowledgements	117

List of publications

This thesis is based on the work contained in the following papers, referred to by Roman numerals in the text:

- I. **Viljamaa, S.**, Ahlgren Kalman, T., Kumar, V., Wang, W., Delhomme, N., Hvidsten, T. R., Street, N. R. And Niittylä, T. (2022). Genome-wide map of transcriptional regulation in developing aspen wood. (Manuscript)
- II. Ahlgren Kalman, T., **Viljamaa, S.**, Delhomme, N., Niittylä, T. and Street, N. R. (2022). A practical guide for DAP-seq data analysis in plant genomes. (Manuscript)
- III. Wang, W., Talide, L., **Viljamaa, S.** and Niittylä, T. (2022) Aspen growth is not limited by starch reserves. *Current Biology*.
<https://doi.org/10.1016/j.cub.2022.06.056>
- IV. Wang, W., **Viljamaa, S.**, Hodek, O., Moritz, T. and Niittylä, T. (2022) Sucrose synthase activity is not required for cellulose biosynthesis in Arabidopsis. *The Plant Journal*.
<https://doi.org/10.1111/tpj.15752>

Papers III and IV are reproduced with the permission of the publishers.

The contribution of Sonja Viljamaa to the papers included in this thesis was as follows:

- I. SV designed and conducted experiments, participated in data analysis, and wrote the manuscript together with the other authors.
- II. SV designed and conducted experiments, performed the literature review, and wrote the manuscript together with the other authors.
- III. SV designed and conducted experiments, analysed data, and contributed to the writing of the manuscript.
- IV. SV designed experiments, conducted the carbohydrate analysis, and contributed to the writing of the manuscript.

List of figures

Figure 1. The starch biosynthesis pathway in the plastids of the leaf.	29
Figure 2. The structures of sucrose, glucose and fructose.	32
Figure 3. The irreversible sucrose cleavage reaction catalysed by invertase (INV).	33
Figure 4. The reversible sucrose cleavage reaction catalysed by sucrose synthase (SUS).	35
Figure 5. A simplified overview of sucrose metabolism and its interconnectedness to other processes of plant growth and metabolism, such as the biosynthesis pathways of starch and the cell wall components cellulose, hemicellulose and monolignols.	39
Figure 6. Simplified overview over the current consensus of the transcriptional regulatory network regulating secondary cell wall and wood formation.	51
Figure 7. Overview of the DNA affinity purification sequencing (DAP-seq) experiment.	63

Abbreviations

^{13}C	Carbon-13, a stable isotope
^{14}C	Carbon-14, a radioactive isotope
4CL	4-coumarate:CoA ligase
ADP	Adenosine diphosphate
AGPase	ADP-glucose pyrophosphorylase
ATP	Adenosine triphosphate
C	Carbon
C3'H	Coumaroyl 3'-hydroxylase
CAD	Cinnamyl alcohol dehydrogenase
CaMV	Cauliflower mosaic virus
CesA	Cellulose synthase
CINV	Cytosolic invertase
CO ₂	Carbon dioxide
CRISPR/cas9	Clustered regularly interspaced short palindromic repeats/CRISPR associated
cPGM	Cytosolic phosphoglucomutase
CWINV	Cell wall-localized invertase
DAP-seq	DNA affinity purification sequencing
DW	Dry weight

Fru	Fructose
Fru-6-P	Fructose-6-phosphate
Glc	Glucose
Glc-1-P	Glucose-1-phosphate
Glc-6-P	Glucose-6-phosphate
HXK	Hexokinase
INV	Invertase
MYB	MYELOBLASTOSIS
NAC	NO APICAL MERISTEM, ATAF1/2, CUP-SHAPED COTYLEDON2
NSC	Non-structural carbohydrate
P	Phosphate
PGI	Phosphoglucoisomerase
PGM	Phosphoglucomutase
pPGM	Plastidial phosphoglucomutase
PP _i	Pyrophosphate
RNAi	RNA interference
Rubisco	Ribulose 1,5-bisphosphate carboxylase/oxygenase
SCW	Secondary cell wall
Suc	Sucrose
SUS	Sucrose synthase
TF	Transcription factor
Triose-P	Triose phosphate
UDP	Uridine diphosphate
UGPase	UDP-glucose pyrophosphorylase
VIN	Vacuolar invertase
VND	VASCULAR-RELATED NAC-DOMAIN

1. Introduction

Wood of trees is a versatile, renewable and economically important resource that humanity has been using for thousands of years as fuel and as raw material for tools, furniture, construction, as well as pulp and paper. Wood, also known as secondary xylem, provides trees with rigidity that enables upright growth, as well as a conduit for water and nutrient transport. The evolution of xylem combined with secondary growth enabled plant life on land and provided trees with the ability to grow in width and height. On an ecological scale, the wood of both living and dead trees provides habitats and nutrition for diverse species of animals, fungi and insects.

Trees play an important role in the mitigation of climate change. They absorb annually circa two billion tonnes of carbon dioxide (CO₂) from the atmosphere, which makes them the largest terrestrial carbon sink (FAO, 2018). Most of the assimilated carbon (C) is stored as wood (Plomion *et al.*, 2001), which is synthesised from carbon imported from photosynthetic tissues.

Due to the importance of trees for economy, ecology and the climate, it is important to study trees and their wood. Understanding the biology underlying the structure and formation of wood will facilitate the breeding of resilient trees for future climates and allow the harvested biomass to be used in the most effective ways possible. In the following sections I describe our current understanding of how carbon enters trees, how it is then transported and deposited in the wood, and how these processes are regulated.

1.1 Photosynthesis is the source of carbon for wood formation

Plants absorb carbon dioxide in photosynthesis, which takes place in chloroplasts. Inside the chloroplasts, chlorophyll-containing protein complexes capture the energy of sunlight to power a complex reaction chain which converts water and atmospheric carbon dioxide to sugars and oxygen (Stirbet *et al.*, 2020). The reaction chain is called the Calvin-Benson cycle after Melvin Calvin and Andrew Benson, who discovered and characterised the cycle in 1950s by using the radioactive isotope carbon-14 (^{14}C , Benson, 1951).

In the Calvin-Benson cycle, carbon is fixed into triose phosphate (triose-P) sugars in a reaction catalysed by the enzyme called Rubisco (ribulose 1,5-bisphosphate carboxylase/oxygenase). These triose-Ps can be exported from chloroplasts into the cytosol and converted in a multi-step reaction chain into sucrose, which is used in the tree for energy and building blocks for metabolism and growth. In addition to its use locally in the leaf, sucrose is exported to other parts of the plant.

The triose-Ps can also be used inside the leaf chloroplasts for the biosynthesis of starch, which is a storage compound that can be metabolised to produce energy and sugars for example at night, during periods of stress or when photosynthesis is otherwise limited (Smith & Zeeman, 2020). In trees starch is an important reserve during winter dormancy, and some starch reserves can be utilised even decades after their synthesis (Richardson *et al.*, 2013).

Photosynthetic assimilates available for metabolism are often collectively called non-structural carbohydrates (NSC). They function as storage compounds, mobile forms of carbon, energy sources and as substrates for primary and secondary metabolism (Chapin *et al.*, 1990; Kozłowski, 1992; Hartmann & Trumbore, 2016). In this thesis I am focusing on starch and soluble sugars (glucose [Glc], fructose [Fru] and sucrose [Suc]) as the major NSCs in trees, while the other non-structural carbon compounds in trees include amino acids, oligosaccharides and sugar alcohols (Chapin *et al.*, 1990; Hoch *et al.*, 2003). In addition to NSCs, lipids are another important source of non-structural carbon for some tree genera such as *Pinus* and *Tilia* (Chapin *et al.*, 1990; Hoch *et al.*, 2003).

For most trees, sucrose is the main mobile form of carbon (Rennie & Turgeon, 2009; Ruan, 2014). However, some tree species can transport

carbon as sugar alcohols, such as mannitol or sorbitol (Dominguez & Niittylä, 2021). Sucrose is transported via phloem, but it is not well understood what determines where and when the sucrose and its carbon is directed in the tree.

1.2 Source and sink tissues in plants: the concept and terminology

The movement of carbon between different parts of a plant is often described in terms of source-sink dynamics, a term first used in a plant context by Mason and Maskell (1928). Source tissues are defined as net producers and exporters of carbon, while sink tissues are net importers of carbon (Ho, 1988; White *et al.*, 2016). During growth, the main carbon sources in trees are fully expanded and actively photosynthesizing leaves, but even storage organs such as roots or the stem can function as sources during the remobilization of stored NSCs (Yu *et al.*, 2015). Sink tissues in trees include the developing wood, apical meristems, and developing leaves, flowers, seeds, and fruits. The expanding young leaves are net sinks since they both assimilate carbon from the atmosphere and at the same time receive it from other leaves and organs (Larson *et al.*, 1980).

The functions of sink and source organs and tissues can be further described in terms of activity and strength. Sink activity is defined as the metabolic activity of carbon storage or consumption in sink organs, and sink strength is described as the competitive ability of a sink organ or tissue to import carbon (Ho, 1988; Yu *et al.*, 2015). Sink strength is affected both by sink activity and sink size (Ho, 1988; White *et al.*, 2016). Additionally, the distance between the sink and a source affects the sink strength – the larger the distance, the weaker the sink in relation to the source (Ho, 1988). Source activity and strength on the other hand are defined by the rate of carbon assimilation and carbon export activity (Yu *et al.*, 2015; White *et al.*, 2016).

In addition to carbon storage in sink organs, respiration as well as exudation of carbohydrate compounds via roots to *e.g.* symbiotic fungi are other important carbon sinks for trees (De Vries, 1975; Klein & Hoch, 2015). Source and sink dynamics are tightly connected to the concept of carbon allocation, which describes how the assimilated carbon is partitioned into different functional pools in the plant (Hartmann *et al.*, 2020).

1.3 Source-sink relationships in trees

Communication between sources and sinks is thought to be important for plant growth and development. It is also potentially a key component in plant productivity, which is why it has been studied intensively in agriculturally important crop species. Two recent reviews on agricultural research performed mainly on cereals highlight the role of phytohormones, nutrients and minerals, environmental cues, and the transported sugar compounds themselves as important players in the signalling network for source-sink communication (Yu *et al.*, 2015; Chang & Zhu, 2017).

1.3.1 Regulation of carbon allocation in trees – who decides: the source or the sink?

The character of source-sink relationships and which of the partners controls carbon allocation into woody biomass is a major open question in tree biology. Is this process dominated by the source or the sink, or by an interplay of the two?

Traditionally, the carbon-centric view where the source is limiting has been popular in the literature for process-based models of plant and forest growth (*e.g.* Sitch *et al.*, 2003; Krinner *et al.*, 2005; De Kauwe *et al.*, 2014). In process-based models, biological systems such as single trees or whole forest stands are subdivided into their functional components defined by parameters such as leaf area, net primary production (*i.e.* the carbon assimilated by the plant within a certain time frame), tree age, and stem volume and height (Gupta & Sharma, 2019). Interactions between the components themselves and with the environment are simulated to obtain a view of the behaviour of the whole system (Mäkelä *et al.*, 2000; Gupta & Sharma, 2019).

However, the focus on source as the limiting factor may be unfounded in the tree context. As the photosynthetic source tissues in the leaf assimilate atmospheric CO₂, their activity could be limited by CO₂ availability. However, the current atmospheric CO₂ concentration (ca. 400 ppm) is significantly higher than the pre-industrial or even prehistorical CO₂ concentration (180-290 ppm) to which the current tree species have adapted to (Siegenthaler *et al.*, 2005; Pires & Dolan, 2012). This could mean that CO₂ availability does not limit source activity or tree growth. However, some studies show increased photosynthesis, biomass and/or yield under elevated CO₂ (475-600 ppm) conditions (*e.g.* Ainsworth & Long, 2005). Additionally,

studies have shown that the availability of nutrients such as nitrogen and phosphorus or for example the micronutrient molybdenum in the soil can limit tree growth in natural ecosystems more than the atmospheric CO₂ concentration (Barron *et al.*, 2008; Cleland & Harpole, 2010).

Körner (2015) suggests two main reasons for the popularity of source limitation models. The first of these is that CO₂ assimilation -related processes in the plant are relatively well understood and they have been more straightforward to model than nutrient uptake and tissue growth (Körner, 2015). The second suggested reason is based on interpretation of data from classical studies of plant productivity such as that of Monteith (1977), where the yield of crop plants was seen to correlate linearly with the solar radiation intercepted by the plant. However, in Monteith's model many other factors affecting plant development during the growing season, such as evaporation, are not taken into account when interpreting the results, which casts doubt on the factors actually behind the increasing yield (Körner, 2015).

Recently, the sink limitation of tree growth has received more attention in literature. Several studies have shown that the activity of sink tissues can influence the source tissues in trees. For example, in partially defoliated *Eucalyptus globulus* saplings (*i.e.*, where source capacity has been reduced) an increase in photosynthesis was recorded in the remaining leaves (Eyles *et al.*, 2013). This was interpreted as a response to the change in source:sink ratio of the tree, where the high demand from developing sinks such as new leaves or wood biosynthesis in the trunk would be the cause for increased carbon assimilation in the sources (Eyles *et al.*, 2013). The response could therefore indicate that in benign conditions the leaves are not photosynthesizing as much as they could because sink tissue demands are limiting. In ponderosa pine (*Pinus ponderosa*), reduced growth and increased carbon storage was observed in experiments where water availability or temperature was limited, which suggested that the activity of sinks instead of source tissues would be limiting in this case (Körner, 2003; Sala & Hoch, 2009; Körner, 2013).

The results of source-sink manipulation can be difficult to interpret, as illustrated by manipulation of lignin biosynthesis in transgenic hybrid poplar (*Populus alba x grandidentata*) trees. Coleman *et al.* (2008a, 2008b) used RNA interference (RNAi) under the constitutive cauliflower mosaic virus (CaMV) 35S promoter to generate trees in which wood formation was impaired via the silencing of coumaroyl 3'-hydroxylase (C3'H), an essential

enzyme involved in the biosynthesis of G- and S-type lignin in the secondary cell walls of wood. The transgenic trees grew smaller in height, stem diameter and root biomass than the wild-type trees, and exhibited altered leaf morphology as well as a collapsed xylem phenotype. In addition, the transgenic trees accumulated high levels of soluble sugars and starch in their leaves while both stomatal conductance and photosynthesis were reduced (Coleman *et al.*, 2008b). Taken together, the researchers concluded that the inhibition of lignin deposition had reduced the sink strength of wood, where the carbon of the soluble sugars would normally be transported and deposited, and resulted in the accumulation of photosynthates in leaves, which in its turn would limit the leaf photosynthetic activity via a feedback loop (Coleman *et al.*, 2008b). However, considering the tree phenotype it is possible that the defects in vessel elements and their influence on water transport as well as local source leaf effects would cause diminished growth, as well as or instead of the reduced sink strength.

In an earlier study, Hoch and Körner (2003) measured the NSC and lipid concentrations of different tissues of three pine species growing at the treeline ecotone in different latitudes and climates. Treeline trees are known to grow slower than those at the lower altitudes, and it has been suggested that the low temperatures at high altitudes could either limit the photosynthesis and source activity, or slow down the meristematic growth and affect growth via hindering sink activity (Körner, 1998; Hoch & Körner, 2003). The NSC and lipid concentrations observed in this experiment increased with increasing altitude in all measured organs, and the NSC concentrations in all the species were similar at the treeline at the end of the growing season (Hoch & Körner, 2003). These findings support the sink limitation hypothesis, since if the source and photosynthetic activity were limiting, the size of mobile carbon pools measured at higher altitudes would be expected to be smaller than at the lower altitude. However, the increased NSC and lipid concentrations may also reflect a local adaptation to the alpine conditions, and that carbon allocation to storage could be a plastic response to the low temperature that functions independently of the carbon sinks and tree growth (Wiley & Helliker, 2012). Thus, the decreased growth and increased NSC concentrations could be caused by active storage to avoid carbon starvation, and not as a result of sink limitation of growth.

It is likely that the interplay between sources and sinks is complex and context-dependent, and that source and sink tissues work together to regulate

growth. This view is supported by studies in crop species, which have shown that plants can transition from sink limitation to source limitation when they switch from vegetative growth to the reproductive stage. When wheat (*Triticum aestivum*) was treated with elevated CO₂, which is expected to increase source activity (*i.e.* photosynthesis), highest increases in seed yield were observed when the treatment was applied during the vegetative growth period just before the transition to flowering (Havelka *et al.*, 1984). This indicated that the seed yield was limited by the source in this experiment.

In trees, computational modelling evidence supporting source and sink interplay in growth regulation was published by Schiestl-Aalto *et al.* (2015), who used a model of tree growth and carbon allocation and compared its predictions to measurements of a stand of Scots pine (*Pinus sylvestris*) grown in southern Finland. The data collected from the field included measurements for gross primary productivity, secondary growth as well as the length of shoots and needles. The model successfully predicted growth dynamics of wood and needles both within and between different growth years, but only if variables related to both source limitation and sink activity, affected by the environment, were included in the calculations (Schiestl-Aalto *et al.*, 2015).

The mechanism of source and sink interplay is thought to function via complex feedback and feedforward loops. For example, accumulation of photosynthates in the leaf often leads to the downregulation of photosynthesis via a feedback loop (Paul & Pellny, 2003; Smith & Stitt, 2007). Recently, a feedforward loop from source to sink related to the transition between juvenile and adult growth stages of the model plant *Arabidopsis* (*Arabidopsis thaliana*) was identified, involving among others sucrose and glucose signalling, a putative MYB-family transcription factor protein called PAPI/MYB75 as well as the enzymes cytosolic invertase CINV1 and hexokinase HXK1 (Meng *et al.*, 2021). CINV1 was already earlier linked to source-sink dynamics, and HXK1 was shown to play a role in glucose sensing (Moore *et al.*, 2003; Barnes & Anderson, 2018). Meng *et al.* (2021) built on these observations and proposed a mechanism in which the sucrose produced in photosynthesis induces the activity of the PAPI/MYB75 transcription factor, which promotes the expression of CINV1. The invertase enzyme hydrolyses sucrose into fructose and glucose, which is sensed by HXK1 (Moore *et al.*, 2003). Via a yet unknown mechanism, HXK1 triggers a regulatory module involving the microRNA precursor miR156 and a transcription factor called *SPL9*, which are

previously identified regulators of the juvenile-to-adult transition phase (Yang *et al.*, 2013). SPL9 was shown to activate *PAP1/MYB75* expression, leading again to the promotion of CINV1 activity, the production of glucose and the continuation of the feedforward loop (Meng *et al.*, 2021).

Furthermore, other factors such as plant hormones and nitrogen and sugar signalling, either alone or interacting with each other, have been shown to regulate carbon sources and sinks and their interplay (Lastdrager *et al.*, 2014). It is expected that future studies will reveal more complex interactions involving sources and sinks, and that researchers will focus on how these are regulated.

1.3.2 Tree source-sink dynamics in space and time

Source-sink dynamics of trees should be considered both spatially and in time. This is not an easy task as trees are large and long-lived modular organisms whose different parts are considered semi-autonomous (Sprugel *et al.*, 1991). Modularity means that trees (and plants in general) are composed of multiple repeating units that have been constructed using the same architectural pattern (*e.g.*, roots, shoots), and semi-autonomy that these units can in some regards be independent from other parts of the tree. A good example of this is a mature source leaf or even a whole branch that produces all the carbon it needs but that relies on other parts of the tree for water and nutrients.

In experimental plant science it is common to first perform experiments on fast-growing model organisms such as *Arabidopsis* and then extrapolate the results to other species. However, it can be questioned whether this is a suitable strategy when considering carbon dynamics of trees. In contrast to the herbaceous and annual *Arabidopsis* in which most of the carbon-storing tissues participate in photosynthesis, the main carbon-storing organs in trees are branches, roots and stemwood, whose tissues are usually non-photosynthetic (Palacio *et al.*, 2014; Furze *et al.*, 2019). In wood, NSC storage takes place in the ray parenchyma cells (Plavcová & Jansen, 2015). These are absent in the secondary xylem of *Arabidopsis* hypocotyl (Chaffey *et al.*, 2002). Therefore, the differences in anatomy, size and lifestyle make *Arabidopsis* a poor model for carbon dynamics of perennial woody species and highlight the need to perform these studies on trees.

In trees, NSC concentrations have been shown to vary between species as well as between the different organs and tissues of the same tree (Körner, 2003; Furze *et al.*, 2019). The latter observation can be linked to the trees' modular structure. A meta-analysis performed on 121 studies of 177 plant species grown in natural conditions in different biomes revealed that across all studied plant species, concentrations of total NSC and soluble sugars were in general highest in leaves, intermediate in belowground organs and lowest in the stem (Martínez-Vilalta *et al.*, 2016). The same study observed that when looking at starch levels alone they were similar in leaves and belowground organs, but two times lower in the stem (Martínez-Vilalta *et al.*, 2016).

In studies performed on *Populus* species, highest total NSC concentrations were observed in the roots (Landhäusser & Lieffers, 2003; Blumstein *et al.*, 2020). In the study of Blumstein *et al.* (2020) the root NSC concentration was 1.6 ± 0.3 times higher than that of the stem. The relatively high root starch content may be linked to the ecological niche of *Populus* as pioneer species that have adapted to environments which often experience disturbances, such as herbivory browsing (Bollmark *et al.*, 1999). The existence of large belowground NSC reserves is important for resprouting after the disturbance (Bollmark *et al.*, 1999). The observed variation between tissues, organs and species highlights the need to study the dynamics of starch, total NSCs and carbon allocation specifically in trees, while also considering other sources of variation such as the season or the time of day during sampling.

1.3.3 Seasonal variation of non-structural carbon resources in trees

Seasonal variations in tree NSC levels in the temperate regions are well documented. Since aspens and poplars (*Populus* spp.) are frequently used as models, I will focus on describing the seasonal NSC dynamics in this genus.

In the three-year-old branch wood of orchard-grown poplar trees (*Populus x canadensis* 'robusta'), starch accumulated during the growing season (May-October) to a maximum concentration of 15-18 $\mu\text{g}/\text{mg}$ of dry weight (DW), after which it started to decrease to a winter minimum (December-February) of 0.5-3 $\mu\text{g}/\text{mg}$ DW (Sauter & van Cleve, 1994). The decrease in branch starch during autumn and winter coincided with an increase in total soluble sugar content (including glucose, fructose, sucrose,

xylose, maltose, galactose, raffinose and stachyose), which increased to 17-32 µg/mg DW (Sauter & van Cleve, 1994). A similar increase in starch content during the growing season was observed in the branch sapwood of most temperate deciduous tree species studied by Hoch *et al.* (2003) as well as in stem cores of deciduous and evergreen species studied by Richardson *et al.* (2013). The latter study also reports an increase in sugar concentrations during the dormant season (Richardson *et al.*, 2013). The soluble sugars are thought to contribute to osmoprotection and the freezing tolerance of the tree during the winter.

In the beginning of the growing season, starch reserves from mainly the roots and the stem are mobilized into soluble sugars which are used as energy and material for biosynthesis of structural carbohydrates in the new leaves, roots and wood (Landhäusser & Lieffers, 2003; Gough *et al.*, 2010; Regier *et al.*, 2010). In their study, Landhäusser and Lieffers (2003) noticed a rapid decrease in NSC concentrations of the large branches of the tree crown, which coincided with an increase of sugar concentrations in new shoots and breaking buds of quaking aspen (*P. tremuloides*). Based on this it is feasible for the stem and the branches to be the main source of NSC supporting bud flush during the spring (Landhäusser & Lieffers, 2003).

Results contrasting the seasonal NSC accumulation patterns reported by Sauter and van Cleve (1994) were presented earlier by Bonicel *et al.* (1987). They report a decreasing trend in starch content during the growing season in both the stem and branch wood of young, 10- to 22-month-old poplar trees (*Populus trichocarpa x deltoides*) grown in a forest in south-eastern France. It is unlikely that tree age would explain these results, as similar starch deposition patterns to those reported by Sauter and van Cleve (1994) were presented by Regier *et al.* (2010), who used 19-month-old clones of poplar (*Populus deltoides x nigra* cv. 'Dorskamp') in their study conducted in Switzerland. Geographical location is also unlikely as the main cause, since the studies of both Bonicel *et al.* (1987), Sauter and van Cleve (1994) and Regier *et al.* (2010) were conducted in the temperate region of Europe. The use of different methods and instruments for starch extraction and quantification might explain some of the differences between the studies presented (Quentin *et al.*, 2015), but it cannot explain the completely different seasonal starch pattern observed by Bonicel *et al.* (1987).

It has been shown that the starch reserves of *Populus* sp. trees are depleted during environmental stress conditions such as drought (Wiley *et al.*, 2017)

and although no stress conditions are reported by Bonicel *et al.* (1987), this could be an explanation for the observed decrease in stem and branch starch content during the growing season. As the timing of the highest stem starch concentration has been shown to vary between young trees of different hybrid poplar clones (Nguyen *et al.*, 1990), genetic differences between the studied trees could also provide an explanation for some of the contradictory differences in the reported NSC patterns.

In addition to the temperate region, seasonal NSC variation has been studied in forest ecosystems ranging from tropical (Würth *et al.*, 2005) to sub-tropical (Liu *et al.*, 2018), Mediterranean (Mooney & Hays, 1973; Davidson *et al.*, 2021), semiarid (Peltier *et al.*, 2021), arctic (Chapin & Shaver, 1988) and boreal forests (Landhäusser & Lieffers, 2003; Schiestl-Aalto *et al.*, 2019). Combined, these studies show that the variation in NSC dynamics in relation to seasons differs between tree species, and it seems to have components that are affected both by the species, seasonality and different years (Würth *et al.*, 2005; Liu *et al.*, 2018; Davidson *et al.*, 2021).

All in all, the patterns of seasonal NSC variation reported in studies on *Populus* (e.g. Sauter & van Cleve, 1994; Landhäusser & Lieffers, 2003; Gough *et al.*, 2010; Regier *et al.*, 2010, excluding Bonicel *et al.*, 1987) are in accordance with seasonal NSC trends reported from other species of temperate forest trees (Hoch *et al.*, 2003). However, comparing the different *Populus* studies with each other is not easy as there is little to no overlap between the sampled tissues and organs or the age of sampled trees, and for example data on the NSC dynamics during the winter dormancy is missing in many studies.

1.3.4 Diel patterns of non-structural carbon during growth of trees

The level of starch stored in photosynthesizing leaves is known to fluctuate during the day and night, due to carbon flux into starch during the day and cleavage to soluble sugars during the night. This has been studied for example in the leaves of the model plant *Arabidopsis*, but studies conducted on trees are still scarce.

Tixier *et al.* (2018) studied the diurnal patterns of starch and soluble carbohydrates in different tissues and organs of seven-year-old, orchard-grown almond trees (*Prunus dulcis*) and observed that the time of day has a significant effect on local NSC concentrations in all the studied tissues

except the central region of the tree trunk. However, there were some notable differences compared to starch dynamics in *Arabidopsis* leaves. The almond tree starch concentrations observed in leaf and branch samples increased during the day and decreased overnight, but in twigs and the trunk starch accumulation was observed during the night (Tixier *et al.*, 2018). This combined with $^{13}\text{CO}_2$ pulse analyses performed on branches of slightly younger trees indicated that the newly assimilated carbon of the NSCs would disperse downward from branches to the trunk and roots, and thus mix vertically during the diel cycle (Tixier *et al.*, 2018).

In a recent study, organic electrochemical transistors were implanted into the vascular tissues of young, greenhouse-grown hybrid aspen trees (*P. tremula x tremuloides*) to monitor the glucose and sucrose levels of the xylem sap during a 48 h diel cycle (Diacci *et al.*, 2021). While no changes were observed in the glucose content, the xylem sap sucrose content increased during night-time and decreased during the day (Diacci *et al.*, 2021). A similar fluctuation was observed for total soluble carbohydrates in the almond tree xylem sap (Tixier *et al.*, 2018).

Taken together, diel patterns in NSC concentrations and deposition can be observed both at the level of single tissues as well as the whole tree. The NSC dynamics of different tissues and organs are not necessarily synchronized in time (Tixier *et al.*, 2018), which might reflect on how the NSC compounds are transported, stored and utilised. Despite an extensive literature search I have not found any other publications studying the diel NSC patterns in the woody tissues of trees than those mentioned above, which highlights this as a major gap in our knowledge.

1.3.5 Availability and mixing of NSC resources in trees

It is important to know the availability of long-term stored NSC reserves in addition to those that have been assimilated by the tree more recently, in order to get a clear picture of the NSC dynamics on a whole-tree level. When both deciduous and coniferous, approximately 100-year-old trees were sampled, NSC was detected even in the innermost stem core-sections with an age of ca. 80-100 years (Hoch *et al.*, 2003). However, it is unclear whether the trees still can access such carbon stored deep in the stem. Both Richardson *et al.* (2013) as well as Carbone *et al.* (2013) investigated this using the ^{14}C “bomb spike” method in which the ^{14}C content of plant samples

is compared to historical knowledge of the atmospheric ^{14}C concentration. This concentration spiked in the 1950s and 1960s due to nuclear weapons testing and has been decreasing since then due to mixing with carbon reserves in the biosphere and oceans, and the release of ^{14}C -free carbon from anthropogenic sources such as use of fossil fuels (Levin & Kromer, 2004; Levin *et al.*, 2010). In their studies, Richardson *et al.* (2013) and Carbone *et al.* (2013) determined that the mean age of NSC and soluble sugars in 2 cm stem cores of field-grown mature trees was circa 10 years. Surprisingly, the ages of starch and sugar reserves in the stem cores were quite similar, which the researchers interpreted as an indication of local starch turnover in the tissue (Richardson *et al.*, 2013).

Later, Richardson *et al.* (2015) used the same ^{14}C method to study the dynamics of NSC stored in the stem, branches, and roots of field-grown white pine (*Pinus strobus*) and red oak (*Quercus rubra*). The ^{14}C found in sugars of branches and outermost growth rings of the stems in both species indicated that it had been fixed during the current growing season, and the carbon age increased steadily when examining older growth rings in these tissues, suggesting less mixing of old and new NSC reserves (Richardson *et al.*, 2015). Similar results were published by Trumbore *et al.* (2015), who studied oak trees (*Quercus* sp.). Both research groups observed that the carbon in NSC fractions was younger than the structural carbon (*i.e.*, cellulose) from which it was extracted, which indicates that the predominant direction for younger NSC compounds is to move inward into the stem (Richardson *et al.*, 2013; Richardson *et al.*, 2015; Trumbore *et al.*, 2015).

Different models have been made to conceptualize the dynamics of the NSC pool or pools in trees. One of them was suggested by Richardson *et al.* (2013), who used a mathematical model called FöBAAR (FOrest Biomass, Allocation, Assimilation and Respiration, developed by Keenan *et al.*, 2012) to model seasonal carbon allocation, using different parameters for variables such as NSC pool size and timescale for carbon turnover. Based on the results, Richardson *et al.* (2013) proposed a model in which trees would have two functional pools of NSC instead of just one. A ‘fast’ pool would contain recently assimilated NSC which would have an approximate turnover rate of several months to a year. These compounds would mainly be used for tree growth and metabolism. On the other hand, a ‘slow’ pool would be composed of older NSC with a turnover of tens of years, which would be used if the reserves in the ‘fast’ pool are depleted (Richardson *et al.*, 2013;

Richardson *et al.*, 2015). An alternative to the two functional pool model was suggested by Trumbore *et al.* (2015), who combined computer modelling of NSC allocation to stem year rings with NSC measurements from slow- and fast-growing individuals of California live oak (*Quercus agrifolia*). Instead of two separate NSC pools, they argue for the existence of only one NSC pool, where both newly assimilated and old NSC compounds would reside and mix (Trumbore *et al.*, 2015).

Models such as the ones presented above are useful tools in formulating hypotheses, but they cannot yet predict the NSC situation in a particular tree. Carbon fluxes into or out of the different NSC pools are easiest to track when the pool size changes, and even then this indicates the net, not gross, change (Hartmann & Trumbore, 2016). A more accurate picture of whole tree -level NSC dynamics can be obtained by for example using the radioactive ^{14}C or the stable isotope ^{13}C (Hartmann *et al.*, 2015; Richardson *et al.*, 2015; Dominguez *et al.*, 2021).

1.4 NSC storage in trees: active, passive or something in between?

It is not clear how the storage of NSC compounds in trees is regulated (Sala *et al.*, 2012). However, various models have been proposed to describe the process. In their classical review, Chapin *et al.* (1990) define storage as "resources that build up in the plant and can be mobilized in the future to support biosynthesis for growth or other plant functions". They divide NSC storage in plants into three general classes: accumulation, reserve formation and recycling (Chapin *et al.*, 1990). Accumulation is described as a passive process in which storage compounds pile up as resource supply exceeds demand for growth and maintenance. Reserve formation on the other hand is an active process where storage compounds are synthesized on the expense of growth and defence. Finally, recycling is described as an active process where compounds originally invested in growth or defence are broken down and reused to support future growth (Chapin *et al.*, 1990).

More recently, Dietze *et al.* (2014) use the terms active, quasi-active and passive to describe NSC storage. Active storage, like the reserve formation in Chapin *et al.* (1990), is described as storage at the expense of growth, even when the growth conditions would be favourable. Quasi-active storage

describes a situation in which storage occurs due to downregulation of growth. Lastly, passive storage is said to occur when growth is limited by factors other than carbon and the excess carbohydrates are stored. However, the storage processes are not mutually exclusive, and it is possible that all of them can occur in the tree in different developmental stages and growth conditions (Dietze *et al.*, 2014).

Our understanding of NSC storage mechanisms relies heavily on experimental work in *Arabidopsis*. Evidence from studies on *Arabidopsis* grown in varying daylengths indicates that it can adjust its metabolism strategy between storage and growth, so that storage is upregulated when carbon uptake is low (Smith & Stitt, 2007; Gibon *et al.*, 2009). When carbon-starved *Arabidopsis* plants subjected to a prolonged night were returned to light, they accumulated storage carbohydrates instead of growing (Gibon *et al.*, 2004b). This would indicate that in *Arabidopsis* storage is an active process.

In trees, evidence for active storage was reported by Huang *et al.* (2021), who documented down-regulation of growth and photosynthesis in Norway spruce (*Picea abies*) saplings grown in reduced CO₂, while their respiration rate was maintained at the same level as under normal atmospheric CO₂ conditions. When the carbon starvation was prolonged, the biosynthesis of storage-related NSC compounds was upregulated and growth-related processes were downregulated, which indicated a shift from growth to storage (Huang *et al.*, 2021). Young Norway spruce saplings subjected to reduced CO₂ or drought treatments in the experiments of Hartmann *et al.* (2015) allocated recently assimilated carbon into storage even under the stress conditions, which led to the researchers' conclusion that storage cannot be a passive overflow process, and that active components such as up-regulation of storage associated genes or down-regulation of growth associated genes are likely involved, at least under stress (Wiley & Helliker, 2012; Hartmann *et al.*, 2015). Similarly, NSC accumulation and active NSC synthesis were documented in three-year-old seedlings of Scots pine (*Pinus sylvestris*) in drought conditions and even after rewetting (Galiano *et al.*, 2017). Contrasting results were obtained for large-leaved linden (*Tilia platyphyllos*), where the already high total NSC concentrations stayed the same under drought conditions, which the researchers interpreted as evidence for a passive overflow strategy of storage (Galiano *et al.*, 2017). However, all the tree experiments mentioned above represent the trees'

storage strategies under stress conditions and might not represent how the storage dynamics work during growth in unstressed field conditions or in greenhouse conditions with optimal amounts of water and nutrients.

Therefore, like in the question of sources or sinks as the main drivers of carbon allocation, it is probable that also for NSC storage the situation is dynamic and adapting to environmental and developmental factors. For example, in long-lived trees the strategy could change depending on the developmental stage, so that one strategy would be more preferred at the seedling stage and another in a mature tree. This is proposed for example by Sala *et al.* (2012) and Hartmann and Trumbore (2016), who discuss that storage is not a purely passive or active process, but rather involves both. The current evidence as outlined above seems to support this view.

1.5 Starch as the storage polymer

Starch is the most important storage carbohydrate in plants (Zeeman *et al.*, 2007). It is a large, osmotically inert polymer composed of glucose residues that are packed into semicrystalline granules in plastids: a temporary starch storage is produced after photosynthesis in chloroplasts, while starch that is stored for a longer time is produced in specialized plastids called amyloplasts (Pérez & Bertoft, 2010; Pfister & Zeeman, 2016).

The substrate for starch synthesis is adenosine diphosphate-glucose (ADP-Glc) and it is derived from the triose-P produced in photosynthesis in the chloroplasts (figure 1). First, the triose-P is converted into fructose-6-phosphate (Fru-6-P), which is further converted by the plastidial isoform of phosphoglucosomerase (PGI) enzyme into glucose-6-phosphate (Glc-6-P). Glc-6-P in its turn is the substrate for the synthesis of glucose-1-phosphate (Glc-1-P) in a reversible reaction catalysed by the plastidial isoform of the enzyme called phosphoglucomutase (PGM). Finally, ADP-glucose pyrophosphorylase (AGPase) uses Glc-1-P as its substrate in an irreversible reaction requiring the energy source adenosine triphosphate (ATP) to produce ADP-Glc and pyrophosphate (PPi).

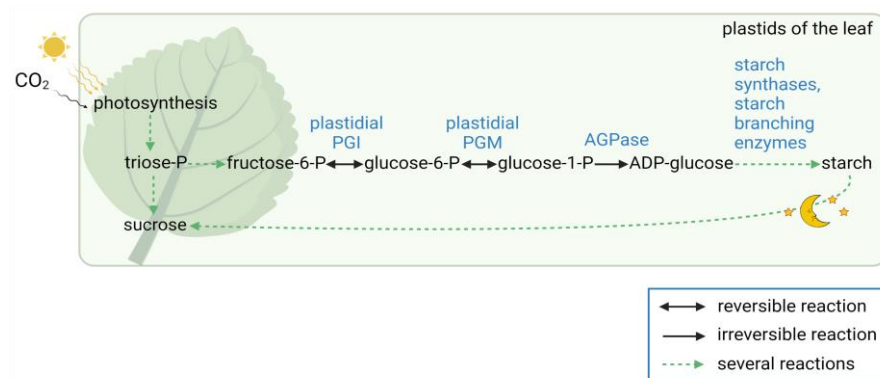


Figure 1. The starch biosynthesis pathway in the plastids of the leaf.

Abbreviations: CO₂, carbon dioxide; P, phosphate; PGI, phosphoglucoisomerase; PGM, phosphoglucomutase; AGPase, ADP-glucose pyrophosphorylase. Figure created with BioRender.com.

Starch synthase enzymes use the ADP-Glc as substrate and add it to existing glucose chains on the surface of growing starch granules, forming α -1,4-linkages and producing branched amylopectin and linear amylose (Recondo & Leloir, 1961; Iglesias & Preiss, 1992; Pfister & Zeeman, 2016). The α -1,6-linked branches of amylopectin are created by starch branching enzymes (Tetlow & Emes, 2014). Some of the added branches are eventually removed by debranching enzymes, to achieve the final semicrystalline structure of the starch granule (James *et al.*, 1995; Smith & Zeeman, 2020).

The abovementioned “classical” pathway of starch synthesis in the leaf has been challenged by an alternative model in which the starch and sucrose synthesis pathways would be interconnected (*e.g.* Streb *et al.*, 2009; Bahaji *et al.*, 2014). The hypothesis proposes ADP-Glc production in the cytosol via sucrose synthase (SUS) -mediated sucrose cleavage in the presence of ADP, and its transport into the chloroplast for starch synthesis via a yet unknown transporter (Baroja-Fernandez *et al.*, 2001; Munoz *et al.*, 2005; Streb *et al.*, 2009). However, in a recent study, *Arabidopsis* mutants deficient in SUS activity in leaf mesophyll cells, where starch biosynthesis takes place, or lacking it completely, were shown to have similar levels of both ADP-Glc and starch than wild-type plants (Fünfgeld *et al.*, 2022). As a contrast, ADP-Glc and starch levels lower than in wild-type plants were observed in plants

lacking the plastidial PGM or AGPase enzymes, both of which are essential enzymes for the starch biosynthesis pathway (Caspar *et al.*, 1985; Lin *et al.*, 1988; Fünfgeld *et al.*, 2022). This recent evidence provides strong support for the classical pathway of starch biosynthesis in the leaf.

However, in the amyloplasts of non-photosynthetic tissues in trees, starch is derived from the cytosolic cleavage of sucrose in reactions catalysed by sucrose synthase and/or invertase enzymes, followed by a forking pathway leading to the production of Glc-1-P via Fru-6-P, Glc-6-P or UDP-glucose (UDP-Glc). The interconversion between Glc-6-P and Fru-6-P is catalysed by the cytosolic isoform of PGI, while the cytosolic PGM catalyses the reaction between Glc-6-P and Glc-1-P. Glc-1-P is then imported to amyloplasts via the hexose-P translocator and used for ADP-Glc and starch biosynthesis.

1.6 Studying starchless mutants helps in understanding NSC dynamics

Mutants lacking or failing to degrade starch have been used to study the importance and dynamics of this storage compound as well as that of other NSCs. Caspar *et al.* (1985) used ethyl methanol sulfonate (EMS) mutagenesis to generate mutant lines of *Arabidopsis* and performed a starch iodine staining screen to find plants whose leaves did not contain starch. As a result, they discovered a mutant plant whose leaves, stem and roots lacked starch at the detection level of the iodine assay. Only trace amounts of starch could be quantified enzymatically from the leaves, which might indicate a slight “leakiness” of the mutated gene. In a later study even hypocotyls, flower stalks and roots of the mutant were verified to lack starch (Caspar & Pickard, 1989). Biochemical analysis of the plant material revealed that there were two PGI and three PGM isozymes in the wild-type plants, but that the mutant plants completely lacked the activity of the plastidial isozyme of PGM (Caspar *et al.*, 1985). The researchers concluded that the loss of plastidial PGM, which prevented the production of Glc-1-P and thus the further synthesis of ADP-Glc, explained the starchless phenotype (Caspar *et al.*, 1985; Caspar & Pickard, 1989).

After these initial studies, three PGM isoforms have been characterized in most plants: two cytosolic PGM (cPGM) isoforms which are essential for synthesis of sucrose and cell wall components, and the single plastidial PGM

(pPGM), which is needed for synthesis of starch in the chloroplasts of leaves (Caspar *et al.*, 1985; Manjunath *et al.*, 1998; Malinova *et al.*, 2014). Arabidopsis plants lacking both cytosolic PGM isoforms have reduced growth and seed production, while mutants lacking both the cytosolic and plastidial isoforms are dwarfish, unable to flower and die prematurely (Malinova *et al.*, 2014).

The *pgm* mutant plants characterized by Caspar *et al.* (1985) that lack only the plastidial isoform grew just like the wild-type plants in continuous light, but had a strongly reduced growth rate and produced less biomass unless grown under continuous light or very long days. The reduced growth was initially hypothesized to be caused by downregulation of photosynthesis, as the mutants had reduced photosynthetic capacity when grown in 12h photoperiod, and/or by increased respiration rate, which was 1.5 times higher during the night in *pgm* plants and which in the end would lead to a reduction in net carbon assimilation (Caspar *et al.*, 1985). When Schulze *et al.* (1994) studied plant resource allocation and growth dynamics in both rosette leaves and flower stalks of Arabidopsis, they observed that the relative growth rate of *pgm* was higher than that of the wild-type during flowering. Based on this, they suggested that the reduced growth of *pgm* at the rosette stage could be due to reduced carbon sinks (Schulze *et al.*, 1994). Later, large-scale time series experiments showed that the *pgm* mutant plants become carbon depleted at the end of the night, which is currently considered the most likely cause for the growth reduction (Gibon *et al.*, 2004a; Gibon *et al.*, 2004b; Bläsing *et al.*, 2005). Interestingly, the transcriptome of the *pgm* plants at the end of night resembled that of wild-type plants grown in 6-h extended night conditions (Gibon *et al.*, 2004a), further supporting end of the night carbon depletion as the cause of the reduced growth.

The *pgm* mutant plants have been a valuable tool in studying plant resource allocation and growth dynamics. In addition to Arabidopsis, starch defect mutants with an impaired PGM have been studied at least in pea (*Pisum sativum*; Harrison *et al.*, 1998; Harrison *et al.*, 2000), tobacco (*Nicotiana glauca*; Hanson & McHale, 1988) and potato (*Solanum tuberosum*; Tauberger *et al.*, 2000; Fernie *et al.*, 2001). Unlike the *pgm* mutants of Arabidopsis, these mutants did not exhibit major growth phenotypes when grown in greenhouse conditions and under a diel light cycle. The severity of the *pgm* impairment in these studies ranged from the ca. 1.3 % remaining PGM activity and near starchlessness of tobacco, to the

reduction of seed starch content from 50 % of the wild-type to the ca. 1 % of the pea mutant, and to the ca. 40 % reduction of tuber starch content in potato (Hanson & McHale, 1988; Harrison *et al.*, 1998; Tauberger *et al.*, 2000). These examples show that *Arabidopsis* is not a good model system for the role of starch across plant species. This is a particular problem for trees where no starch mutants exist, and this shortcoming was addressed in this thesis work.

1.7 Sucrose cleavage pathways as key determinants of sink strength in trees

In most trees, the disaccharide sucrose (figure 2) is the major transported form of carbon and therefore the source of energy as well as raw material for carbon skeletons of various compounds in heterotrophic tissues including wood. Once the sucrose has been transported into developing wood, it needs to be cleaved. This can take place via two pathways: either via the activity of invertase (INV) or sucrose synthase (SUS) enzymes.

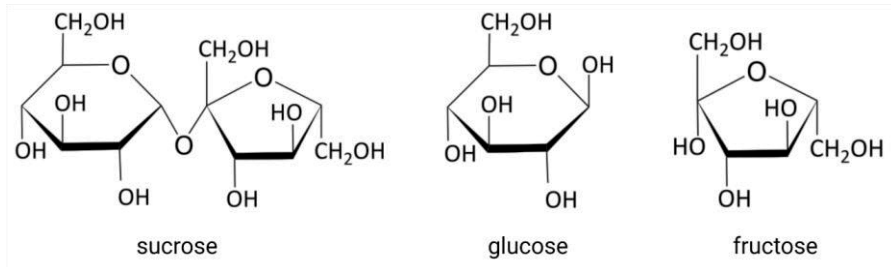


Figure 2. The structures of sucrose, glucose and fructose.

Sucrose is a disaccharide composed of glucose and fructose monosaccharide units that are connected by an α -1,2-glycosidic linkage.

1.7.1 Sucrose cleavage by invertases

Invertases (INVs, figure 3) cleave sucrose into glucose and fructose in an irreversible reaction (Sturm & Tang, 1999). The different types of invertases are classified by their subcellular location and pH optimum of activity into cell wall- (CWINVs) and vacuole- (VINs) localised acidic invertases and cytoplasm-localised neutral invertases (CINs), also called neutral/alkaline invertases (Sturm, 1999; Bockock *et al.*, 2008; Ruan, 2014).

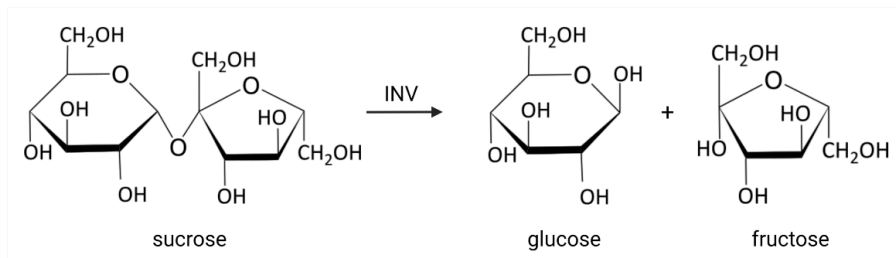


Figure 3. The irreversible sucrose cleavage reaction catalysed by invertase (INV).

Studies of CWINVs in *Arabidopsis* and crop species have associated their activity with sink strength. For example, a mutation in the maize *ZmCWIN2* resulted in reduced CWINV activity and led to a phenotype with miniaturized seeds (Cheng *et al.*, 1996). In another study, CWINV-encoding genes from *Arabidopsis*, rice and maize (*Zea mays*) were expressed in an elite line of maize, driven by the constitutive CaMV 35S promoter (Li *et al.*, 2013). Compared to the wild-type, constitutive expression of the transgene lead to larger shoot biomass and an overall increased grain yield, which was caused by enlarged ears, increased seed number and seed size. The researchers also reported an increase in seed starch content (Li *et al.*, 2013). These findings make CWINVs especially interesting targets in breeding for increased crop yield, and perhaps also in directing more carbon to wood of trees. However, results from studies using constitutive promoters should be interpreted with caution. It has been shown that 35S-driven expression can vary between and within tissues, and that it can be affected by *e.g.* plant developmental stage or abiotic stress conditions (Pret'ová *et al.*, 2001; Boyko *et al.*, 2010; Kiselev *et al.*, 2021). Complementing the 35S studies with studies using native tissue-specific promoters could provide a more realistic picture of the processes *in planta*.

Six putative CWINV genes have been identified in *Arabidopsis* (Sherson *et al.*, 2003), although two of them were later confirmed to lack invertase activity and instead be involved in degradation of fructans (De Coninck *et al.*, 2005). In *Populus trichocarpa*, five CWINV-encoding genes (named *PtCINI-5*) have been identified (Bocock *et al.*, 2008; Chen *et al.*, 2015). *PaxgINV2* of hybrid poplar (*Populus alba* x *grandidentata*) showed high transcript abundance in actively growing tissues and was therefore

hypothesised to function in providing them with carbon and energy (Canam *et al.*, 2008), and thus be involved in the regulation of source-sink dynamics.

Vacuolar invertases are involved in the regulation of sugar storage in the vacuole. High VIN activity was linked to cotton fibre elongation (Wang *et al.*, 2010) and to the elongation of Arabidopsis roots and hypocotyls, in the latter case possibly by increasing the osmotic potential of the vacuole by the production of glucose and fructose (Sergeeva *et al.*, 2006). This would cause increased water uptake and an increase in turgor pressure, which would lead to cell expansion. Via the regulation of cell expansion, VINs could also take part in the regulation of source-sink dynamics. In black cottonwood (*Populus trichocarpa*), three vacuolar invertase genes (*PtVIN1-3*) have been characterized (Bocock *et al.*, 2008). A study on *Populus tremula x alba* indicated that VIN, especially the isoform VIN2, could work together with the tonoplast-localised sucrose transporter PtaSUT4 in the regulation of sucrose compartmentalization within the cell and transport throughout the tree (Payyavula *et al.*, 2011).

The role of cytosolic invertases was for long less clear than that of the other invertases (Ruan *et al.*, 2010), but recently studies have started to elucidate their role in plant metabolism. Studies on lotus (*Lotus japonicus*), Arabidopsis and rice have shown that mutations in *CIN*s can affect the growth and development of roots, reproductivity and overall plant growth rate (Jia *et al.*, 2008; Barratt *et al.*, 2009; Welham *et al.*, 2009). Compared to the wild-type, Arabidopsis *cinv1cinv2* double mutants had defects in producing the nucleotide sugar uridine diphosphate (UDP) glucose (UDP-Glc) and cellulose as well as an altered cellulose microfibril organization while other cell wall matrix polysaccharides were not substantially affected, indicating an important role for CIN on the UDP-Glc biosynthesis pathway (Barnes & Anderson, 2018). Seedlings of these double mutants were grown on media with different exogenous sugar concentrations and their starch levels were measured, which revealed higher starch levels in *cinv1cinv2* than in the Columbia-0 (Col-0) wild-type and indicated that CINV could also play a role in carbon partitioning between cellulose and starch biosynthesis (Barnes & Anderson, 2018). These results illustrate that CINVs clearly play a central role in primary metabolism.

In *Populus* the picture of cytosolic invertases is complex. There are 16 alkaline/neutral invertases in the *Populus* genome (Bocock *et al.*, 2008), but only *CIN8/12*, which is expressed during secondary cell wall formation, has

been assigned a function (Rende *et al.*, 2017). RNAi lines where the transgene expression was driven by a secondary cell wall-localised promoter (*GT43B*) were generated to study the *CIN12* function in *Populus tremula x tremuloides* (Rende *et al.*, 2017). In developing wood of the transgenic trees, the concentration of UDP-Glc, an important cellulose biosynthesis precursor, was reduced by 53-78 % compared to the wild-type trees. The researchers concluded that the reduced *CIN12* expression explained the reduction in average cellulose fibril diameter and lower crystalline cellulose content of the transgenic trees (Rende *et al.*, 2017). Put together, both the Arabidopsis and *Populus* data imply an important role for CIN as the supplier of UDP-Glc for cellulose biosynthesis.

1.7.2 Sucrose cleavage by sucrose synthases

In presence of UDP, sucrose synthases (SUSs, figure 4) catalyse the reversible cleavage of sucrose into UDP-glucose and fructose (Geigenberger & Stitt, 1993). Although SUSs can also synthesize sucrose, the direction of the reaction for cleavage is favoured *in vivo* (Geigenberger & Stitt, 1993). Studies have shown that heterologously expressed recombinant SUSs can also use other nucleoside phosphates such as ADP as a substrate during the cleavage to produce other nucleotide sugars, but compared to UDP the affinity for other nucleoside diphosphates is lower (Murata *et al.*, 1966). The reaction catalysed by SUS enzymes is pH-dependent with optimal sucrose degradation activity occurring between pH 5.5 and 7.5, while optimal sucrose synthesis activity is observed between pH 7.5 and 9.5 (Schmolzer *et al.*, 2016).

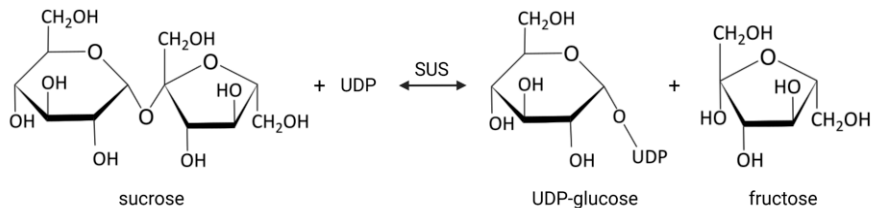


Figure 4. The reversible sucrose cleavage reaction catalysed by sucrose synthase (SUS).

The model organism *Arabidopsis* has six *SUS* genes (*SUS1-6*) which have different but overlapping spatial and temporal patterns of expression (Bieniawska *et al.*, 2007), while as many as 15 *SUS* genes have been identified in the genome of *Populus* (Tuskan *et al.*, 2006; An *et al.*, 2014).

SUS isoforms can be found in various compartments of the plant cell. Initial enzyme assay studies on soybean (*Glycine max*) and castor bean (*Ricinus communis*) identified *SUS* activity in the cytosol (Nishimura & Beevers, 1979; Morell & Copeland, 1985), and immunolocalization studies performed on cotton fibres (*Gossypium hirsutum*) indicated that *SUS* could be localized at the plasma membrane (Amor *et al.*, 1995). In maize, different *SUS* isoforms have been localized both to the plasma membrane and to the cytosol (Carlson & Chourey, 1996; Duncan *et al.*, 2006). These and other studies indicate that the cytosolic and plasma membrane localizations of *SUS* are most common. Other reported *SUS* localizations include the Golgi apparatus of maize (Buckeridge *et al.*, 1999), the tonoplast (Etxeberria & Gonzalez, 2003), and plastid membranes of maturing *Arabidopsis* seeds, where *SUS* was suggested to be involved in controlling carbon flow into starch or lipid synthesis (Nunez *et al.*, 2008).

A specific cotton *SUS* isoform called *SusC* was localized to the cell wall during secondary cell wall synthesis and a later *in situ* immunolocalization experiment in cotton indicated *SUS* distribution close to the plasma membrane of elongating cotton fibres, along the orientation of cellulose microfibrils (Amor *et al.*, 1995; Haigler *et al.*, 2001; Brill *et al.*, 2011). When the expression of *SUS* was suppressed in cotton using transgenic sense and antisense constructs, seed fibre initiation and elongation were repressed (Ruan *et al.*, 2003). These findings have been interpreted as indications of *SUS* involvement in cellulose biosynthesis and have given rise to a popular model, in which a plasma membrane localized *SUS* would directly supply cellulose synthase (*CesA*) complexes (*CSCs*) with their substrate UDP-Glc (Haigler *et al.*, 2001; Stein & Granot, 2019).

The cotton studies have been complemented with studies in other species, some of which have supported the *SUS-CSC* model. For example, the overexpression of *Populus simonii* × *nigra* sucrose synthase *PsnSuSy2* under the constitutive 35S promoter in tobacco lead to increased cellulose content, fibre length and cell wall thickness, while the lignin content decreased (Wei *et al.*, 2015). The overexpression of cotton *SUS* both under a constitutive (2x 35S) and tissue-specific (*Petroselinum crispum* 4-coumarate:CoA ligase

[4CL]) promoter in hybrid poplar (*P. alba x grandidentata*) resulted in slightly increased cellulose formation (Coleman *et al.*, 2009). In another hybrid poplar study on *P. deltoides x trichocarpa*, the SUS isoforms SUS1 and SUS2 were identified as potentially associated with cellulose synthases, as they were pulled down with the CSC complexes in an immunoprecipitation assay (Song *et al.*, 2010).

The SUS-CSC model was challenged by Barratt *et al.* (2009), who built on Bieniawska *et al.* (2007) experiments in which single knockout mutant plants lacking individual SUS isoforms as well as double knockout mutants lacking two of the most closely related SUS isoforms (*sus2/sus3*, *sus5/sus6*) grew, developed and reproduced normally. This indicated that none of the isoforms were essential for plant development and cell wall biosynthesis, neither individually nor in the tested pairs. Later, Barratt *et al.* (2009) generated quadruple *SUS* knockout mutants (*sus1/sus2/sus3/sus4*) of *Arabidopsis* and observed no defects in plant growth, development or cell wall composition. The remaining two isoforms SUS5 and SUS6 were suggested to play a role in callose biosynthesis, as they were localized to the phloem sieve plates, and as the callose-containing layer lining the pores of sieve elements was thinner in the *sus5/sus6* double knockout mutants than in the wild-type plants (Barratt *et al.*, 2009).

Additional results challenging the SUS-CSC model were presented by Gerber *et al.* (2014), who generated transgenic RNAi lines (*SUSRNAi*) of *Populus tremula x tremuloides* where both *SUS1* and *SUS2* were targeted by the same RNAi construct driven by the constitutive 35S promoter. Only trace amounts of SUS activity could be detected in the developing wood of these trees but despite this, no dramatic growth phenotypes or clear differences in xylem anatomy or dry weight percentages of the wood polymers (including cellulose) were observed when the transgenic trees were grown in glasshouse conditions. This is in agreement with the earlier result from the *Arabidopsis* experiment of Barratt *et al.* (2009) and supports the hypothesis that SUS activity would not be essential for cellulose synthesis. However, as the wood density of the transgenic trees was lower than that of the wild-types and there was less lignin, cellulose and hemicellulose per volume of wood, the researchers concluded that SUS has an important role in supplying carbon to the synthesis of all the main cell wall polymers and not to cellulose specifically (Gerber *et al.*, 2014).

The results of Barratt *et al.* (2009) were later challenged by Baroja-Fernández *et al.* (2012). They claim that unfavourable reaction conditions, including too high pH and too long reaction times, were used in the studies of Bieniawska *et al.* (2007) and Barratt *et al.* (2009), which might have affected the SUS activity and caused misleading results. Additionally, in the earlier studies SUS activity was measured in the synthesis direction instead of the cleavage direction, which have different pH optima (Schmolzer *et al.*, 2016). Baroja-Fernández *et al.* (2012) repeated the earlier experiments in the sucrose breakdown direction using optimized reaction conditions and reported that the remaining activity of SUS5 and SUS6 in the *sus1/sus2/sus3/sus4* mutant would be enough to compensate for the lack of other SUS isoforms and to support normal growth as well as starch biosynthesis. However, no explanation was provided for how the phloem-localized isoforms SUS5 and SUS6 would compensate for SUS activity throughout the plant tissues. Together with my colleagues, I have addressed this debate as a part of my PhD project, and in Wang *et al.* (2022) we present strong evidence for SUS not being essential for cellulose biosynthesis in Arabidopsis.

1.7.3 Sucrose metabolism is tightly connected to other important metabolic pathways

Sucrose provides the majority of carbon for wood and NSC formation in stems and its cleavage by SUS and INV is an important process for plant growth and metabolism (figure 5). The existence of two sucrose cleavage pathways with multiple subcellular localisations highlights the flexibility in the system, although it is still unclear how carbon fluxes are divided between both pathways (Mahboubi & Niittylä, 2018; Stein & Granot, 2019). It is likely that there are differences in this between different tissues, cell types and developmental stages of the plant. For example, studies on potato and lentil (*Lens culinaris*) indicated that sucrose cleavage via INV could be the major pathway in actively growing organs, while cleavage via SUS would be the preferred route in storage organs in these species (Ross *et al.*, 1994; Chopra *et al.*, 2003).

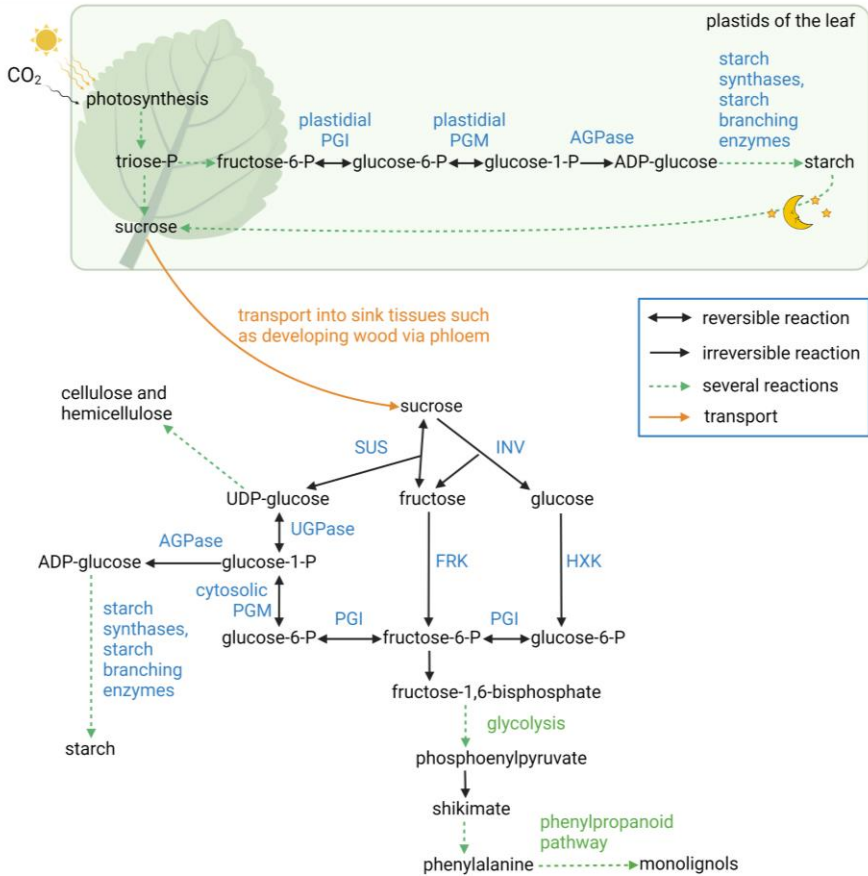


Figure 5. A simplified overview of sucrose metabolism and its interconnectedness to other processes of plant growth and metabolism, such as the biosynthesis pathways of starch and the cell wall components cellulose, hemicellulose and monolignols.

Abbreviations: CO₂, carbon dioxide; AGPase, ADP-glucose pyrophosphorylase; ADP, adenosine diphosphate; UGPase, UDP-glucose pyrophosphorylase; UDP, uridine diphosphate; PGM, phosphoglucomutase; PGI, phosphoglucoisomerase; FRK, fructokinase; HXK, hexokinase; P, phosphate.

Figure created with BioRender.com.

The energy costs of the two sucrose cleavage reactions are different. Sucrose catalysis into Glc-6-P by INV and hexokinase requires two molecules of ATP, but only one molecule of the inorganic pyrophosphate (PP_i) is needed for the reactions via SUS, UDP-glucose pyrophosphorylase (UGPase) and PGM (Geigenberger, 2003). PP_i is produced as a byproduct in biosynthetic reactions where ATP is hydrolysed, such as during the synthesis of DNA, RNA and proteins, and if it is assumed that recycled PP_i is used in the reactions of the SUS pathway, the total energy cost becomes even lower (Geigenberger, 2003; Ferjani *et al.*, 2014). The difference in energy costs may have an effect on where and when each pathway is utilised.

Current results indicate that cleavage via INV could be the more critical pathway for overall plant growth and survival. In the Barratt *et al.* (2009) experiment described above, the growth and development of *Arabidopsis sus1/sus2/sus3/sus4* mutant plants was normal. The recent study of Fünfgeld *et al.* (2022) as well as the results of this PhD work published in Wang *et al.* (2022) show that even complete loss of SUS activity does not cause obvious growth defects. In contrast, mutant plants lacking the two neutral/alkaline invertases (*cinv1/cinv2*) that are highly expressed in the cytosol of root cells had significantly reduced growth when compared to the wild-type controls (Barratt *et al.*, 2009). Glucose, fructose, sucrose and starch contents were the same between the quadruple *SUS* mutant and the wild-type plant and there was no difference between INV activity between the two, which indicates that sucrose catabolism via the cytosolic INV activity would be enough to provide the non-photosynthetic tissues with the carbon they need (Barratt *et al.*, 2009).

Recent work has shown that the pathway via SUS has a vital role in tree growth. Dominguez *et al.* (2021) investigated the role of SUS in *P. tremula* x *tremuloides* carbon allocation on the whole-tree level, using both metabolite profiling and ¹³CO₂ pulse labelling to study the incorporation and allocation of carbon. The total carbon content of the glasshouse-grown *SUSRNAi* trees was significantly reduced, which together with a decrease in ¹³C-sucrose as well as an overall decrease in ¹³C-labelled, developing wood-related metabolites in the transgenic trees revealed SUS as a key enzyme in determining carbon allocation at the whole tree level. The authors also observed an increase in acidic invertase activity in two of three analysed *SUSRNAi* lines, which suggested that acid INV are partially compensating for the reduced SUS activity (Dominguez *et al.*, 2021). A partial

compensation effect was also implied in the trees grown out in field conditions, where the stem diameter and height growth of *SUSRNAi* trees at first was like that of the wild-type but became statistically significantly reduced as time passed. The growth phenotypes suggest that SUS is needed for tree growth in natural growth conditions (Dominguez *et al.*, 2021). All in all, Dominguez *et al.* (2021) concluded that the incorporation of carbon from sucrose into developing wood was reduced in the transgenic *SUSRNAi* trees. This reduced the sink activity of wood, which in its turn reduced the phloem loading and transport of sucrose as feedback. The results indicate that SUS activity has a central role in coordinating sink activity and carbon allocation on the whole-tree level.

To summarise, sucrose catabolism via SUS and INV is tightly connected to the biosynthesis of both the storage polymer starch and the major components that are needed to build up the plant cell walls. In the following sections I will connect this knowledge to the formation of wood.

1.8 Wood formation is the main carbon sink during growth of trees

Wood (secondary xylem) is formed by the activity of the vascular cambium, which is a cylindrical secondary meristem located around the stem. Vascular cambium is derived from the procambium, which in its turn originates from the apical meristem of the tree (Larson, 1994). Cells of the vascular cambium, the so-called cambial initials, can divide periclinally (*i.e.*, parallel to the stem surface and epidermis) to produce files of xylem cells to the pith-side (inside) and files of phloem cells to the bark-side (outside) of the stem (Schuetz *et al.*, 2013). The xylem mother cells are known to divide more often than phloem mother cells, which leads to the production of more xylem than phloem (Fromm, 2013).

Cambial cells also divide anticlinally to produce more cambial initials, so that the meristematic cylinder is not disrupted during stem diameter growth. The cambial initial cells can be categorized into two different types: the elongated fusiform initials that develop into cells of the axial system (phloem and xylem) and the more compact, almost isodiametric ray initial cells which produce the radial system (ray parenchyma and ray tracheids; (Fromm, 2013).

After leaving the cambium, the cells of xylem go through the four main stages of wood development: cell expansion, secondary cell wall (SCW) deposition, maturation and programmed cell death (Mellerowicz *et al.*, 2001; Plomion *et al.*, 2001). The newest, still expanding cells are surrounded by the primary cell wall, which is mainly composed of pectins, cellulose and hemicellulose. The primary cell wall is loosened during the cell expansion, which allows the cell to grow to its final size while simultaneously synthesising and adding new cell wall material (Cosgrove, 2005). After the cell has expanded to its final size, xylem cells deposit a rigid, multi-layered secondary cell wall, which is built onto the inner side of the primary cell wall (Li *et al.*, 2016).

In angiosperm trees such as aspen (*Populus tremula*), wood is mainly composed of three different types of cells: vessels, fibres and ray parenchyma, each with its own specialized function (Mellerowicz *et al.*, 2001). Vessel elements are the water-conducting structures of wood. After expanding to their final size, they deposit a thick, lignified SCW that contributes to additional mechanical strength and waterproofing. Sides of these cells have small pits that connect the cells to neighbouring ray cells, while the ends of the vessel elements have openings called perforation plates (Murakami *et al.*, 1999; Jacobsen *et al.*, 2018). These connect multiple vessel elements to each other, which is how the long pipes for water transport are formed (Jacobsen *et al.*, 2018). Before water transport can begin, the cell contents of the vessel elements must be removed so that the cells become hollow. This occurs via programmed cell death that takes place within a few days after maturation. The lignification of vessel cell walls continues even after death, in some cases with the help of their neighbouring cells (Pesquet *et al.*, 2010; Bollhöner *et al.*, 2012; Smith *et al.*, 2013).

The main function of the long and thin fibre cells is to provide mechanical support for the tree. During their growth and starting already within the cambial zone, fibres undergo intrusive tip growth and penetrate between other cells of wood (Gorshkova *et al.*, 2012). Like vessel elements, also fibres undergo programmed cell death, but this occurs slightly later than in vessels, presumably to allow for more time to synthesise the thick, strong SCW required for mechanical strength (Courtois-Moreau *et al.*, 2009; Schuetz *et al.*, 2013).

Cells of the ray parenchyma are involved in horizontal nutrient transport within the wood. Rays are also the most long-lived of the three main cell

types of wood: the ray parenchyma cells of *Populus sieboldii* x *P. grandidentata* were observed to die within five years of differentiation, and the timing of death was shown to correlate with connectivity to neighbouring vessel elements and the cell's position within a ray (Nakaba *et al.*, 2011). As both wood fibres and vessels are dead when they are mature and ray parenchyma only makes up ca. 10-14 % of the volume of wood in *Populus*, it can be stated that wood is mainly composed of dead cells (Spicer, 2014).

It was initially estimated that approximately 1000 Arabidopsis genes would be involved in or connected to processes related to biosynthesis, modification and turnover of the cell wall (Carpita *et al.*, 2001; Somerville *et al.*, 2004). A later estimation based on a genome-wide co-expression network analysis indicated that the number might be closer to 2800 (Cai *et al.*, 2014). When the same analysis was performed on *Populus trichocarpa*, at least 588 putative cell wall -related genes were identified based on their gene ontology annotations (Cai *et al.*, 2014). However, it is likely that not all *Populus* cell wall -related genes were detected in this study, and it is rather expected that the number would be similar to, or higher than in Arabidopsis (Tuskan *et al.*, 2006). In support of this conclusion, a co-expression network analysis performed on developing wood -expressed *Populus tremula* genes defined 41 transcriptional modules containing a total of 2560 genes, all of them associated with wood formation (Sundell *et al.*, 2017).

In the following sections I will briefly describe the formation and structure of the main wood polymers cellulose, lignin and hemicellulose which as combined represent the main carbon sink in trees.

1.9 Carbon allocation to the main wood polymers

Approximately 40-50 % of wood consists of cellulose, which makes it the most abundant terrestrial biopolymer (Plomion *et al.*, 2001). For example, in different *Populus* species and hybrids wood cellulose content varies between ca. 42-49 % (McDougall *et al.*, 1993; Sannigrahi *et al.*, 2010; Kačík *et al.*, 2012). Cellulose is composed of β -1,4-linked glucosyl residues which are attached together by inter- and intramolecular hydrogen bonds and Van der Waals forces to form semicrystalline microfibrils (McFarlane *et al.*, 2014). These microfibrils are the main load-bearing elements of plant cell walls (Verbancic *et al.*, 2018). The cellulose microfibrils are synthesized at the plasma membrane by rosette-like cellulose synthase (CesA) complexes

(CSCs; (Mueller & Brown, 1980; Kimura *et al.*, 1999; Hill *et al.*, 2014). In addition to the CesAs, several proteins such as CELLULOSE SYNTHASE INTERACTING1 (CSI1)/POM2 and KORRIGAN are associated with the CSC complex and influence cellulose biosynthesis (Allen *et al.*, 2021).

Cellulose microfibrils are surrounded by hemicelluloses which are a diverse group of branched polysaccharides whose backbone consists of β -1,4-linked subunits. In angiosperms, the group includes xyloglucans, glucans, mannans and glucomannans, and in *Populus* species they make up ca. 16-23 % of the cell wall (Sannigrahi *et al.*, 2010; Scheller & Ulvskov, 2010). Hemicellulose biosynthesis takes place in the Golgi apparatus, from which they are delivered to the cell wall by transport vesicles (Cosgrove, 2005). First, the polymer backbone is synthesized by polysaccharide synthases, after which glycosyltransferase enzymes attach the branched side-chains to complete the polymer (Perrin *et al.*, 2001). The composition of these side chains differs between plant species and cell types (Scheller & Ulvskov, 2010).

The nucleotide sugar UDP-Glc is the precursor of both cellulose and hemicellulose biosynthesis. As described earlier, UDP-Glc is produced via the cleavage of sucrose in the developing wood. Therefore, influencing the production of UDP-Glc or the action of the enzymes and their interactors could provide interesting control points for studying carbon allocation into cellulose and hemicellulose.

Lignin is the second most abundant terrestrial biopolymer that accounts for ca. 15-40 % of wood, depending on the tree species (Sarkanen & Ludwig, 1971). In the wood of *Populus* species lignin accounts for ca. 15-25 %, varying between different clones and growth conditions (Lapierre *et al.*, 1999; Bose *et al.*, 2009; Studer *et al.*, 2011). In wood, lignin provides the cells with additional stiffness, strength and waterproofing (Boerjan *et al.*, 2003). Lignin is composed of three monolignols, *p*-coumaryl alcohol, coniferyl alcohol, and sinapyl alcohol, which form *p*-hydroxyphenyl (H), guaiacyl (G) and syringyl (S) subunits of the lignin polymer, respectively (Boerjan *et al.*, 2003). The ratio between these monomers in the lignin polymer varies between species and cell type, and for example the lignin of angiosperm hardwoods (including *Populus* species) is mainly composed of the G- and S-subunits with only traces of H-subunits (Boerjan *et al.*, 2003).

The lignin monomer biosynthesis pathway is linked to the primary metabolism carbon flux via the amino acid phenylalanine, which is produced

via the shikimate pathway (Maeda & Dudareva, 2012; Vanholme *et al.*, 2019). Most of the reactions on the pathway take place in the cytosol, while some of the enzymes are associated with the endoplasmic reticulum (Boerjan *et al.*, 2003; Gou *et al.*, 2018). In the first steps of the lignin biosynthesis pathway, the enzyme phenylalanine ammonia-lyase (PAL) catalyses the deamination of phenylalanine into cinnamic acid, which is then converted into *p*-coumaric acid by cinnamate-4-hydroxylase (C4H). After this the pathway forks to form a complicated metabolic grid, where a total of 21 monolignol genes encoding for 20 proteins, including the ones mentioned above, catalyse 37 reaction fluxes between 24 metabolites, finally resulting in the biosynthesis of the monolignol subunits (Wang *et al.*, 2018). The grid-like structure is created by many of the pathway enzymes (*e.g.* 4-coumarate:CoA ligase [4CL] and cinnamyl alcohol dehydrogenase [CAD]) having several substrates, and it has been speculated that this would be important in regulating the carbon flow via the different intermediate compounds to control the biosynthesis (Vanholme *et al.*, 2019).

After synthesis, the monolignols are exported across the plasma membrane to the cell wall, where they are radicalised by laccases and/or peroxidases and incorporated into the growing lignin polymer (Morreel *et al.*, 2004; Perkins *et al.*, 2019). The exact export method is yet unknown, and both diffusion and active transport have been suggested as possible mechanisms (Perkins *et al.*, 2019). The downregulation of monolignol biosynthesis genes caused the lignin content of different transgenic lines of *Populus trichocarpa* to vary between 9,4-25 % of wood dry weight, compared to the average 21,7 % of wood dry weight that was observed in untreated wild-type trees (Wang *et al.*, 2018). This is why the biosynthesis of monolignol subunits has been suggested as a possible control point of carbon allocation into the lignin pathway.

1.10 Primary metabolism is a key component in defining sink strength in developing wood

Recent studies by Sundell *et al.* (2017) and Roach *et al.* (2017) provided evidence for the importance of transcriptional regulation in carbon allocation to wood. In their study, Sundell *et al.* (2017) generated thin, consecutive cryosections of wild-growing aspen stems and used RNA sequencing methods to construct high-spatial-resolution transcriptome profiles that span

the whole region of wood development, starting from the differentiation of cambial cells into xylem precursors, continuing to cell elongation and expansion, maturation, and ending in the programmed cell death of tracheary elements and xylem fibres. The results of the study were collected to a database called AspWood, which can currently be accessed via the Plant Genome Integrative Explorer (PlantGenIE) online resource (Sundell *et al.*, 2015). This study revealed previously unknown transcriptome modularity in developing wood, with specific transcription factor proteins being expressed in certain wood developmental zones (Sundell *et al.*, 2017). More detailed investigation of these modules, their TFs and how their expression is regulated is required to obtain information on the regulation of wood formation and thus also carbon allocation to wood.

Roach *et al.* (2017) selected eight central primary metabolism enzymes based on their importance in sugar metabolism and confirmed or hypothesized roles in biosynthesis of the secondary cell wall polymers, measured their activities across phloem, cambium and developing wood, and compared the enzyme activity patterns with the AspWood transcript levels of the corresponding genes. The activities of most of the enzymes increased during secondary cell wall formation, and in many cases this was matched with an increase in both transcript levels as well as sugar, hexose phosphate (including Fru-6-P, Glc-6-P and Glc-1-P) and UDP-glucose content (Roach *et al.*, 2017). For example, the transcript levels of two of the fifteen *SUS* genes in aspen (Potri.018G063500 [*SUS1*]) and Potri.006G136700 [*SUS2*]) were upregulated in the secondary cell wall forming region of wood (Roach *et al.*, 2017; Roach *et al.*, 2018). Their expression peak correlated with the highest *SUS* enzyme activity, and with the greatest accumulation of carbon into the cell wall. Similarly, the highest enzyme activity peak of UDP-glucose pyrophosphorylase (UGPase), an enzyme catalysing the reversible reaction of Glc-1-P and UDP into UDP-Glc, occurred in the zone of secondary cell wall formation and coincided with the increase of two transcripts (Potri.004G074600 and Potri.004G074400). The increase in *SUS* and UGPase activities was similar to the progressive increase in the concentrations of sucrose, glucose and fructose through the phloem and the first sections of the secondary cell wall forming region. Based on this, the researchers hypothesized that both *SUS* and UGPase could be important primary metabolism enzymes involved in production of UDP-glucose for cell wall biosynthesis in aspen wood (Roach *et al.*, 2017).

These findings show that there is a positive relationship between increased primary metabolism enzyme activity and increased carbon allocation to cell walls during wood development, more specifically secondary cell wall formation. The activities of many of the enzymes closely followed the level of its gene transcript(s), which indicated that carbon allocation in developing wood is under transcriptional regulation (Roach *et al.*, 2017). However, it is not yet known what these regulators are and how this gene expression is regulated. This was one of the major questions addressed in this PhD thesis, and to make the connection I will next describe the current understanding of transcriptional regulation of wood and secondary cell wall formation.

1.11 Transcription factor proteins as regulators of sink strength and carbon allocation to wood

Transcription of genes is regulated primarily by proteins called transcription factors (TFs). TFs recognize and bind to specific, short regions on the DNA called *cis*-regulatory elements (CRE) or TF binding sites (TFBSs). The requirements for TF binding include that the TF can recognize the CRE in question, the DNA chromatin structure is open and available for binding, and that the CRE is not already occupied by a TF (Weber *et al.*, 2016). Depending on the mode of action, TF binding can either initiate or suppress the transcription of a gene. When binding to DNA, TF proteins can either function alone, as hetero- or homomers, or in a complex with other TFs and/or cofactors. The part of the TF protein that recognizes the CRE on the DNA strand and binds to it is called the DNA-binding domain (DBD).

The CREs are typically located in non-coding DNA upstream from the transcription start site (TSS) of the gene or genes they regulate, but they can also be located downstream or within a coding region of a gene (Bennetzen & Wang, 2018; Ricci *et al.*, 2019). CREs contain conserved, usually short regions of DNA called TF binding motifs. Binding motifs can be identified using *in vivo* and *in vitro* methods, where the *in vivo* methods are particularly useful in characterizing binding events in specific biological conditions (*e.g.* under a stress treatment or at a certain developmental stage) and the *in vitro* methods contain different large-scale approaches for screening many interactions at once (Inukai *et al.*, 2017). Chromatin immunoprecipitation

sequencing (ChIP-seq) is one of the commonly used *in vivo* methods for screening for TF binding sites on the genomic DNA, after which bioinformatics algorithms such as those in the MEME Suite can be used to search for enriched binding motifs (Bailey *et al.*, 2009; Bailey *et al.*, 2015; Inukai *et al.*, 2017). Graphs called position weight matrices (PWMs) are often used to illustrate the binding motif and the probabilities of each base at different positions of the binding site (Stormo *et al.*, 1982; Schneider & Stephens, 1990; Stormo, 2013). Well-characterized DNA-binding motifs and their PWMs have been collected into curated databases such as JASPAR (<https://jaspar.genereg.net/>; Khan *et al.*, 2018).

A set of general TFs is needed to initiate gene transcription performed by RNA polymerase II, which is the polymerase responsible for the transcription of protein coding genes. The binding site of these TFs is called the core promoter and it is usually located near the TSS. This core promoter usually contains *cis*-regulatory elements such as the TATA box (located 25-30 bp upstream from TSS), CAAT box (ca. 80 bp upstream from TSS), initiator region and/or the downstream promoter element, but not all of them are present in all core promoters and might instead be replaced by other regulatory elements (Bilás *et al.*, 2016).

In addition to the initiation of transcription via binding the core promoter, TFs function as important activators or enhancers that promote the expression of genes, or as repressors or silencers that downregulate or prevent gene expression (Slattery *et al.*, 2014). Studies on the fruit fly (*Drosophila melanogaster*) have shown that TF binding can even be neutral or non-functional with no clear effect on gene expression (*e.g.* (Fisher *et al.*, 2012)). In this thesis work and the following sections I will focus on TFs with enhancing and repressing properties.

Identification of transcriptional enhancers and silencers in plants has been challenging as their binding sites can be located far away from the gene or genes that they regulate (Galli *et al.*, 2020). However, an assay for transposase-accessible chromatin with sequencing (ATAC-seq) experiment on root tip nuclei of Arabidopsis, barrel medic (*Medicago truncatula*), tomato and rice showed that most (ca. 75 %) of the open chromatin sites that are available for TF binding are located within 3 kb upstream of the TSS (Maher *et al.*, 2018). In maize leaf protoplasts, a ChIP-seq experiment revealed that most TF binding peaks were located $\pm 2,5$ kb from the closest gene, more often on the upstream (5') side (Tu *et al.*, 2020). Therefore, the

location of *cis*-regulatory elements seems similar between different plant species. Combining the ChIP-seq and ATAC-seq data showed that ca. 74 % of the TFs intersected with open chromatin regions, which supports the mapping of open chromatin as an effective strategy for identifying biologically relevant TF binding sites (Tu *et al.*, 2020).

TFs are classified into families based on similarities in the amino acid sequences of their DNA-binding domains (Luscombe *et al.*, 2000). Many TF families are common across several kingdoms of life, but they can perform different functions in different organisms. One such TF superfamily is MYELOBLASTOSIS (MYB), which contains a well-conserved DBD called the MYB domain. The length and number of repeating structures in this domain is used to classify the MYB proteins into different sub-groups. In addition to plants, genes belonging to the MYB family are found in vertebrates, insects and fungi (Lipsick, 1996; Weston, 1998). Most of the MYB genes in plants belong to the subfamily R2R3-MYB, and among others they have an important function in regulating the formation of secondary cell walls (McCarthy *et al.*, 2009; Dubos *et al.*, 2010).

There are also several TF families specific to plants. Plant-specific TF families are mainly related to biological processes as well as development and growth of organs that only occur in plants. These include, for example, the WRKY TF family involved in biotic and abiotic stress responses as well as the NO APICAL MERISTEM, ATAF1/2, CUP-SHAPED COTYLEDON2 (NAC)-family, which, in addition to having functions related to stress, plays an important role in wood formation (Yamasaki *et al.*, 2013).

When considering the development of secondary xylem, it is known that the development and differentiation of vessel elements is a process carefully controlled by TF proteins (Kubo *et al.*, 2005; Yamaguchi *et al.*, 2008; Shi *et al.*, 2017). The exact molecular mechanism for fibre cell differentiation is still unknown, but it has been suggested that both mechanical signals and transcriptional regulation might be involved (Brown, 1964; Gorshkova *et al.*, 2012).

In the early 2000s ca. 1500 putative TFs were identified in the model plant *Arabidopsis*, estimated then to represent approximately 5 % of its genes (Riechmann *et al.*, 2000). According to the latest version of the online PlantTFDB database, the current estimate of loci coding for *Arabidopsis* TFs is 1717, classified into 58 families (Tian *et al.*, 2020). In comparison, the

current PlantTFDB estimate for the model tree *Populus trichocarpa* is 2466 TF-coding loci, which reflects the so-called “salicoid” whole genome duplication event ca. 58 million years ago (Tuskan *et al.*, 2006; Dai *et al.*, 2014; Tian *et al.*, 2020). The AspWood database with transcriptome data of wood-expressed, annotated protein-coding genes of aspen contains 1688 genes that were classified as TFs (Sundell *et al.*, 2017). This is approximately 5.9 % of all the wood-expressed genes, and ca. 68 % of the TF-coding loci recorded in PlantTFDB, emphasizing the importance of TFs for wood formation.

1.11.1 TFs in wood formation: Hierarchy and master regulations

According to the current model, transcriptional regulation of secondary cell wall formation is a hierarchical process with multiple tiers (figure 6; (Hussey *et al.*, 2013; Zhang *et al.*, 2018). This means that so called master regulator TFs on the first and highest tier of the regulatory “pyramid” regulate the expression of genes encoding for TFs on tiers two and three, and the pathway eventually leads to the activation of genes involved in the synthesis of secondary cell wall components. Different research groups have assigned the genes in the network into either four or five tiers (Taylor-Teeple *et al.*, 2015; Zhang *et al.*, 2018; Chen *et al.*, 2019).

Most of the studies on both the transcriptional control of SCW formation and the role of single TF proteins in this process have been performed on the model plant *Arabidopsis*. Studies performed on woody species such as *Populus* have indicated that the master regulator TFs on the first two tiers of the network are well conserved between the two angiosperm species. On the third tier there are more *Populus* TFs, which makes the network more complicated and comparisons with *Arabidopsis* on this tier more challenging (Zhang *et al.*, 2018). Additionally, alternative splicing of some of the first-layer master regulator TFs was observed both in *Populus* and *Eucalyptus* but not in *Arabidopsis*, which might indicate an additional layer of complexity in trees compared to herbs (Li, Q *et al.*, 2012; Zhao *et al.*, 2014).

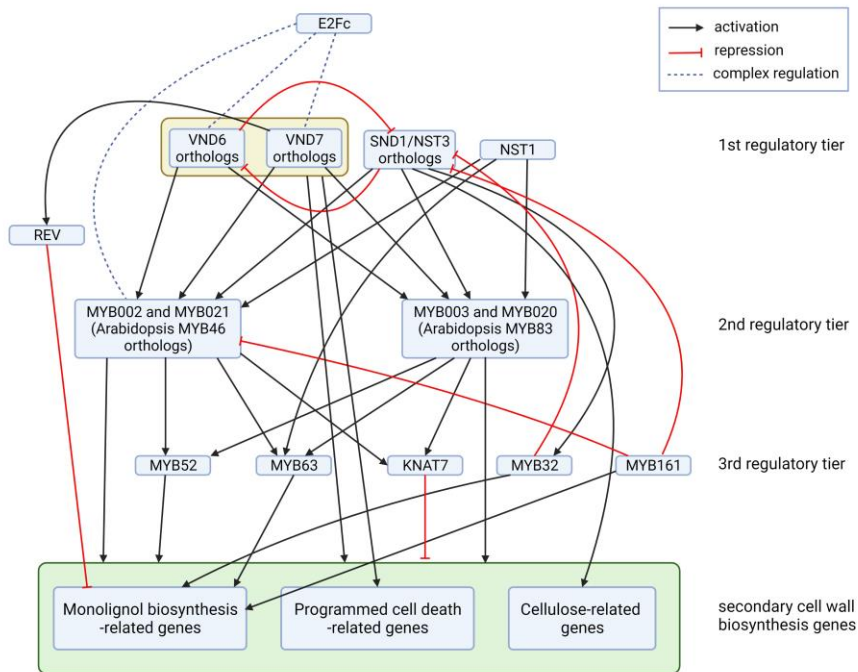


Figure 6. Simplified overview over the current consensus of the transcriptional regulatory network regulating secondary cell wall and wood formation.

The consensus network is based on studies on *Arabidopsis thaliana* and *Populus trichocarpa*. Several known interactions have been omitted for clarity. The network has three tiers, with the master regulators VND6, VND7, SND1/NST3 and NST1 on the first tier, MYB46, MYB83 and their *Populus* homologs on the second tier, and various transcription factors belonging to the MYB as well as other families on the third tier. The fourth and lowest tier of the network contains genes involved in or related to the biosynthesis of secondary cell wall components. Some transcription factors are involved in the network without being assigned to a specific tier, such as E2Fc and REV. Not all of the interactions have been experimentally verified in both *Populus* and *Arabidopsis*.

Abbreviations: VND, VASCULAR-RELATED NAC-DOMAIN; SND, SECONDARY WALL-ASSOCIATED NAC DOMAIN1; NST, NAC SECONDARY WALL THICKENING PROMOTING FACTOR; MYB, MYELOBLASTOSIS; KNAT7, KNOTTED ARABIDOPSIS THALIANA7; REV, REVOLUTA. Figure created with BioRender.com.

The first-tier master regulators are NAC-domain proteins

In Arabidopsis, the NAC-domain proteins VASCULAR-RELATED NAC-DOMAIN6 (VND6) and VND7 are considered the master regulators of xylem vessel element formation, with VND6 being preferentially expressed in metaxylem and VND7 in protoxylem vessels to initiate their differentiation (Kubo *et al.*, 2005). The role of these NACs as regulators of SCW formation was first reported in a mesophyll cell culture of the model organism *Zinnia elegans*, where the NAC TF Z567 was upregulated during transdifferentiation of mesophyll cells into tracheary elements (Demura *et al.*, 2002). Later, Arabidopsis homologs of this gene were identified in suspension cells and named VND1-7, and in the same study the functions of VND6 and VND7 in meta- and protoxylem vessel differentiation were discovered (Kubo *et al.*, 2005). By overexpressing VND6 and VND7 it is possible to induce vessel cell formation and ectopic SCW deposition in tissues whose cells normally do not form SCW, such as leaves, and their inactivation causes the lack of vessel element formation (Kubo *et al.*, 2005; Mitsuda *et al.*, 2005; Yamaguchi *et al.*, 2008). These observations were strong indicators for the status of VND6 and VND7 as central regulators of SCW formation.

A saying in both Finnish and Swedish states that “a dear child has many names”, and this also describes scientists’ relation to *Populus* orthologs of VND6 and 7 very well. The six *Populus* genes orthologous to *AtVND6* have been called VNS01-06, WND3A/B-5A/B, VND6-A1/A2-VND6-C1/C2 as well as PNAC008-011 and PNAC070-071, and the two *AtVND7* orthologs have been referred to as VNS07-08, WND6A/B, VND7-1/2 as well as PNAC056 and PNAC058 (Hu *et al.*, 2010; Zhong *et al.*, 2010b; Ohtani *et al.*, 2011; Li, Q *et al.*, 2012; Wang *et al.*, 2020). The non-uniform nomenclature in the literature can make comparison of studies challenging, and highlights the importance of including either a locus ID (*e.g.* Potri.013G113100 for WND6A) or a GenBank accession number, so that verification of gene identity will be easier. In the RNAseq study of Sundell *et al.* (2017), the expression of *Populus* homologs of *AtVND6* peaked within the cell expansion zone and at the end of SCW deposition zone, which is consistent with their role in determining vessel cell fate as well as SCW formation and cell death during vessel element formation, respectively. Only one of the homologs of *AtVND7* was expressed in the dataset with a clear peak in the SCW formation zone, indicating its role in SCW deposition in *Populus*

(Sundell *et al.*, 2017). As the AspWood database was constructed using wood samples from a mature tree, it does not contain protoxylem which occurs during the very early development of the vasculature (Ruzicka *et al.*, 2015). This could explain why only one of the two aspen homologs of *AtVND7* was expressed in the dataset.

Fibre formation is regulated by SECONDARY WALL-ASSOCIATED NAC DOMAIN1 (*SND1*), which is also known as ARABIDOPSIS NAC DOMAIN CONTAINING PROTEIN12 (*ANAC012*) and as NAC SECONDARY WALL THICKENING PROMOTING FACTOR3 (*NST3*), and by *NST1*, which together are considered the master regulators of fibre formation (Zhong *et al.*, 2006; Ko *et al.*, 2007; Mitsuda *et al.*, 2007; Mitsuda & Ohme-Takagi, 2008). Repression of both *SND1/NST3* and *NST1* expression suppressed the formation of secondary cell walls in interfascicular fibres of inflorescence stems and the secondary xylem of Arabidopsis hypocotyls, but knocking out only one of the genes was not enough to cause a visible fibre wall phenotype (Mitsuda *et al.*, 2007). Based on this finding it can be concluded that the two TFs act redundantly to regulate interfascicular fibre wall biosynthesis.

Four *Populus* orthologs of *SND1/NST3* have been described, and they have been called *VNS09-12*, *WND1A/B-2A/B*, *SND1-A1/2-B1/B2* as well as *PNAC084-086* and *PNAC017* (Hu *et al.*, 2010; Zhong *et al.*, 2010b; Ohtani *et al.*, 2011; Li, Q *et al.*, 2012; Wang *et al.*, 2020). When a quadruple knockout mutant of all *VNS* genes (*vns09 vns10 vns11 vns12*) of hybrid aspen (*Populus tremula x tremuloides*) was generated using CRISPR/cas9 (Clustered regularly interspaced short palindromic repeats/CRISPR associated), the formation of SCW was completely suppressed in xylem ray parenchyma cells as well as xylem and phloem fibres, but the SCW of vessel elements developed normally (Takata *et al.*, 2019). This demonstrates the essential role of *Populus NST/SND* genes in the SCW biosynthesis in xylem and phloem fibres and xylem ray parenchyma.

Alternative splicing was shown to play a role in *SND1*-mediated regulation in *Populus trichocarpa*, when the splice variant named *SND1-A2^{IR}* was found to inhibit the expression of other members of the *PtrSND1* family as well as the downstream target *PtrMYB021*, but not that of *SND1-A1* (Li, Q *et al.*, 2012). In a later study, *VND6-C1^{IR}*, a splice variant of the vessel element master regulator *VND6*, was shown to function similarly and in tandem with *SND1-A2^{IR}* in suppressing both *PtrSND1s*, including *SND1-*

AI, and *PtrVND6s*, but excluding its cognate *VND6-C1* (Lin *et al.*, 2017). This indicates that the regulatory process in *Populus* is not as straightforward and top-down as initially assumed based on results from *Arabidopsis* studies.

The four first-tier TFs, VND6, VND7, SND1/NST3 and NST1, as well as NST2, which has a master regulator role in SCW formation in the anther endothecium, are collectively referred to as the secondary wall NAC (SWN) proteins (Mitsuda *et al.*, 2005; Zhou *et al.*, 2014). In woody plants such as *Populus*, the functional orthologs of SWNs are even called wood associated NAC domain transcription factors, WNDs (Zhong & Ye, 2010).

MYB46 and MYB83 are the second-tier master regulators

The current consensus in the literature is that the second layer of the transcriptional network is composed only of two TFs. The second-tier *Arabidopsis* TFs MYB46 (At5g12870) and MYB83 (At3g08500) could even be called second-tier master regulators, as they are able to cause ectopic SCW deposition when over-expressed (Zhong *et al.*, 2007; McCarthy *et al.*, 2009).

In trees, orthologs of these MYB TFs have been identified in eucalyptus, pine and *Populus* (Goicoechea *et al.*, 2005; Bomal *et al.*, 2008; McCarthy *et al.*, 2010; Zhong *et al.*, 2010a). Based on a phylogenetic analysis of the *Populus trichocarpa* orthologs, PtrMYB002 (Potri.001G258700) and PtrMYB021 (Potri.009G053900) are the closest orthologs of AtMYB46, and PtrMYB003 (Potri.001G267300) and PtrMYB020 (Potri.009G061500) the closest orthologs of AtMYB83 (McCarthy *et al.*, 2010; Jiao *et al.*, 2019). Based on their ability to cause ectopic lignification as well as ectopic deposition of cellulose and xylan, McCarthy *et al.* (2010) classified PtrMYB003 and PtrMYB020 as the functional orthologs of AtMYB46 and AtMYB83.

Both AtMYB46 and AtMYB83 are directly regulated by the first-tier master regulators AtVND6 and VND7, AtNST1 and AtSND1/AtNST3 (Zhong *et al.*, 2007; McCarthy *et al.*, 2009). In *Populus* the SND1 homolog PtrSND1-B1 (also known as PtrWND2A) directly targets PtrMYB021 as well as another MYB called PtrMYB074 (Potri.015G082700, also known as PtrMYB050; (Zhong *et al.*, 2010b; Lin *et al.*, 2013; Chen *et al.*, 2019). A recent study by Wang *et al.* (2020) reports that three additional *Populus trichocarpa* first-tier master regulators, SND1-A1 (WND1A), SND1-A2

(WND1B) and SND1-B2 (WND2B) can activate the expression of both PtrMYB021 and PtrMYB074.

AtMYB46, AtMYB83 and their *Populus* homologs are known to directly regulate several other TFs as well as genes related to the synthesis of SCW components. AtMYB46 and AtMYB83 are known to bind to a specific 7 bp *cis*-element called the secondary wall MYB-responsive element (SMRE, ACC[A/T]A[A/C][T/C]), and both of them were suggested to activate the same direct target genes (Zhong & Ye, 2012). These direct targets include five other MYB TFs (*e.g.* MYB52 and MYB63) as well as KNOTTED ARABIDOPSIS THALIANA7 (KNAT7), which is a third-tier negative regulator of SCW formation in both *Arabidopsis* and *Populus* (Li, E *et al.*, 2012; Zhong & Ye, 2012). The 1,5 kb promoters of MYB63 and MYB52 were noted to contain eight and five repeats of the SMRE binding sites, respectively, which is highly enriched compared to the theoretical occurrence of this motif calculated as one in 2 048 bp (Zhong & Ye, 2012). Other direct targets of MYB46 and MYB83 include genes that are either hypothesized or known to be related to cell wall modification, programmed cell death, and the biosynthesis of xylan and lignin (Zhong & Ye, 2012). The lignin biosynthesis-related genes include *e.g.* phenylalanine ammonia-lyase (PAL) genes, cinnamoyl-CoA reductases and laccases (Zhong & Ye, 2012). As mentioned earlier, PAL is particularly interesting in the context of carbon allocation to wood as it catalyses the reaction in which primary metabolism branches towards lignin biosynthesis.

TFs and cell wall biosynthesis-related genes on the third and fourth tiers

The third tier of the regulatory network is mainly composed of TFs of the MYB family, but it also includes several NAC TFs as well as some TFs of other families, like BEL-like homeodomain (BLH) and bZIP family TFs (Zhong & Ye, 2012; Chen *et al.*, 2019). In some models, genes related to cell wall biosynthetic processes have been placed on the third tier in addition to the TFs, while other models place the cell wall genes on their own, lower tier (Taylor-Teeple *et al.*, 2015; Chen *et al.*, 2019; Wang *et al.*, 2020). In this thesis I consider the third tier as the lowest tier in the TF regulatory network, followed by the genes involved in biosynthesis of the cell wall components.

The expression of both third-tier TFs and cell wall-related genes on the fourth tier can be regulated by both first- and second-tier TFs. For example, a transcriptome analysis of the master regulator VND7 indicated possible

direct binding to the promoters of over sixty direct target genes, including the cellulose synthase genes *CesA4* and *CesA8* as well as the laccase LAC4, which plays a role in lignin biosynthesis (Yamaguchi *et al.*, 2011). In another experiment, an electrophoretic mobility shift assay (EMSA) confirmed an earlier suggestion that *AtMYB32* would be a direct target of the master regulator AtSND1 and resulted in the finding that AtMYB32 could function as a negative regulator of *AtSND1* in a feedback loop (Zhong *et al.*, 2010b; Wang *et al.*, 2011). AtMYB32 has been hypothesized to directly regulate several lignin biosynthesis -related genes (Preston *et al.*, 2004). The third-tier TF AtMYB63, mentioned in the previous section as a direct target of AtMYB46 and AtMYB83, was in an overexpression study indicated to be also a target of the master regulator NST1 (Zhou *et al.*, 2009). AtMYB63 was shown to directly regulate the expression of several monolignol biosynthesis associated genes such as *PAL1* and *cinnamyl alcohol dehydrogenase 6 (CAD6)*, most likely via binding to AC regulatory elements in their promoters (Zhou *et al.*, 2009). As additional examples, the promoters of the fourth-tier cellulose synthase genes *CESA4* and *CESA8* as well as that of *KORRIGAN*, an endoglucanase involved in cellulose biosynthesis, contain a TF binding motif called "tracheary element-regulating *cis*-element" (TERE; (Taylor-Teeple *et al.*, 2015). Several *in vitro* analyses as well as an *in planta* ChIP-seq experiment revealed that this motif can be bound by the master regulators SND1 and NST2, which indicates these three genes could be directly regulated by the first-tier TFs (Taylor-Teeple *et al.*, 2015).

1.11.2 From a strictly hierarchical pyramid towards a complex transcriptional network

The regulatory process of SCW formation is often presented as a top-down pyramid, although the reality is more complex, as described above. New studies are revealing previously unknown interactions and changing the pyramid into a complex network, where "lower-level" TFs can regulate the expression of those on "higher levels". An example of a lower-tier TF regulating the expression of higher-tier TFs was presented by Wang *et al.* (2020), who showed that PtrMYB161, a third-tier MYB, could bind to the promoters and repress the expression of four first-tier TFs, PtrSND1-A1, -A2, -B1 and -B2, as well as the second-tier regulator PtrMYB021.

In some cases, even the concentration of the TF seems to play a regulatory role. This applies to EF2c, a regulator added to the SCW network by Taylor-Teeples *et al.* (2015). Based on a large-scale yeast one-hybrid (Y1H) assay in the Arabidopsis root xylem, the researchers hypothesized that EF2c would be an upstream regulator of *VND6*, *VND7*, *MYB46* and several SCW biosynthesis genes as it was noted to bind their promoters. In experiments performed on an *E2Fc*-overexpressor line with impaired turnover of the protein, moderate levels of *E2Fc* activated *VND7* expression, while high or low levels of *E2Fc* caused the repression of *VND7* (Taylor-Teeples *et al.*, 2015). This indicates that the regulatory function of E2Fc can change based on its concentration.

Interactions in the regulatory network can even take place within the same tier. An EMSA analysis performed on AtSND1 revealed that the protein can directly bind to its own promoter, which the researchers interpreted as evidence for a positive feedback loop (Wang *et al.*, 2011). In another study, data from yeast two-hybrid (Y2H) experiments combined with bimolecular fluorescence complementation (BiFC) indicated that the third-tier TFs PtrMYB090, PtrMYB161 and PtrWBLH1 can all form dimers with each other (Chen *et al.*, 2019). As all these TFs can bind to the promoter of the lignin biosynthesis pathway gene *PtrCCoAOMT2*, the researchers suggested that the TF-TF complexes could regulate *CCoAOMT* expression either as individual protein pairs or in a larger complex (Chen *et al.*, 2019).

There are several important regulators and interactors of the TFs in the secondary cell wall regulatory network that have not been assigned to a specific tier of the “pyramid”. One such regulator is VND-INTERACTING2 (VNI2), which based on protein-protein binding experiments can interact both with the master regulator *VND7* as well as *VND1-5* and several other NAC TFs (Yamaguchi *et al.*, 2010). It was classified as a transcriptional repressor since a transient reporter assay suggested that VNI2 limits the expression of *VND7*-induced genes specific to vessel elements (Yamaguchi *et al.*, 2010). Additionally, VNI2 is induced by the plant hormone abscisic acid, and its overexpression in Arabidopsis leaves was shown to prolong leaf longevity and to increased resistance to salt stress (Yang *et al.*, 2011). This suggests that VNI2 could link together the SCW -related TF network via its interaction with *VND7* with processes related to stress tolerance and senescence (Lindemose *et al.*, 2013), and possibly even function as a transcriptional hub or a control point between them. The class III

homeodomain-leucine zipper (HD-Zip III) TFs, including REVOLUTA (REV) and PHABULOSA (PHB), are other interesting interactors of TFs and genes of the network. In *Arabidopsis*, the master regulator VND7 can bind the promoters of *PHB* and *REV*, and REV was noted to bind the promoter of *PAL4* (Raes *et al.*, 2003; Taylor-Teeples *et al.*, 2015). The amount of *PAL4* transcripts increased in the *rev-5* loss-of-function mutant and decreased when *REV* was transiently induced, indicating REV as a repressor of *PAL4* (Taylor-Teeples *et al.*, 2015).

Simple and straightforward interactions between a TF and its direct target(s) as well as more complex feedback- and feed-forward loops between several transcriptional activators, repressors and their targets can be considered as network motifs – repeating circuits of the transcriptional regulatory network (Alon, 2007; Hussey *et al.*, 2013). These structures exist in order to help with regulating the levels and activities of the TF proteins and their target genes during the different plant developmental processes, such as SCW deposition and wood formation (Hussey *et al.*, 2013).

By identifying interactions between TF proteins and their target genes it will be possible to characterize regulatory hubs, which could be used as interesting targets for genetic modification or traditional breeding. For example, changes in the thickness of secondary cell walls and/or the amount of wood tissue affect the source-sink balance and the carbon allocation of the whole tree.

2. Research aims and objectives

The aim of this PhD project was to study carbon allocation, tree growth and source-sink relationships, both on transcriptional as well as whole-plant level. The more specific objectives of the project were:

In **paper I**, to chart transcription factor (TF) proteins involved in the regulation of sink strength in developing wood, and to generate a developing wood transcriptional regulatory network in European aspen.

In **paper II**, to critically consider the bioinformatics analysis methods used in processing data from DAP-seq experiments and how these can impact biological interpretations, and to suggest guidelines as well as quality control checks for the data analysis.

In **paper III**, to assess the role of starch during tree growth and using low starch hybrid aspen trees, shed light on the following questions:

- Does the lack of starch limit the growth of the aspen tree, either at a diel time scale, or during seasonal processes such as bud set, dormancy, and bud flush?
- Does the aspen tree use an active or passive mechanism for starch storage?
- Is aspen growth limited by the source or the sink tissues?

In **paper IV**, to investigate the role of sucrose synthase (SUS) in cellulose biosynthesis of *Arabidopsis thaliana*. The central question of this study was:

- Is SUS activity required for supplying the substrate UDP-glucose for cellulose biosynthesis in *Arabidopsis*?

3. Material and methods

3.1 Arabidopsis and aspen as model organisms

During this PhD thesis work, Arabidopsis (*Arabidopsis thaliana*), European aspen (*Populus tremula*) and hybrid aspen (*Populus tremula x tremuloides*) were used as model organisms.

Arabidopsis, also known as thale cress or mouse-ear cress, is an annual herbaceous plant that can complete its entire lifecycle in six weeks (Meinke *et al.*, 1998). Its small size, fast growth, and availability of various types of mutants make it an ideal plant to grow and study in laboratory conditions. After its relatively small genome of about 125 Mbp was sequenced in 2000, Arabidopsis cemented its place as the main model organism of plant science (The Arabidopsis Genome, 2000; Krämer, 2015). Even though Arabidopsis is herbaceous, its hypocotyl undergoes secondary growth under short day conditions, which makes it a suitable model for studying the development and formation of secondary xylem (Chaffey *et al.*, 2002). Results from experiments performed on Arabidopsis are often extrapolated to trees. However, the small size and annual lifestyle of Arabidopsis mean that not all of its growth and developmental processes are comparable with perennial trees, which is why tree model species are needed as well.

Members of the *Populus* genus are widely used as model species for trees. As pioneer species they are fast-growing and propagate clonally via root-shoots, which are properties that make it easy to amplify them from cuttings in laboratory conditions. The North American black cottonwood (*Populus trichocarpa*) was the first woody species whose whole genome was sequenced, which further strengthened its role as a major deciduous woody model plant (Tuskan *et al.*, 2006). The genomes of both *Populus trichocarpa* and its relative European aspen (*Populus tremula*) are well conserved and of

a moderate size, approximately 480 Mbp (Tuskan *et al.*, 2006; Lin *et al.*, 2018). A wide array of genome editing tools such as *Agrobacterium*-mediated transformation, RNAi and CRISPR/cas9 have been established for use on *Populus* species, and the existence of curated databases containing genetic and transcriptional information facilitate the comparison of experimental results.

Populus species can hybridize with each other. A particular *Populus tremula x tremuloides* hybrid aspen clone called “T89” originating from Czech Republic is widely used in experimental work, mainly due to its higher transformation efficiency compared to *P. tremula* (Nilsson *et al.*, 1992; Ellis *et al.*, 2010).

In this PhD study, I collected samples of field-grown European aspen for DNA extraction and generation of a sequencing library in papers I and II. In paper III, I studied hybrid aspen trees. CRISPR/cas9-mediated gene modification was used to generate starchless mutant lines lacking *PGM1* and *PGM2* activity. Two mutant lines, *pgm1pgm2* line1 and line 2, and the wild-type T89 were grown in controlled growth conditions in greenhouse and in an automated phenotyping facility. In some of the experiments, the growth conditions were manipulated by adjusting the daylength and light intensity, but otherwise the trees were well-watered and fertilized.

In paper IV I made use of the model plant *Arabidopsis*. The quadruple and sextuple knockout mutants *sus^{quad}*, *sus^{sext}-1* and *sus^{sext}-2* lacking sucrose synthase (SUS) isoforms were compared to the starchless *pgm* mutant and the Col-0 wild-type to investigate the role of SUS in cellulose biosynthesis.

3.2 DNA affinity purification sequencing (DAP-seq)

DNA affinity purification sequencing (DAP-seq) is a recently developed high-throughput screening method for discovering and mapping TF-DNA interactions as well as TF binding sites and binding motifs (O'Malley *et al.*, 2016; Bartlett *et al.*, 2017), which I utilized in projects I and II. An overview of the experimental protocol is shown in figure 7.

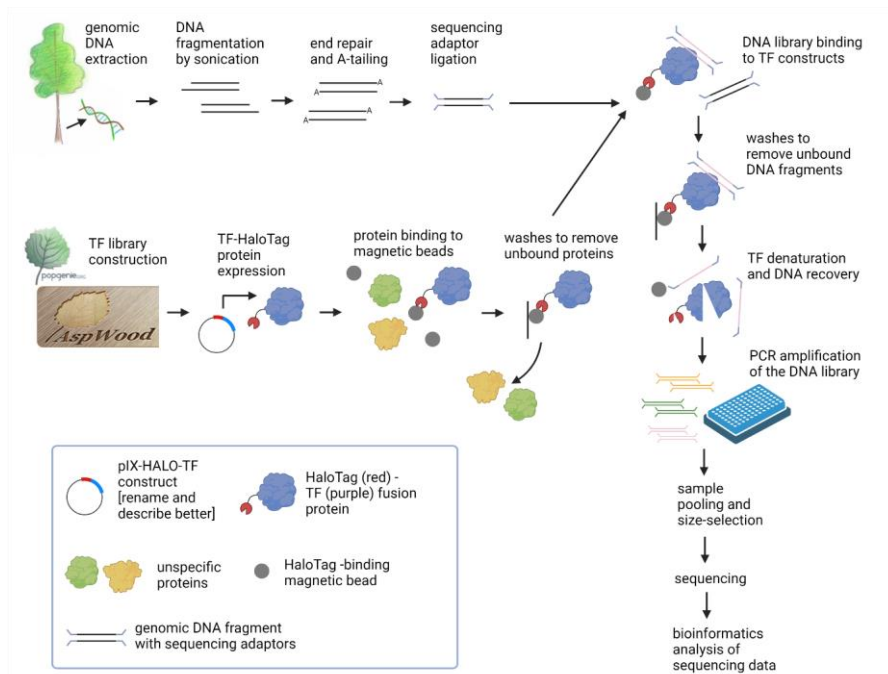


Figure 7. Overview of the DNA affinity purification sequencing (DAP-seq) experiment. The experimental procedure is based on O'Malley *et al.* (2016) and Bartlett *et al.* (2017). **Abbreviations:** TF, transcription factor. Figure created with BioRender.com

Briefly, the *Populus tremula* coding sequences (CDSs) for TFs of interest were retrieved from the PopGenIE database and cloned into the pIX-HALO plasmid, which contains the sequence coding for the 33 kDa HaloTag (Los *et al.*, 2008; England *et al.*, 2015; Sundell *et al.*, 2015). A cell-free expression system (a commercial kit using wheat germplasm cells) was used to express the TF-HaloTag -protein *in vitro*, and the proteins were bound to magnetic beads with the help of the HaloTag. A sequencing library constructed of fragmented *P. tremula* genomic DNA was added to the reaction, which allows the binding of TFs onto the DNA. Unspecific products were washed away, the TF proteins were denatured, and the remaining DNA was amplified with PCR. Tagged primers were used to enable the pooling of samples during sequencing. After pooling, the samples were purified using an automated DNA size selection system (BluePippin, Sage Science) and the

fragment size was confirmed with an automated electrophoresis instrument (Bioanalyzer, Agilent). Finally, the samples were sent for sequencing and the generated data was analysed in a bioinformatics pipeline.

A trimming algorithm was used to remove poor-quality reads, short fragments and sequencing adaptors from the raw sequencing data (Bolger *et al.*, 2014). After this, the trimmed reads were aligned to the *P. tremula* reference genome (Li, 2013; Schiffthaler *et al.*, 2019), sorted, and indexed (Danecek *et al.*, 2021). Reads from negative control samples containing only the empty pIX-Halo vector without a TF insert were merged into a single sample in order to generate a negative control, which was used to remove background noise in the following steps of the bioinformatics pipeline. Genomic regions that were significantly enriched with sequencing reads were defined as peaks, and they were identified by using a peak-calling programme on each TF sample (Zhang *et al.*, 2008). Regions where more than five samples had peaks as well as regions where the pIX-HALO negative control sample had peaks were removed from the data, after which the locations of the remaining peaks were intersected with that of gene bodies, transcription start sites, repeats and intergenic regions of *P. tremula* (Quinlan & Hall, 2010; Schiffthaler *et al.*, 2019). In paper II, scripts of the MEME Suite were used for discovery and mapping of motifs to the reference genome (Gupta *et al.*, 2007; Grant *et al.*, 2011; Bailey *et al.*, 2015), and the identified motifs were compared to those available in databases such as JASPAR and PlantTFDB (Fornes *et al.*, 2020; Tian *et al.*, 2020).

At the time of writing, the DAP-seq method has been applied in previous studies to chart TF-DNA binding events in annual plant species such as *Arabidopsis* (O'Malley *et al.*, 2016; Bartlett *et al.*, 2017), maize (Galli *et al.*, 2018; Ricci *et al.*, 2019; Dong *et al.*, 2020) and rice (Cerise *et al.*, 2021), and even in fungi (Wu *et al.*, 2020), bacteria (Trouillon *et al.*, 2020), and animals (de Mendoza *et al.*, 2019a; de Mendoza *et al.*, 2019b). DAP-seq has even been applied on a selection of woody species including eucalyptus (Brown *et al.*, 2019), persimmon (Yang *et al.*, 2019), apple (Chen *et al.*, 2020) and poplar (Ramos-Sánchez *et al.*, 2019; Yao *et al.*, 2020). These tree studies were targeted approaches focused on either single or a small number of TFs, and the effectivity of the method for large-scale screening studies in woody species was therefore unexplored prior to the work in this thesis.

Native genomic DNA is used as starting material for the DAP-seq DNA library, which means that secondary modifications such as methylations are

retained (Bartlett *et al.*, 2017). This helps in mapping regions which are accessible for binding *in planta*. However, as the native DNA is fragmented during library preparation, the chromatin structure and possible secondary modifications that can hinder or enhance TF binding are not taken into account in the experiment. To address this issue, we performed an additional Assay for Transposase-Accessible Chromatin sequencing (ATAC-seq) experiment to chart genomic regions with open chromatin footprints (Buenrostro *et al.*, 2013). These indicate sites where binding by TFs and other proteins is possible, and which could be potential promoter regions of genes. In paper I, the results from the ATAC-seq experiment were compared with the DAP-seq peaks to assess their overlap.

4. Results and discussion

4.1 Genome-wide map of transcriptional regulation in developing aspen wood (paper I)

In paper I we performed a large-scale DNA affinity purification sequencing (DAP-seq) screen on transcription factors (TFs) expressed in the developing wood of aspen (*Populus tremula*). The aim was to discover new TF targets and to chart the regulatory TF network orchestrating wood formation in trees. We combined the results of our DAP-seq screen with an Assay for Transposase-Accessible Chromatin sequencing (ATAC-seq) experiment to identify high-confidence TF binding sites and their genomic locations. Additionally, we used *in silico* network analysis methods to combine these results with gene expression data recorded in the AspWood database to chart both novel and previously identified TF-target interactions in developing wood. Finally, we integrated our results into the PlantGenIE database, providing a useful resource for future studies.

TFs of interest were selected from the AspWood database, which was generated using high-resolution RNA-seq data from sequential developing wood cryosections of aspen (Sundell *et al.*, 2017). The sections span the whole region of phloem and wood development, starting from cambial cells differentiating into xylem precursors and continuing to cell elongation and expansion, maturation and finally to the programmed cell death of xylem fibres and tracheary elements (Sundell *et al.*, 2017). The AspWood dataset revealed detailed spatial information on gene expression across developing wood and provided the foundation for the TF selection in this project.

The TFs were selected based on their expression patterns. Most of the TFs were chosen based on their centrality in the secondary cell wall (SCW) co-expression network and expression patterns during wood development, especially in the regions of SCW formation, SCW deposition and xylem maturation. Additional TFs were included based on a previous study that identified unique expression patterns during tension wood formation (Seyfferth *et al.*, 2018). The selected TFs included both previously studied master regulators of SCW biosynthesis such as the *Populus* orthologs of VND6 and 7, SND1/NST3, MYB46 and MYB83, as well as lesser-known proteins classified as TFs based on sequence homology.

The coding sequences of the TFs were extracted from the PopGenIE database and cloned into the pIX-HALO plasmid vector, which contains the sequence coding for the 33 kDa HaloTag (Los *et al.*, 2008; England *et al.*, 2015; Yazaki *et al.*, 2016). The N-terminal -located HaloTag couples covalently and irreversibly with its specific ligand, which in the DAP-seq experiment was coupled to magnetic beads, helping with immobilization and preventing protein loss during the washing steps of protein purification (England *et al.*, 2015). The final TF library contained 661 pIX-HALO-TF constructs (paper I, supplementary table 1), which represent ca. 40 % of transcripts classified as TFs in the AspWood database and 27 % of the total of 2466 TF-coding loci of the model species *Populus trichocarpa*, a close relative of aspen (Sundell *et al.*, 2017; Tian *et al.*, 2020). The 49 TF families represented in the library cover 92 % of those present in the AspWood developing wood dataset (paper I, supplementary figure 1). Hence, our library provides a good overview of potential TF-DNA interactions in developing wood.

The DAP DNA library was prepared using genomic DNA extracted from scrapings of aspen developing wood, as it is expected to contain the cell-, tissue- and organ-specific methylation marks that can influence TF binding (O'Malley *et al.*, 2016; Huang & Ecker, 2018). During the DAP-seq screen, 653 of the 661 TFs (98.8 %) produced a total of 1 221 900 TF binding peaks, with peak counts varying between a minimum of 460 and maximum of 21 326 peaks per sample. The eight samples that were excluded from this number during the filtering process had peaks that either overlapped only with the negative control sample consisting of an empty pIX-HALO vector without a TF construct, causing these peaks to be classified as noise, or had TF binding peaks overlapping with those of many other samples. The

maximum peak number was in line with previously published DAP-seq results, where a maximum of 16 414 TF binding peaks were reported for eucalyptus, 19 867 for maize and between 20 000 and 28 323 for rice (Brown *et al.*, 2019; Du *et al.*, 2020; Cerise *et al.*, 2021; Wu *et al.*, 2021). However, due to the use of fragmented genomic DNA for library construction, these maximum peak numbers probably far exceed the number of accessible TF binding sites *in vivo*.

In addition to methylation, it is known that TF binding is affected by chromatin accessibility and that accessible binding sites are usually located on nucleosome-free chromatin regions, which differ between species and tissues (Sullivan *et al.*, 2014; Maher *et al.*, 2018; Brown *et al.*, 2019). To chart these open chromatin regions, we performed an Assay for Transposase-Accessible Chromatin sequencing (ATAC-seq) using nuclei isolated from aspen developing wood and investigated the intersection of the DAP-seq and ATAC-seq peaks. We noticed that all of the 653 peak-producing DAP-seq samples had peaks intersecting the open chromatin regions identified by ATAC-seq, resulting in a total of 207 787 intersecting peaks, which is ca. 17 % of all the DAP-seq peaks. Most of the open chromatin -located binding sites were found in the 5' untranslated regions (5'UTRs), followed by 3'UTRs, coding sequences (CDSs) and promoters (paper I, figure 1). Meanwhile, long terminal repeat (LTR) sequences and intergenic regions were the least peak-enriched (paper I, figure 1). Previous DAP-seq studies have reported similar patterns with most abundant TF binding in 5'UTR and the proximal promoter regions (O'Malley *et al.*, 2016; Galli *et al.*, 2018; Dong *et al.*, 2020; Cerise *et al.*, 2021), and depletion of TF binding peaks in the intergenic regions (Galli *et al.*, 2018). Similar results were reported even when charting the *Eucalyptus grandis* developing wood DNase I hypersensitivity sites that indicate open chromatin sites and thus genomic regions that are accessible for TF binding, with most of these sites located in 5'UTR, promoters and exons, and depletion in the 3'UTR and intergenic regions (Brown *et al.*, 2019). In summary, we report that combining the DAP-seq results with ATAC-seq charting of open chromatin regions helps in identifying putative high-confidence and biologically relevant TF binding sites for further validation.

Next, we used the Inferelator algorithm (Arrieta-Ortiz *et al.*, 2015) to chart the interactions and connections in the TF regulatory network of aspen developing wood. With the help of RNA-seq expression data in the

AspWood database, we selected a set of 93 TFs and 559 target genes that were clearly turned on or off during wood formation and used them together with the DAP/ATAC-seq data for prediction and ranking of TF-target interactions, and finally for regulatory network construction. After filtering the datasets for interactions with a high enough confidence score, the constructed transcriptional regulatory network contained a total of 89 TFs and 510 target genes and included both novel and previously published TF-target gene interactions (paper I, figure 2a, supplementary table 2). The novel interactions can be used as starting points for future studies to help in unravelling new regulatory connections in wood formation, and the previously published ones can be used to verify and increase the robustness of the TF-target connections we report.

To illustrate the different kinds of TF-target interactions captured by DAP-seq, we highlight two previously published TF-target interactions that are also present in our network (paper I, figure 2b and 2c). The TF MYB20 and its inferred target are co-expressed and have similar expression patterns (paper I, figure 2b), with the expression of MYB20 peaking in the beginning of SCW deposition and most likely activating the expression of its target, which follows closely behind. The expression patterns of VND6-A1 and its target (paper I, figure 2c) however do not follow this co-expression pattern, but instead their peaks are separate. The TF expression reaches its peak in the middle of cell expansion, decreases, and rises again to a smaller peak during SCW deposition. Meanwhile, the expression of its target seems to be repressed during cell expansion, but it increases to a high peak during SCW deposition. The *in vivo* -existence of this putative interaction should still be verified in a later experimental study, but our results indicate that relying on TF-target co-expression alone when searching for new putative interactions might cause one to miss interesting candidates. This is further supported by an analysis of the AspWood gene expression profiles, which shows that TFs and their targets tend to belong to different co-expression clusters (paper I, table 1).

Finally, to make our results more accessible for use in future research, we integrated the DAP-seq peaks and ATAC-seq open chromatin regions as new tracks into the JBrowse *Populus* genome browser available in <https://plantgenie.org/> (paper I, figure 3). Our update to the database, which already contained the AspWood developing wood RNA-seq expression data, provides a useful resource for future research projects on wood formation.

Originally, the aim of this study was to also investigate the TF binding motifs on the genomic DNA to identify both previously studied and novel motifs. We wanted to use any previously identified motifs found in our dataset for additional verification of our DAP-seq interactions, and to use any novel motifs identified as a starting point for studying and characterizing possibly new TF-target relationships in the developing wood and SCW transcriptional regulatory network. The specificity of both known and novel motifs could have been tested for example by producing synthetic promoters with variants of the predicted binding site in order to test the binding specificity of the TF, and/or synthetic promoters containing multiple copies of the predicted binding site in order to test if this would have had an effect on the level of target gene expression. Unfortunately, it was not possible to derive reliable binding motifs from the data, likely because of limiting sequencing depth (paper II). Despite this shortcoming, the TF binding sites are dependable and provide a starting point for further analysis.

4.2 A practical guide for DAP-seq data analysis in plant genomes (paper II)

In paper II, we review the bioinformatics methods used for analysing data from DAP-seq experiments and identify a lack of clear and established data analysis guidelines for the method. We present an improved data analysis pipeline as well as guidelines with quality control checks that aim for better experimental reproducibility and good scientific practice.

First, we performed a literature review on all the 65 currently available publications where the DAP-seq method has been used (paper II, table 1). The majority of these studies have been performed on plants and with a focus on well-studied model species such as maize, rice and Arabidopsis. Although the DAP-seq method is well suited for large-scale screening of TF networks, only three publications described screens of over 100 TFs while most of the studies are focused on characterizing interactions of single or a few TFs (paper II, table 1). During the review process we noticed that many of the studies fail to report the exact parameters that were used for data analysis. For example, 14 of the publications did not report which program they used for aligning the reads to a reference genome after sequencing, and the algorithm that was used for peak calling was not specified in six of the studies

(paper II, table 1). Furthermore, 32 of the studies that had specified the peak caller did not elaborate on which version of the program or which parameters were used, making the analysis impossible to repeat and thus not complying with the FAIR data principles of Findability, Accessibility, Interoperability, and Reusability (Wilkinson *et al.*, 2016).

The data generated in DAP-seq studies is similar to that produced in ChIP-seq (O'Malley *et al.*, 2016), which allows the use of existing scripts and pipelines that in their original purpose have well established quality control checks and data analysis guidelines (Bailey *et al.*, 2013). However, such checks and guidelines do not yet exist specifically for the processing of DAP-seq data. Therefore, we decided to use our own aspen DAP-seq dataset (paper I) and two publicly available datasets for a comparative analysis as well as for highlighting especially important parts of the pipeline.

We selected the previously published Arabidopsis (O'Malley *et al.*, 2016) and maize (Galli *et al.*, 2018) DAP-seq datasets for the comparative study. The genomes of these two species are different from that of aspen, which is of a moderate size and very heterozygous, with a moderate number of repeat regions (Lin *et al.*, 2018). Arabidopsis is a species with a small (ca. 125 Mbp) and homozygous genome with a low repeat content, while the genome of maize is larger (ca. 2300 Mbp), heterozygous and repeat-rich (Gaut *et al.*, 2000; The Arabidopsis Genome, 2000; Michael & VanBuren, 2015). We hypothesized that the differences in genome characteristics of the three species could have an impact on peak calling and investigated this by running MACS2 (Zhang *et al.*, 2008) on all the datasets (paper II, figure 1a-d). We noticed that fewer peaks were identified in Arabidopsis and aspen than maize, but that adjusting the parameters for peak identification made the peak counts between the species more comparable (paper II, figure 1d).

After mapping peaks to the reference genome, an algorithm such as MEME-ChIP (Machanick & Bailey, 2011) is usually used to search for TF binding motifs. The identified motifs can then be compared to previously identified motifs published in a curated database such as the JASPAR CORE collection (Fornes *et al.*, 2020). We inspected the length of the motifs in this database and noticed that the majority of the listed plant motifs were between 5-15 bp long (paper II, figure 2). Interestingly, if one uses the default parameters in the MEME-ChIP peak calling program (Machanick & Bailey, 2011; Bailey *et al.*, 2015), the maximum length of motifs identified is 15 bp as well. This could explain, at least in part, the motif length distribution in

the database and is something the scientist should be aware of when interpreting results.

According to the MEME-ChIP analysis guidelines, it is common to hide repeat regions by replacing them with 'N' before searching for DNA binding motifs in a dataset (Machanick & Bailey, 2011), https://web.mit.edu/meme_v4.11.4/share/doc/meme-chip.html). This treatment is called hardmasking. However, many plant genomes such as maize and aspen are rich in repeat regions and long terminal repeat (LTR) sequences (Michael & VanBuren, 2015), and these regions are thought to be important sources for new TF binding motifs (Naito *et al.*, 2009; Zhao *et al.*, 2022). Thus, we hypothesized that if a such genome is hardmasked, many sites containing TF binding motifs might be missed during the analysis. We noticed that more motifs could be identified when the unmasked genome of aspen was used for motif calling instead of the hardmasked one (paper II, figure 3a), and that about a third of the mapped motif occurrences intersected a repeat region (paper II, figure 3b), confirming our hypothesis and suggesting that the different genome characteristics of different plant species should be considered during data analysis.

The aspen and Arabidopsis datasets were also compared in regard to the percentage of TF binding peaks overlapping to the highest-ranking motif identified by MEME (paper II, figures 7 and 8). Using the same default analysis parameters on the two species resulted in less motifs identified in the aspen samples than in Arabidopsis (paper II, figure 7 and 8a), and adjusting the parameters only increased the number of samples with identified motifs (paper II, figure 8b and c). Next, we studied the peak signal strength and the overlap between peaks and motifs in all the three datasets (paper II, figure 9). For Arabidopsis, the overlap between called peaks and JASPAR motifs identified in the dataset was high (ca. 75 %), while in maize this statistic was much lower, between 2-40 % (paper II, figure 9a and c). Despite the low overlap, these data were used to define the maize motifs that were entered in the JASPAR CORE database and that are now used for further studies by the scientific community. For aspen, the peak-motif overlap was very poor (paper II, figure 9e), explaining our difficulties in calling motifs in this dataset. The low overlap could be a result of low signal to noise ratio in our data as was likely due to insufficient sequencing depth. The use of this analysis therefore represents an important quality control step

to help inform whether sufficient sequencing data has been generated for a DAP-seq library.

Finally, we studied sample clustering based on motif similarity (paper II, figure 10). While the Arabidopsis TF binding motifs clustered together based on motif similarity and TF family (paper II, figure 10a), the aspen samples formed clusters containing TFs from several families (paper II, figure 10c). We suspect this is a further indication of poor signal to noise ratio in the aspen dataset and follows from the poor motif calling.

Put together, this study highlights potential pitfalls of the DAP-seq analysis pipeline and suggests checks that should be performed to ensure good data quality.

4.3 Aspen growth is not limited by starch reserves (paper III)

In paper III we investigate carbon partitioning in aspen trees and focus on the role of starch in aspen growth and carbon storage. We reveal that carbon availability is not limiting aspen tree growth under greenhouse growth conditions and that the trees utilise a passive storage mechanism. Finally, we hypothesize that aspen tree growth under greenhouse conditions is limited by the activity of sink tissues.

First, we identified two plastidial *PHOSPHOGLUCOMUTASE* genes (*PGM1* and *PGM2*) in the hybrid aspen (*Populus tremula x tremuloides*) genome (paper III, supplementary figure 1). By using CRISPR/cas9, we generated low-starch mutant aspen lines containing premature stop codons in the second exons of both genes (paper III, figure 1a). In leaves, the PGM enzyme converts glucose-6-phosphate (Glc-6-P) to Glc-1-P and its activity is essential in the pathway leading to ADP-Glc, which is the main substrate for starch biosynthesis (Pfister & Zeeman, 2016). Mutants lacking *pgm* have earlier been generated and characterized in several herbaceous plant species, including Arabidopsis (Caspar *et al.*, 1985). To our knowledge, this is the first study on *pgm* mutants in a woody species to elucidate the role of starch during tree growth.

The *pgm1pgm2* mutant trees were verified as lacking starch by iodine staining of fully expanded source leaves, phloem tissue and root tips, as well as in a quantitative enzymatic assay of the leaves (paper III, figure 1b-e). A mild growth phenotype with hanging leaves resulting in a slightly reduced

canopy area was observed in both *pgm1pgm2* mutant lines (paper III, figure 2b and 2d). Height growth rate (paper III, figure 2a), stem thickness, wood density as well as the biomass of leaves, stems and roots were the same as that of the wild-type (paper III, supplementary table 1) when the trees were grown in an 18-h/6-h day/night cycle. Additionally, no significant differences were observed between the *pgm1pgm2* lines and the wild-type in wood carbohydrate and lignin content or carbohydrate:lignin ratio (paper III, supplementary figure 3). These results lead us to the conclusion that lack of starch in the aspen *pgm* mutants causes no major defects in tree growth under long-day conditions.

Next, we investigated the tree growth in short-day conditions, as previous studies have shown that *pgm* mutants of *Arabidopsis* have considerably slower growth rate and produce less biomass than the wild-type when grown in a short day photoperiod (Caspar *et al.*, 1985). Although dormancy is induced in the wild-type aspen genotype used in the study in daylengths shorter than 15 h, it will still continue to grow for ca. 3-4 weeks after moving to short day (Howe *et al.*, 1996; Olsen *et al.*, 1997; Böhlenius *et al.*, 2006). In contrast to the study on *Arabidopsis*, no differences in growth rate were observed when the *pgm1pgm2* trees were grown in 14-h/10-h or 8-h/16-h day lengths (paper III, Supplementary figure 4). Combined, the normal growth rate in short-day conditions together with the results from the long-day experiment show that starch is not essential for aspen growth.

Previous studies have reported diel patterns in non-structural carbon (NSC) concentrations of herbs and tree species (Gibon *et al.*, 2004b; Graf *et al.*, 2010; Tixier *et al.*, 2018). I measured the contents of starch and soluble sugars in fully expanded, mature source leaves of wild-type aspen trees at different timepoints, and like in the previous studies, observed a diel pattern in starch turnover in the aspen leaves. The levels of starch were highest at the end of day and lowest at the end of night (paper III, figure 3a). We also observed a reduction in leaf sucrose content between the end of day and the end of night in both wild-type and the *pgm* mutants (paper III, figure 3c), which combined with the lack of a major growth phenotype indicates that the sucrose pool alone may be enough to supply carbon for growth and essential metabolic processes in *pgm1pgm2* during the night. When I compared the soluble sugar concentrations of fully expanded source leaves of the *pgm1pgm2* lines and the wild-type, harvested from long-day grown trees in the middle of the light period, I noticed no statistically significant

differences in either glucose, fructose or sucrose (paper III, figure 3b). This was in contrast to the *Arabidopsis pgm* mutant, which accumulates more soluble sugars than the wild-type in the light (Gibon *et al.*, 2006). Additionally, we selected three marker genes of carbon depletion (Tarancón *et al.*, 2017) and analysed their expression in source leaves of wild-type and *pgm1pgm2* trees at the end of 16-h night using quantitative real-time PCR. No significant differences in the marker gene expression were observed between *pgm* and the wild-type (paper III, figure 3e). Together with the previous data, these results highlight that sucrose and starch are used in aspen during the night, but that starch is not a critical compound.

Since the starch biosynthesis pathway is blocked in the mutant trees, and if all other aspects were equal, more assimilated carbon might be available for other processes such as growth. As this was not the case, we hypothesized that there could be differences in the CO₂ assimilation between the *pgm1pgm2* and the wild-type trees. This was studied by measuring the CO₂ assimilation in trees that were grown under different light intensities. Up to ca. 30 % reduced CO₂ uptake was observed in the *pgm1pgm2* mutant lines compared to the wild-type under irradiances higher than 100 $\mu\text{mol quanta m}^{-2} \text{s}^{-1}$ in trees that had been growing under light intensities of both 180-200 $\mu\text{mol quanta m}^{-2} \text{s}^{-1}$ and 500 $\mu\text{mol quanta m}^{-2} \text{s}^{-1}$ (paper III, figure 4a and 4c). However, no significant differences were noted in leaf transpiration (paper III, figure 4b and 4d) which was used as a proxy for stomatal conductance, which indicates that the reduced CO₂ intake is not due to reduced stomatal conductance. Additionally, we measured chlorophyll content and photosynthetic parameters of the source leaves to find out if the reduced CO₂ assimilation would be explained by impaired light absorption. The chlorophyll content of *pgm1pgm2* was increased compared to the wild-type while the other photosynthesis parameters were similar (paper III, supplementary table 2), and we conclude that this does not explain the diminished CO₂ assimilation. All in all, the combination of reduced CO₂ intake with normal growth and wood density in the *pgm1pgm2* trees suggests that their growth is not limited by carbon assimilation under benign greenhouse growth conditions. This would indicate that aspen tree growth is limited by processes downstream from the CO₂-assimilating source tissues, suggesting sink activity as the growth-limiting factor.

Previous studies on the aspen tree have indicated that starch reserves of the stem and roots are important for supplying carbon for new growth during

the spring as well as for resprouting after herbivory (Bollmark *et al.*, 1999; Landhüsser & Lieffers, 2003; Gough *et al.*, 2010; Regier *et al.*, 2010), indicating that the lack of starch might hamper these processes. We induced growth cessation, bud set and dormancy in both wild-type and the *pgm1pgm2* lines by moving them from long-day conditions with 18-h light period into short-day conditions with a 14-h day light period for ten weeks. After this the trees were subjected to ten weeks of cold temperature (+4 °C), which was followed by returning them to 18-h long day conditions and warm temperature (22 °C during the light period, 18 °C during the dark) to induce dormancy break and bud flush. No differences were observed during the dormancy nor during bud flush (paper III, supplementary figure 4), which indicates that starch is not critical for these processes in aspen trees growing in benign greenhouse growth conditions. In the future, it would be very interesting to grow these mutants in a field experiment over several years in order to see if, and potentially how, their growth and survival over the changing seasons would be affected by the lack of starch reserves.

According to the current understanding, the herbaceous *Arabidopsis* can actively adjust its metabolism between storage and growth by upregulating carbon storage as starch, especially when grown in short photoperiods or where carbon uptake is limited (Gibon *et al.*, 2004b; Smith & Stitt, 2007; Gibon *et al.*, 2009). An active carbon storage strategy was suggested also for the conifers Norway spruce and Scots pine based on experiments performed under stress conditions and described in more detail in section 1.4 of this thesis (Hartmann *et al.*, 2015; Galiano *et al.*, 2017; Huang *et al.*, 2021). In contrast, the deciduous large-leaved linden (*Tilia platyphyllos*) was suggested to employ a passive overflow strategy in a study performed under drought stress (Galiano *et al.*, 2017). However, these results might not represent the storage strategies for trees growing in benign growth conditions. Based on our study it seems that the hybrid aspen tree uses a passive overflow carbon storage strategy to store carbon into starch, at least when grown in the greenhouse with no competition and an optimised amount of water and nutrients. Sampling wild-type aspen trees grown in field conditions and/or under for example limited water or nutrients could give us more information on if a passive carbon storage strategy is used even then, or if the aspen tree is able to actively adjust its metabolism like *Arabidopsis* and the conifer species in the abovementioned studies.

4.4 Sucrose synthase activity is not required for cellulose biosynthesis in Arabidopsis (paper IV)

In paper IV we address the debate on whether sucrose synthase (SUS) enzymes are required for cellulose biosynthesis in *Arabidopsis thaliana*. We show that mutant plants lacking all six sucrose synthase isoforms grow normally, have no defects in stem anatomy and have leaf and stem cellulose contents comparable to the wild-type plants. All in all, our results show that SUS activity is not needed for cellulose biosynthesis in Arabidopsis.

UDP-glucose (UDP-Glc) is the substrate of cellulose synthase (CesA) enzymes, which produce the major cell wall component cellulose. A popular model based on studies on several plant species suggests that SUS could directly supply the CesA complexes with the UDP-Glc substrate (Haigler *et al.*, 2001; Stein & Granot, 2019). This model has been challenged by conducting studies on Arabidopsis mutant plants lacking four of the six SUS isoforms (Barratt *et al.*, 2009), but these conclusions were questioned by the suggestion that the activity of the remaining two isoforms could be enough to produce necessary amounts of UDP-Glc for cellulose biosynthesis (Baroja-Fernández *et al.*, 2012).

Recently, Fünfgeld *et al.* (2022) generated two Arabidopsis sextuple mutant lines which lack all the six SUS isoforms (*sus1sus2sus3sus4sus5sus6*; *sus^{sext}*, lines -1 and -2). In their study, these mutants were used to investigate the role of SUS in starch biosynthesis (Fünfgeld *et al.*, 2022). In paper IV these same lines were used to assess the possible role of SUS in cellulose biosynthesis. When the mutants were grown in the greenhouse under long day conditions (16 h day, 8 h night), both *sus^{sext}-1* and *sus^{sext}-2* grew like the Col-0 wild-type without a visible growth phenotype (paper IV, figure 1a). We also grew the quadruple mutant *sus^{quad}* and in accordance with previously published results saw no growth phenotype (Barratt *et al.*, 2009). The stems of these plants were sectioned, dyed with toluidine blue and studied under microscope, and no anatomical defects were detected in any of the *sus* mutants (paper IV, figure 1b). Abnormalities in secondary cell wall biosynthesis often lead to thinner cell walls or a collapsed xylem phenotype (Taylor *et al.*, 2000; Brown *et al.*, 2005), and we interpreted the lack of such disturbances in the *sus^{sext}* and *sus^{quad}* plants as an indication of normal secondary cell wall biosynthesis. Additionally, the presence of possible primary cell wall defects was investigated by comparing the hypocotyl lengths of etiolated seedlings

(paper IV, figure 1c and 1d), but even here no visible phenotypes or differences in the length were observed between the mutants and the wild-type.

To investigate potential differences in cellulose content that might not have been visible on the anatomical or phenotypical level, we measured the cellulose content of both stems and rosette leaves. No differences between the mutant lines and the wild-type were observed (paper IV, figure 2a and 2b). However, when we studied the pool of the cellulose biosynthesis substrate UDP-Glc using a newly developed mass spectrometry method, we noticed that the rosette leaf UDP-Glc pool was in fact larger in the *sus* mutants than in the wild-type, producing a statistically significant difference for both *sus^{sex}* lines (paper IV, figure 2c). These results are surprising as the lack of SUS in the mutants prevents the direct catabolism of sucrose into UDP-Glc and Fru, but they indicate the upregulation of an alternative pathway to produce UDP-Glc. A likely candidate for this would be the multi-step pathway of sucrose catabolism via INV activity, conversion into Glc- or Fru-6-P via hexo- or fructokinases, respectively, interconversion between the two by phosphoglucosomerase (PGI), which is followed by first the conversion of Glc-6-P into Glc-1-P by phosphoglucomutase (PGM), and finally by the production of UDP-Glc in a reaction catalysed by UDP-glucose pyrophosphorylase (UGPase). As an additional control of the UDP-Glc measurements we grew the starchless *pgm* mutant and measured the UDP-Glc content of its rosette leaves at the end of night (paper IV, figure 2d). In line with previously published results, the UDP-Glc concentration of the *pgm* rosette leaves was lower than that of the wild-type plants (Gibon *et al.*, 2006).

In summary, this study concludes the discussion on the specific role of SUS in cellulose biosynthesis by establishing that SUS is not needed for cellulose biosynthesis in Arabidopsis. However, it remains possible that SUS participates in cellulose biosynthesis in the wild-type plants through its contribution to the cytosolic UDP-glucose pool. This is supported by the slightly increased cellulose content of transgenic *Populus* trees expressing a cotton SUS under a wood-specific promoter (Coleman *et al.*, 2009). It also seems likely that SUS could be critical for cellulose biosynthesis in some specific cell types, such as in cotton seed fibres (Ruan *et al.*, 2003). It would be interesting to generate multiple SUS deletion mutants also in *Populus* species, which have 15 *SUS* genes (Tuskan *et al.*, 2006; An *et al.*, 2014). A recent study describes the generation of octuple (8x) tobacco and duodecuple

(12x) *Arabidopsis* mutant plants within only one generation by using multiplex genome editing with a highly optimized CRISPR/cas9 system (Stuttman *et al.*, 2021), which gives hope that similar methods might be applicable to facilitate research even on woody species in the future.

5. Conclusions and future perspectives

In the four projects of this PhD thesis, I have studied factors involved in carbon distribution between the central processes of growth and storage. My aims were to provide new information on carbon allocation, tree growth and source-sink relationships on both transcriptional and whole-plant level.

The transcriptional regulatory network in developing wood of European aspen was charted in **paper I** of this thesis. We report that the open chromatin regions charted via ATAC-seq help in identifying DAP-seq transcription factor (TF) binding sites that are likely to be accessible for binding *in vivo*, and that the majority of the DAP-seq binding sites intersecting the open chromatin regions are found in the 5'UTR, indicating that the regions closest to the transcription start site are important for regulatory binding events. We constructed a developing wood transcriptional regulatory network by combining the DAP-seq peak data with gene expression data from the AspWood database in an *in silico* analysis. This network identified both previously published as well as novel TF-target gene interactions, validating our results and providing interesting starting points for future studies on wood formation. Our results were integrated into the publicly available PlantGenIE web resource, from where they can be accessed in order to provide starting points for future research projects in transcriptional regulation of wood formation.

In **paper II**, we take a critical look at the bioinformatics analysis methods used for the processing of DAP-seq data. We perform a literature review on all currently available publications where the method has been used, identify present and potential problems, and finally present an improved analysis pipeline where we also suggest quality control checks to be performed in future experiments.

In **paper III**, we produced low starch hybrid aspen trees lacking the plastidial isoforms of *PGM1* and *PGM2*. Such mutants were first identified in *Arabidopsis* ca. 40 years ago, but ours is the first study on *pgm* mutants in a woody species, providing a valuable resource for future experiments to elucidate the role of starch in trees. As we observed no major growth defects in the mutant trees compared to the wild-type, we conclude that starch is not an essential carbon reserve for the growth and survival of young aspen trees in benign greenhouse conditions. Additionally, our results suggest a passive overflow starch storage strategy in aspens and indicate that aspen tree growth is limited by the activity of sink tissues instead of the CO₂-assimilating source leaves. This result is in line with the literature supporting the sink limitation hypothesis, but it is expected that the understanding of both source-sink dynamics as well as tree carbon storage strategies will continue to evolve as new studies are performed.

In the future, it would be interesting to grow the *pgm* trees under different stress conditions and for a longer period in the field, in order to study their growth and survival under natural conditions. For example, aspen might be able to actively adjust their storage strategy between active and passive depending on environmental cues, or there might be differences in storage strategy between young saplings and more mature trees. Performing a ¹³CO₂ labelling experiment on the *pgm* mutants as well as unmodified wild-type trees could shed light on carbon partitioning in the source leaf as well as the whole tree.

The scientific community has for long debated on the necessity of sucrose synthase (SUS) enzymes in supplying the UDP-glucose substrate for cellulose biosynthesis. This question was addressed in **paper IV**, where we compared the growth, anatomy, and cellulose contents of wild-type *Arabidopsis* and *sus^{sex1}* mutant plants lacking all six SUS isoforms. As no growth defects were observed in the *sus^{sex1}* mutants and as the cellulose contents of their leaves and stems were comparable to those of the wild-type, we concluded that SUS activity is not required for cellulose biosynthesis in *Arabidopsis*, resolving the long-standing debate.

The studies presented in **papers III and IV** are focused on plant growth and carbon allocation on the levels of primary metabolism and cell wall biosynthesis. However, it is not yet known how the expression of the key primary metabolism genes is regulated, which provides questions for future studies. Using the DAP-seq transcription factor results and the

bioinformatics guidelines suggested in **papers I and II**, combined with for example a Yeast One-Hybrid study, it should be possible to identify putative transcriptional regulators of these genes in the developing wood. Identifying such TF-DNA interactions would help in completing the picture of transcriptional regulation of primary metabolism and give more information on how transcriptional regulators influence carbon allocation into wood and the components of its secondary cell walls. This would provide putative new control points for genetic modification and breeding for desired wood traits, as well as contribute to our understanding on how trees grow.

References

- Ainsworth EA, Long SP. 2005.** What have we learned from 15 years of free - air CO₂ enrichment (FACE)? A meta - analytic review of the responses of photosynthesis, canopy properties and plant production to rising CO₂. *New Phytologist* **165**(2): 351-372.
- Allen H, Wei D, Gu Y, Li S. 2021.** A historical perspective on the regulation of cellulose biosynthesis. *Carbohydrate polymers* **252**: 117022.
- Alon U. 2007.** Network motifs: theory and experimental approaches. *Nature Reviews Genetics* **8**(6): 450-461.
- Amor Y, Haigler CH, Johnson S, Wainscott M, Delmer DP. 1995.** A membrane-associated form of sucrose synthase and its potential role in synthesis of cellulose and callose in plants. *Proceedings of the National Academy of Sciences* **92**(20): 9353-9357.
- An X, Chen Z, Wang J, Ye M, Ji L, Wang J, Liao W, Ma H. 2014.** Identification and characterization of the *Populus* sucrose synthase gene family. *Gene* **539**(1): 58-67.
- Arrieta-Ortiz ML, Hafemeister C, Bate AR, Chu T, Greenfield A, Shuster B, Barry SN, Gallitto M, Liu B, Kacmarczyk T, et al. 2015.** An experimentally supported model of the *Bacillus subtilis* global transcriptional regulatory network. *Mol Syst Biol* **11**(11): 839.
- Bahaji A, Li J, Sanchez-Lopez AM, Baroja-Fernandez E, Munoz FJ, Ovecka M, Almagro G, Montero M, Ezquer I, Etxeberria E, et al. 2014.** Starch biosynthesis, its regulation and biotechnological approaches to improve crop yields. *Biotechnol Adv* **32**(1): 87-106.
- Bailey T, Krajewski P, Ladunga I, Lefebvre C, Li Q, Liu T, Madrigal P, Taslim C, Zhang J. 2013.** Practical guidelines for the comprehensive analysis of ChIP-seq data. *PLoS computational biology* **9**(11): e1003326.
- Bailey TL, Boden M, Buske FA, Frith M, Grant CE, Clementi L, Ren J, Li WW, Noble WS. 2009.** MEME SUITE: tools for motif discovery and searching. *Nucleic Acids Res* **37**(Web Server issue): W202-208.
- Bailey TL, Johnson J, Grant CE, Noble WS. 2015.** The MEME suite. *Nucleic acids research* **43**(W1): W39-W49.
- Barnes WJ, Anderson CT. 2018.** Cytosolic invertases contribute to cellulose biosynthesis and influence carbon partitioning in seedlings of *Arabidopsis thaliana*. *The Plant Journal* **94**(6): 956-974.
- Baroja-Fernandez E, Munoz FJ, Akazawa T, Pozueta-Romero J. 2001.** Reappraisal of the currently prevailing model of starch biosynthesis in photosynthetic tissues: a proposal involving the cytosolic production of

- ADP-glucose by sucrose synthase and occurrence of cyclic turnover of starch in the chloroplast. *Plant and Cell Physiology* **42**(12): 1311-1320.
- Baroja-Fernández E, Muñoz FJ, Li J, Bahaji A, Almagro G, Montero M, Etxeberria E, Hidalgo M, Sesma MT, Pozueta-Romero J. 2012.** Sucrose synthase activity in the *sus1/sus2/sus3/sus4* Arabidopsis mutant is sufficient to support normal cellulose and starch production. *Proceedings of the National Academy of Sciences* **109**(1): 321-326.
- Barratt DP, Derbyshire P, Findlay K, Pike M, Wellner N, Lunn J, Feil R, Simpson C, Maule AJ, Smith AM. 2009.** Normal growth of Arabidopsis requires cytosolic invertase but not sucrose synthase. *Proceedings of the National Academy of Sciences* **106**(31): 13124-13129.
- Barron AR, Wurzburger N, Bellenger JP, Wright SJ, Kraepiel AML, Hedin LO. 2008.** Molybdenum limitation of symbiotic nitrogen fixation in tropical forest soils. *Nature Geoscience* **2**(1): 42-45.
- Bartlett A, O'Malley RC, Huang SC, Galli M, Nery JR, Gallavotti A, Ecker JR. 2017.** Mapping genome-wide transcription-factor binding sites using DAP-seq. *Nat Protoc* **12**(8): 1659-1672.
- Bennetzen JL, Wang X. 2018.** Relationships between gene structure and genome instability in flowering plants. *Molecular plant* **11**(3): 407-413.
- Benson AA. 1951.** Identification of ribulose phosphates in $C^{14}O_2$ photosynthesis products. *Journal of the American Chemical Society* **73**(6): 2971-2972.
- Bieniawska Z, Paul Barratt DH, Garlick AP, Thole V, Kruger NJ, Martin C, Zrenner R, Smith AM. 2007.** Analysis of the sucrose synthase gene family in Arabidopsis. *Plant J* **49**(5): 810-828.
- Bilas R, Szafran K, Hnatuszko-Konka K, Kononowicz AK. 2016.** Cis-regulatory elements used to control gene expression in plants. *Plant Cell, Tissue and Organ Culture (PCTOC)* **127**(2): 269-287.
- Bläsing OE, Gibon Y, Gunther M, Hohne M, Morcuende R, Osuna D, Thimm O, Usadel B, Scheible WR, Stitt M. 2005.** Sugars and circadian regulation make major contributions to the global regulation of diurnal gene expression in Arabidopsis. *Plant Cell* **17**(12): 3257-3281.
- Blumstein M, Richardson A, Weston D, Zhang J, Muchero W, Hopkins R. 2020.** A New Perspective on Ecological Prediction Reveals Limits to Climate Adaptation in a Temperate Tree Species. *Curr Biol* **30**(8): 1447-1453 e1444.
- Bocock PN, Morse AM, Dervinis C, Davis JM. 2008.** Evolution and diversity of invertase genes in *Populus trichocarpa*. *Planta* **227**(3): 565-576.
- Boerjan W, Ralph J, Baucher M. 2003.** Lignin biosynthesis. *Annu Rev Plant Biol* **54**: 519-546.
- Böhlenius H, Huang T, Charbonnel-Campaa L, Brunner AM, Jansson S, Strauss SH, Nilsson O. 2006.** CO/FT regulatory module controls timing of flowering and seasonal growth cessation in trees. *Science* **312**(5776): 1040-1043.

- Bolger AM, Lohse M, Usadel B. 2014.** Trimmomatic: a flexible trimmer for Illumina sequence data. *Bioinformatics* **30**(15): 2114-2120.
- Bollhöner B, Prestele J, Tuominen H. 2012.** Xylem cell death: emerging understanding of regulation and function. *J Exp Bot* **63**(3): 1081-1094.
- Bollmark L, Sennerby-Forsse L, Ericsson T. 1999.** Seasonal dynamics and effects of nitrogen supply rate on nitrogen and carbohydrate reserves in cutting-derived *Salix viminalis* plants. *Canadian Journal of Forest Research* **29**(1): 85-94.
- Bomal C, Bedon F, Caron S, Mansfield SD, Lévasseur C, Cooke JE, Blais S, Tremblay L, Morency MJ, Pavy N, et al. 2008.** Involvement of *Pinus taeda* MYB1 and MYB8 in phenylpropanoid metabolism and secondary cell wall biogenesis: a comparative in planta analysis. *J Exp Bot* **59**(14): 3925-3939.
- Bonice A, Haddad G, Gagnaire J. 1987.** Seasonal variations of starch and major soluble sugars in the different organs of young poplars. *Plant physiology and biochemistry (Paris)* **25**(4): 451-459.
- Bose SK, Francis RC, Govender M, Bush T, Spark A. 2009.** Lignin content versus syringyl to guaiacyl ratio amongst poplars. *Bioresource technology* **100**(4): 1628-1633.
- Boyko A, Molinier J, Chatter W, Laroche A, Kovalchuk I. 2010.** Acute but not chronic exposure to abiotic stress results in transient reduction of expression levels of the transgene driven by the 35S promoter. *New biotechnology* **27**(1): 70-77.
- Brill E, van Thournout M, White RG, Llewellyn D, Campbell PM, Engelen S, Ruan YL, Arioli T, Furbank RT. 2011.** A novel isoform of sucrose synthase is targeted to the cell wall during secondary cell wall synthesis in cotton fiber. *Plant Physiol* **157**(1): 40-54.
- Brown CL 1964.** The influence of external pressure on the differentiation of cells and tissues cultured in vitro. *The formation of wood in forest trees*: Elsevier, 389-404.
- Brown DM, Zeef LA, Ellis J, Goodacre R, Turner SR. 2005.** Identification of novel genes in *Arabidopsis* involved in secondary cell wall formation using expression profiling and reverse genetics. *Plant Cell* **17**(8): 2281-2295.
- Brown K, Takawira LT, O'Neill MM, Mizrachi E, Myburg AA, Hussey SG. 2019.** Identification and functional evaluation of accessible chromatin associated with wood formation in *Eucalyptus grandis*. *New Phytol* **223**(4): 1937-1951.
- Buckeridge MS, Vergara CE, Carpita NC. 1999.** The mechanism of synthesis of a mixed-linkage (1 → 3),(1 → 4) β-D-glucan in maize. Evidence for multiple sites of glucosyl transfer in the synthase complex. *Plant Physiology* **120**(4): 1105-1116.
- Buenrostro JD, Giresi PG, Zaba LC, Chang HY, Greenleaf WJ. 2013.** Transposition of native chromatin for fast and sensitive epigenomic

- profiling of open chromatin, DNA-binding proteins and nucleosome position. *Nature methods* **10**(12): 1213-1218.
- Cai B, Li C-H, Huang J. 2014.** Systematic identification of cell-wall related genes in *Populus* based on analysis of functional modules in co-expression network. *PLoS One* **9**(4): e95176.
- Canam T, Mak SW, Mansfield SD. 2008.** Spatial and temporal expression profiling of cell-wall invertase genes during early development in hybrid poplar. *Tree Physiology* **28**(7): 1059-1067.
- Carbone MS, Czimeczik CI, Keenan TF, Murakami PF, Pederson N, Schaberg PG, Xu X, Richardson AD. 2013.** Age, allocation and availability of nonstructural carbon in mature red maple trees. *New Phytol* **200**(4): 1145-1155.
- Carlson SJ, Chourey PS. 1996.** Evidence for plasma membrane-associated forms of sucrose synthase in maize. *Molecular and General Genetics MGG* **252**(3): 303-310.
- Carpita N, Tierney M, Campbell M 2001.** Molecular biology of the plant cell wall: searching for the genes that define structure, architecture and dynamics. *Plant Cell Walls*: Springer, 1-5.
- Caspar T, Huber SC, Somerville C. 1985.** Alterations in growth, photosynthesis, and respiration in a starchless mutant of *Arabidopsis thaliana* (L.) deficient in chloroplast phosphoglucomutase activity. *Plant Physiology* **79**(1): 11-17.
- Caspar T, Pickard BG. 1989.** Gravitropism in a starchless mutant of *Arabidopsis*. *Planta* **177**(2): 185-197.
- Cerise M, Giaume F, Galli M, Khahani B, Lucas J, Podico F, Tavakol E, Parcy F, Gallavotti A, Brambilla V, et al. 2021.** OsFD4 promotes the rice floral transition via florigen activation complex formation in the shoot apical meristem. *New Phytol* **229**(1): 429-443.
- Chaffey N, Cholewa E, Regan S, Sundberg B. 2002.** Secondary xylem development in *Arabidopsis*: a model for wood formation. *Physiol Plant* **114**(4): 594-600.
- Chang TG, Zhu XG. 2017.** Source-sink interaction: a century old concept under the light of modern molecular systems biology. *J Exp Bot* **68**(16): 4417-4431.
- Chapin F, Shaver G. 1988.** Differences in carbon and nutrient fractions among arctic growth forms. *Oecologia* **77**(4): 506-514.
- Chapin FS, Schulze E, Mooney HA. 1990.** The Ecology and Economics of Storage in Plants. *Annual Review of Ecology and Systematics* **21**(1): 423-447.
- Chen H, Wang JP, Liu H, Li H, Lin YJ, Shi R, Yang C, Gao J, Zhou C, Li Q, et al. 2019.** Hierarchical Transcription Factor and Chromatin Binding Network for Wood Formation in Black Cottonwood (*Populus trichocarpa*). *Plant Cell* **31**(3): 602-626.
- Chen P, Yan M, Li L, He J, Zhou S, Li Z, Niu C, Bao C, Zhi F, Ma F, et al. 2020.** The apple DNA-binding one zinc-finger protein MdDof54 promotes drought resistance. *Hortic Res* **7**(1): 195.

- Chen Z, Gao K, Su X, Rao P, An X. 2015.** Genome-Wide Identification of the Invertase Gene Family in Populus. *PLoS One* **10**(9): e0138540.
- Cheng W-H, Taliercio EW, Chourey PS. 1996.** The Miniature1 seed locus of maize encodes a cell wall invertase required for normal development of endosperm and maternal cells in the pedicel. *The Plant Cell* **8**(6): 971-983.
- Chopra J, Kaur N, Gupta AK. 2003.** Changes in the activities of carbon metabolizing enzymes with pod development in lentil (*Lens culinaris* L.). *Acta Physiologiae Plantarum* **25**(2): 185-191.
- Cleland EE, Harpole WS. 2010.** Nitrogen enrichment and plant communities. *Ann NY Acad Sci* **1195**: 46-61.
- Coleman HD, Park J-Y, Nair R, Chapple C, Mansfield SD. 2008a.** RNAi-mediated suppression of p-coumaroyl-CoA 3'-hydroxylase in hybrid poplar impacts lignin deposition and soluble secondary metabolism. *Proceedings of the National Academy of Sciences* **105**(11): 4501-4506.
- Coleman HD, Samuels AL, Guy RD, Mansfield SD. 2008b.** Perturbed lignification impacts tree growth in hybrid poplar—a function of sink strength, vascular integrity, and photosynthetic assimilation. *Plant Physiology* **148**(3): 1229-1237.
- Coleman HD, Yan J, Mansfield SD. 2009.** Sucrose synthase affects carbon partitioning to increase cellulose production and altered cell wall ultrastructure. *Proceedings of the National Academy of Sciences* **106**(31): 13118-13123.
- Cosgrove DJ. 2005.** Growth of the plant cell wall. *Nature reviews molecular cell biology* **6**(11): 850-861.
- Courtois-Moreau CL, Pesquet E, Sjodin A, Muniz L, Bollhoner B, Kaneda M, Samuels L, Jansson S, Tuominen H. 2009.** A unique program for cell death in xylem fibers of Populus stem. *Plant J* **58**(2): 260-274.
- Dai X, Hu Q, Cai Q, Feng K, Ye N, Tuskan GA, Milne R, Chen Y, Wan Z, Wang Z. 2014.** The willow genome and divergent evolution from poplar after the common genome duplication. *Cell research* **24**(10): 1274-1277.
- Danecek P, Bonfield JK, Liddle J, Marshall J, Ohan V, Pollard MO, Whitwham A, Keane T, McCarthy SA, Davies RM. 2021.** Twelve years of SAMtools and BCFtools. *Gigascience* **10**(2): giab008.
- Davidson AM, Le ST, Cooper KB, Lange E, Zwieniecki MA. 2021.** No time to rest: seasonal dynamics of non-structural carbohydrates in twigs of three Mediterranean tree species suggest year-round activity. *Sci Rep* **11**(1): 5181.
- De Coninck B, Le Roy K, Francis I, Clerens S, Vergauwen R, Halliday AM, Smith SM, Van Laere A, Van Den Ende W. 2005.** Arabidopsis AtcwINV3 and 6 are not invertases but are fructan exohydrolases (FEHs) with different substrate specificities. *Plant, Cell & Environment* **28**(4): 432-443.
- De Kauwe MG, Medlyn BE, Zaehle S, Walker AP, Dietze MC, Wang YP, Luo Y, Jain AK, El-Masri B, Hickler T, et al. 2014.** Where does the carbon

- go? A model-data intercomparison of vegetation carbon allocation and turnover processes at two temperate forest free-air CO₂ enrichment sites. *New Phytol* **203**(3): 883-899.
- de Mendoza A, Hatleberg WL, Pang K, Leininger S, Bogdanovic O, Pflueger J, Buckberry S, Technau U, Hejnol A, Adamska M. 2019a.** Convergent evolution of a vertebrate-like methylome in a marine sponge. *Nature ecology & evolution* **3**(10): 1464-1473.
- de Mendoza A, Pflueger J, Lister R. 2019b.** Capture of a functionally active methyl-CpG binding domain by an arthropod retrotransposon family. *Genome research* **29**(8): 1277-1286.
- De Vries FP. 1975.** The cost of maintenance processes in plant cells. *Annals of Botany* **39**(1): 77-92.
- Demura T, Tashiro G, Horiguchi G, Kishimoto N, Kubo M, Matsuoka N, Minami A, Nagata-Hiwatashi M, Nakamura K, Okamura Y. 2002.** Visualization by comprehensive microarray analysis of gene expression programs during transdifferentiation of mesophyll cells into xylem cells. *Proceedings of the National Academy of Sciences* **99**(24): 15794-15799.
- Diacci C, Abedi T, Lee JW, Gabrielsson EO, Berggren M, Simon DT, Niittylä T, Stavrinidou E. 2021.** Diurnal in vivo xylem sap glucose and sucrose monitoring using implantable organic electrochemical transistor sensors. *Isience* **24**(1): 101966.
- Dietze MC, Sala A, Carbone MS, Czimczik CI, Mantooth JA, Richardson AD, Vargas R. 2014.** Nonstructural carbon in woody plants. *Annu Rev Plant Biol* **65**: 667-687.
- Dominguez PG, Donev E, Derba-Maceluch M, Bunder A, Hedenstrom M, Tomaskova I, Mellerowicz EJ, Niittyla T. 2021.** Sucrose synthase determines carbon allocation in developing wood and alters carbon flow at the whole tree level in aspen. *New Phytol* **229**(1): 186-198.
- Dominguez PG, Niittylä T. 2021.** Mobile forms of carbon in trees: metabolism and transport. *Tree Physiol.*
- Dong Z, Xu Z, Xu L, Galli M, Gallavotti A, Dooner HK, Chuck G. 2020.** Necrotic upper tips1 mimics heat and drought stress and encodes a protoxylem-specific transcription factor in maize. *Proc Natl Acad Sci U S A* **117**(34): 20908-20919.
- Du H, Ning L, He B, Wang Y, Ge M, Xu J, Zhao H. 2020.** Cross-species root transcriptional network analysis highlights conserved modules in response to nitrate between maize and sorghum. *International journal of molecular sciences* **21**(4): 1445.
- Dubos C, Stracke R, Grotewold E, Weisshaar B, Martin C, Lepiniec L. 2010.** MYB transcription factors in Arabidopsis. *Trends Plant Sci* **15**(10): 573-581.
- Duncan KA, Hardin SC, Huber SC. 2006.** The three maize sucrose synthase isoforms differ in distribution, localization, and phosphorylation. *Plant and Cell Physiology* **47**(7): 959-971.

- Ellis B, Jansson S, Strauss SH, Tuskan GA 2010.** Why and how *Populus* became a “model tree”. *Genetics and genomics of Populus*: Springer, 3-14.
- England CG, Luo H, Cai W. 2015.** HaloTag technology: a versatile platform for biomedical applications. *Bioconjugate chemistry* **26**(6): 975-986.
- Etxeberria E, Gonzalez P. 2003.** Evidence for a tonoplast - associated form of sucrose synthase and its potential involvement in sucrose mobilization from the vacuole. *Journal of Experimental Botany* **54**(386): 1407-1414.
- Eyles A, Pinkard EA, Davies NW, Corkrey R, Churchill K, O'Grady AP, Sands P, Mohammed C. 2013.** Whole-plant versus leaf-level regulation of photosynthetic responses after partial defoliation in *Eucalyptus globulus* saplings. *J Exp Bot* **64**(6): 1625-1636.
- FAO. 2018.** The State of the World's Forests 2018 - Forest Pathways to Sustainable Development.
- Ferjani A, Segami S, Asaoka M, Maeshima M 2014.** Regulation of PPi Levels Through the Vacuolar Membrane H⁺-Pyrophosphatase. In: Lüttge U, Beyschlag W, Cushman J eds. *Progress in Botany: Vol. 75*. Berlin, Heidelberg: Springer Berlin Heidelberg, 145-165.
- Fernie AR, Roessner U, Trethewey RN, Willmitzer L. 2001.** The contribution of plastidial phosphoglucomutase to the control of starch synthesis within the potato tuber. *Planta* **213**(3).
- Fisher WW, Li JJ, Hammonds AS, Brown JB, Pfeiffer BD, Weizmann R, MacArthur S, Thomas S, Stamatoyannopoulos JA, Eisen MB. 2012.** DNA regions bound at low occupancy by transcription factors do not drive patterned reporter gene expression in *Drosophila*. *Proceedings of the National Academy of Sciences* **109**(52): 21330-21335.
- Fornes O, Castro-Mondragon JA, Khan A, Van der Lee R, Zhang X, Richmond PA, Modi BP, Correard S, Gheorghe M, Baranašić D. 2020.** JASPAR 2020: update of the open-access database of transcription factor binding profiles. *Nucleic acids research* **48**(D1): D87-D92.
- Fromm J 2013.** Xylem development in trees: from cambial divisions to mature wood cells. *Cellular aspects of wood formation*: Springer, 3-39.
- Fünfgeld MMFF, Wang W, Ishihara H, Arrivault S, Feil R, Smith AM, Stitt M, Lunn JE, Niittylä T. 2022.** Sucrose synthases are not involved in starch synthesis in *Arabidopsis* leaves. *Nature plants*.
- Furze ME, Huggett BA, Aubrecht DM, Stolz CD, Carbone MS, Richardson AD. 2019.** Whole-tree nonstructural carbohydrate storage and seasonal dynamics in five temperate species. *New Phytol* **221**(3): 1466-1477.
- Galiano L, Timofeeva G, Saurer M, Siegwolf R, Martínez - Vilalta J, Hommel R, Gessler A. 2017.** The fate of recently fixed carbon after drought release: towards unravelling C storage regulation in *Tilia platyphyllos* and *Pinus sylvestris*. *Plant, Cell & Environment* **40**(9): 1711-1724.
- Galli M, Feng F, Gallavotti A. 2020.** Mapping Regulatory Determinants in Plants. *Front Genet* **11**: 591194.

- Galli M, Khakhar A, Lu Z, Chen Z, Sen S, Joshi T, Nemhauser JL, Schmitz RJ, Gallavotti A. 2018.** The DNA binding landscape of the maize AUXIN RESPONSE FACTOR family. *Nat Commun* **9**(1): 4526.
- Gaut BS, Le Thierry d'Ennequin M, Peek AS, Sawkins MC. 2000.** Maize as a model for the evolution of plant nuclear genomes. *Proceedings of the National Academy of Sciences* **97**(13): 7008-7015.
- Geigenberger P. 2003.** Response of plant metabolism to too little oxygen. *Current Opinion in Plant Biology* **6**(3): 247-256.
- Geigenberger P, Stitt M. 1993.** Sucrose synthase catalyses a readily reversible reaction in vivo in developing potato tubers and other plant tissues. *Planta* **189**(3): 329-339.
- Gerber L, Zhang B, Roach M, Rende U, Gorzsas A, Kumar M, Burgert I, Niittyla T, Sundberg B. 2014.** Deficient sucrose synthase activity in developing wood does not specifically affect cellulose biosynthesis, but causes an overall decrease in cell wall polymers. *New Phytol* **203**(4): 1220-1230.
- Gibon Y, Blaesing OE, Hannemann J, Carillo P, Höhne M, Hendriks JHM, Palacios N, Cross J, Selbig J, Stitt M. 2004a.** A Robot-Based Platform to Measure Multiple Enzyme Activities in Arabidopsis Using a Set of Cycling Assays: Comparison of Changes of Enzyme Activities and Transcript Levels during Diurnal Cycles and in Prolonged Darkness[W]. *The Plant Cell* **16**(12): 3304-3325.
- Gibon Y, Bläsing OE, Palacios - Rojas N, Pankovic D, Hendriks JH, Fisahn J, Höhne M, Günther M, Stitt M. 2004b.** Adjustment of diurnal starch turnover to short days: depletion of sugar during the night leads to a temporary inhibition of carbohydrate utilization, accumulation of sugars and post - translational activation of ADP - glucose pyrophosphorylase in the following light period. *The Plant Journal* **39**(6): 847-862.
- Gibon Y, Pyl ET, Sulpice R, Lunn JE, Hohne M, Gunther M, Stitt M. 2009.** Adjustment of growth, starch turnover, protein content and central metabolism to a decrease of the carbon supply when Arabidopsis is grown in very short photoperiods. *Plant Cell Environ* **32**(7): 859-874.
- Gibon Y, Usadel B, Blaesing OE, Kamlage B, Hoehne M, Trethewey R, Stitt M. 2006.** Integration of metabolite with transcript and enzyme activity profiling during diurnal cycles in Arabidopsis rosettes. *Genome Biol* **7**(8): R76.
- Goicoechea M, Lacombe E, Legay S, Mihaljevic S, Rech P, Jauneau A, Lapierre C, Pollet B, Verhaegen D, Chaubet-Gigot N, et al. 2005.** EgMYB2, a new transcriptional activator from Eucalyptus xylem, regulates secondary cell wall formation and lignin biosynthesis. *Plant J* **43**(4): 553-567.
- Gorshkova T, Brutch N, Chabbert B, Deyholos M, Hayashi T, Lev-Yadun S, Mellerowicz EJ, Morvan C, Neutelings G, Pilate G. 2012.** Plant Fiber Formation: State of the Art, Recent and Expected Progress, and Open Questions. *Critical Reviews in Plant Sciences* **31**(3): 201-228.

- Gou M, Ran X, Martin DW, Liu C-J. 2018.** The scaffold proteins of lignin biosynthetic cytochrome P450 enzymes. *Nature plants* **4**(5): 299-310.
- Gough CM, Flower CE, Vogel CS, Curtis PS. 2010.** Phenological and Temperature Controls on the Temporal Non-Structural Carbohydrate Dynamics of *Populus grandidentata* and *Quercus rubra*. *Forests* **1**(1): 65-81.
- Graf A, Schlereth A, Stitt M, Smith AM. 2010.** Circadian control of carbohydrate availability for growth in *Arabidopsis* plants at night. *Proc Natl Acad Sci U S A* **107**(20): 9458-9463.
- Grant CE, Bailey TL, Noble WS. 2011.** FIMO: scanning for occurrences of a given motif. *Bioinformatics* **27**(7): 1017-1018.
- Gupta R, Sharma LK. 2019.** The process-based forest growth model 3-PG for use in forest management: A review. *Ecological modelling* **397**: 55-73.
- Gupta S, Stamatoyannopoulos JA, Bailey TL, Noble WS. 2007.** Quantifying similarity between motifs. *Genome biology* **8**(2): 1-9.
- Haigler CH, Ivanova-Datcheva M, Hogan PS, Salnikov VV, Hwang S, Martin K, Delmer DP. 2001.** Carbon partitioning to cellulose synthesis. *Plant Molecular Biology* **47**(1/2): 29-51.
- Hanson KR, McHale NA. 1988.** A starchless mutant of *Nicotiana sylvestris* containing a modified plastid phosphoglucomutase. *Plant Physiology* **88**(3): 838-844.
- Harrison C, Hedley C, Wang T. 1998.** Evidence that the rug3 locus of pea (*Pisum sativum* L.) encodes plastidial phosphoglucomutase confirms that the imported substrate for starch synthesis in pea amyloplasts is glucose-6-phosphate. *The Plant Journal* **13**(6): 753-762.
- Harrison CJ, Mould RM, Leech MJ, Johnson SA, Turner L, Schreck SL, Baird KM, Jack PL, Rawsthorne S, Hedley CL. 2000.** The rug3 locus of pea encodes plastidial phosphoglucomutase. *Plant Physiology* **122**(4): 1187-1192.
- Hartmann H, Bahn M, Carbone M, Richardson AD. 2020.** Plant carbon allocation in a changing world - challenges and progress: introduction to a Virtual Issue on carbon allocation: Introduction to a virtual issue on carbon allocation. *New Phytol* **227**(4): 981-988.
- Hartmann H, McDowell NG, Trumbore S. 2015.** Allocation to carbon storage pools in Norway spruce saplings under drought and low CO₂. *Tree Physiology* **35**(3): 243-252.
- Hartmann H, Trumbore S. 2016.** Understanding the roles of nonstructural carbohydrates in forest trees - from what we can measure to what we want to know. *New Phytol* **211**(2): 386-403.
- Havelka U, Wittenback V, Boyle M. 1984.** CO₂ - Enrichment Effects on Wheat Yield and Physiology. *Crop Science* **24**(6): 1163-1168.
- Hill JL, Hammudi MB, Tien M. 2014.** The *Arabidopsis* cellulose synthase complex: a proposed hexamer of CESA trimers in an equimolar stoichiometry. *The Plant Cell* **26**(12): 4834-4842.

- Ho LC. 1988.** Metabolism and Compartmentation of Imported Sugars in Sink Organs in Relation to Sink Strength. *Annual Review of Plant Physiology and Plant Molecular Biology* **39**(1): 355-378.
- Hoch G, Körner C. 2003.** The carbon charging of pines at the climatic treeline: a global comparison. *Oecologia* **135**(1): 10-21.
- Hoch G, Richter A, Körner C. 2003.** Non-structural carbon compounds in temperate forest trees. *Plant, Cell & Environment* **26**(7): 1067-1081.
- Howe GT, Gardner G, Hackett WP, Furnier GR. 1996.** Phytochrome control of short - day - induced bud set in black cottonwood. *Physiologia Plantarum* **97**(1): 95-103.
- Hu R, Qi G, Kong Y, Kong D, Gao Q, Zhou G. 2010.** Comprehensive analysis of NAC domain transcription factor gene family in *Populus trichocarpa*. *BMC plant biology* **10**(1): 1-23.
- Huang J, Hammerbacher A, Gershenson J, van Dam NM, Sala A, McDowell NG, Chowdhury S, Gleixner G, Trumbore S, Hartmann H. 2021.** Storage of carbon reserves in spruce trees is prioritized over growth in the face of carbon limitation. *Proceedings of the National Academy of Sciences* **118**(33).
- Huang SC, Ecker JR. 2018.** Piecing together cis-regulatory networks: insights from epigenomics studies in plants. *Wiley Interdiscip Rev Syst Biol Med* **10**(3): e1411.
- Hussey SG, Mizrahi E, Creux NM, Myburg AA. 2013.** Navigating the transcriptional roadmap regulating plant secondary cell wall deposition. *Front Plant Sci* **4**: 325.
- Iglesias AA, Preiss J. 1992.** Bacterial glycogen and plant starch biosynthesis. *Biochemical Education* **20**(4): 196-203.
- Inukai S, Kock KH, Bulyk ML. 2017.** Transcription factor-DNA binding: beyond binding site motifs. *Curr Opin Genet Dev* **43**: 110-119.
- Jacobsen AL, Valdovinos - Ayala J, Pratt RB. 2018.** Functional lifespans of xylem vessels: development, hydraulic function, and post - function of vessels in several species of woody plants. *American Journal of Botany* **105**(2): 142-150.
- James MG, Robertson DS, Myers AM. 1995.** Characterization of the maize gene *sugary1*, a determinant of starch composition in kernels. *The Plant Cell* **7**(4): 417-429.
- Jia L, Zhang B, Mao C, Li J, Wu Y, Wu P, Wu Z. 2008.** OsCYT-INV1 for alkaline/neutral invertase is involved in root cell development and reproductivity in rice (*Oryza sativa* L.). *Planta* **228**(1): 51-59.
- Jiao B, Zhao X, Lu W, Guo L, Luo K. 2019.** The R2R3 MYB transcription factor MYB189 negatively regulates secondary cell wall biosynthesis in *Populus*. *Tree Physiol* **39**(7): 1187-1200.
- Kačík F, Ďurkovič J, Kačíková D. 2012.** Chemical profiles of wood components of poplar clones for their energy utilization. *Energies* **5**(12): 5243-5256.

- Keenan TF, Davidson E, Moffat AM, Munger W, Richardson AD. 2012.** Using model-data fusion to interpret past trends, and quantify uncertainties in future projections, of terrestrial ecosystem carbon cycling. *Global Change Biology* **18**(8): 2555-2569.
- Khan A, Fornes O, Stigliani A, Gheorghe M, Castro-Mondragon JA, van der Lee R, Bessy A, Cheneby J, Kulkarni SR, Tan G, et al. 2018.** JASPAR 2018: update of the open-access database of transcription factor binding profiles and its web framework. *Nucleic Acids Res* **46**(D1): D260-D266.
- Kimura S, Laosinchai W, Itoh T, Cui X, Linder CR, Brown Jr RM. 1999.** Immunogold labeling of rosette terminal cellulose-synthesizing complexes in the vascular plant *Vigna angularis*. *The Plant Cell* **11**(11): 2075-2085.
- Kiselev KV, Aleynova OA, Ogneva ZV, Suprun AR, Dubrovina AS. 2021.** 35S promoter-driven transgenes are variably expressed in different organs of *Arabidopsis thaliana* and in response to abiotic stress. *Molecular Biology Reports* **48**(3): 2235-2241.
- Klein T, Hoch G. 2015.** Tree carbon allocation dynamics determined using a carbon mass balance approach. *New Phytologist* **205**(1): 147-159.
- Ko JH, Yang SH, Park AH, Lerouxel O, Han KH. 2007.** ANAC012, a member of the plant - specific NAC transcription factor family, negatively regulates xylary fiber development in *Arabidopsis thaliana*. *The Plant Journal* **50**(6): 1035-1048.
- Körner C. 1998.** A re-assessment of high elevation treeline positions and their explanation. *Oecologia* **115**(4): 445-459.
- Körner C. 2003.** Carbon limitation in trees. *Journal of Ecology* **91**(1): 4-17.
- Körner C. 2013.** Growth controls photosynthesis—mostly. *Nova Acta Leopoldina NF* **114**(391): 273-283.
- Körner C. 2015.** Paradigm shift in plant growth control. *Curr Opin Plant Biol* **25**: 107-114.
- Kozłowski T. 1992.** Carbohydrate sources and sinks in woody plants. *The botanical review* **58**(2): 107-222.
- Krämer U. 2015.** The natural history of model organisms: Planting molecular functions in an ecological context with *Arabidopsis thaliana*. *Elife* **4**: e06100.
- Krinner G, Viovy N, de Noblet-Ducoudré N, Ogée J, Polcher J, Friedlingstein P, Ciais P, Sitch S, Prentice IC. 2005.** A dynamic global vegetation model for studies of the coupled atmosphere-biosphere system. *Global Biogeochemical Cycles* **19**(1).
- Kubo M, Udagawa M, Nishikubo N, Horiguchi G, Yamaguchi M, Ito J, Mimura T, Fukuda H, Demura T. 2005.** Transcription switches for protoxylem and metaxylem vessel formation. *Genes Dev* **19**(16): 1855-1860.
- Landhäusser SM, Lieffers VJ. 2003.** Seasonal changes in carbohydrate reserves in mature northern *Populus tremuloides* clones. *Trees - Structure and Function* **17**(6): 471-476.

- Lapierre C, Pollet B, Petit-Conil M, Toval G, Romero J, Pilate G, Lépé J-C, Boerjan W, Ferret V, De Nadai V. 1999.** Structural alterations of lignins in transgenic poplars with depressed cinnamyl alcohol dehydrogenase or caffeic acid O-methyltransferase activity have an opposite impact on the efficiency of industrial kraft pulping. *Plant Physiology* **119**(1): 153-164.
- Larson PR 1994.** Defining the cambium. *The Vascular Cambium*: Springer, 33-97.
- Larson PR, Isebrands JG, Dickson RE. 1980.** Sink to Source Transition of Populus Leaves. *Berichte der Deutschen Botanischen Gesellschaft* **93**(1): 79-90.
- Lastdrager J, Hanson J, Smeekens S. 2014.** Sugar signals and the control of plant growth and development. *Journal of Experimental Botany* **65**(3): 799-807.
- Levin I, Kromer B. 2004.** The tropospheric $^{14}\text{CO}_2$ level in mid-latitudes of the Northern Hemisphere (1959–2003). *Radiocarbon* **46**(3): 1261-1272.
- Levin I, Naegler T, Kromer B, Diehl M, Francey R, Gomez-Pelaez A, Steele P, Wagenbach D, Weller R, Worthy D. 2010.** Observations and modelling of the global distribution and long-term trend of atmospheric $^{14}\text{CO}_2$. *Tellus B: Chemical and Physical Meteorology* **62**(1): 26-46.
- Li B, Liu H, Zhang Y, Kang T, Zhang L, Tong J, Xiao L, Zhang H. 2013.** Constitutive expression of cell wall invertase genes increases grain yield and starch content in maize. *Plant Biotechnology Journal* **11**(9): 1080-1091.
- Li E, Bhargava A, Qiang W, Friedmann MC, Forneris N, Savidge RA, Johnson LA, Mansfield SD, Ellis BE, Douglas CJ. 2012.** The Class II KNOX gene KNAT7 negatively regulates secondary wall formation in Arabidopsis and is functionally conserved in Populus. *New Phytol* **194**(1): 102-115.
- Li H. 2013.** Aligning sequence reads, clone sequences and assembly contigs with BWA-MEM. *arXiv preprint arXiv:1303.3997*.
- Li Q, Lin YC, Sun YH, Song J, Chen H, Zhang XH, Sederoff RR, Chiang VL. 2012.** Splice variant of the SND1 transcription factor is a dominant negative of SND1 members and their regulation in Populus trichocarpa. *Proc Natl Acad Sci U S A* **109**(36): 14699-14704.
- Li Z, Fernie AR, Persson S. 2016.** Transition of primary to secondary cell wall synthesis. *Science Bulletin* **61**(11): 838-846.
- Lin T-P, Caspar T, Somerville C, Preiss J. 1988.** Isolation and characterization of a starchless mutant of Arabidopsis thaliana (L.) Heynh lacking ADPglucose pyrophosphorylase activity. *Plant Physiology* **86**(4): 1131-1135.
- Lin YC, Li W, Sun YH, Kumari S, Wei H, Li Q, Tunlaya-Anukit S, Sederoff RR, Chiang VL. 2013.** SND1 transcription factor-directed quantitative functional hierarchical genetic regulatory network in wood formation in Populus trichocarpa. *Plant Cell* **25**(11): 4324-4341.
- Lin YC, Wang J, Delhomme N, Schiffthaler B, Sundstrom G, Zuccolo A, Nystedt B, Hvidsten TR, de la Torre A, Cossu RM, et al. 2018.** Functional and evolutionary genomic inferences in Populus through

- genome and population sequencing of American and European aspen. *Proc Natl Acad Sci U S A* **115**(46): E10970-E10978.
- Lin YJ, Chen H, Li Q, Li W, Wang JP, Shi R, Tunlaya-Anukit S, Shuai P, Wang Z, Ma H, et al. 2017.** Reciprocal cross-regulation of VND and SND multigene TF families for wood formation in *Populus trichocarpa*. *Proc Natl Acad Sci U S A* **114**(45): E9722-E9729.
- Lindemose S, O'Shea C, Jensen MK, Skriver K. 2013.** Structure, function and networks of transcription factors involved in abiotic stress responses. *International journal of molecular sciences* **14**(3): 5842-5878.
- Lipsick JS. 1996.** One billion years of Myb. *Oncogene* **13**(2): 223-235.
- Liu W, Su J, Li S, Lang X, Huang X. 2018.** Non-structural carbohydrates regulated by season and species in the subtropical monsoon broad-leaved evergreen forest of Yunnan Province, China. *Sci Rep* **8**(1): 1083.
- Los GV, Encell LP, McDougall MG, Hartzell DD, Karassina N, Zimprich C, Wood MG, Learish R, Ohana RF, Urh M. 2008.** HaloTag: a novel protein labeling technology for cell imaging and protein analysis. *ACS chemical biology* **3**(6): 373-382.
- Luscombe NM, Austin SE, Berman HM, Thornton JM. 2000.** An overview of the structures of protein-DNA complexes. *Genome biology* **1**(1): 1-37.
- Machanick P, Bailey TL. 2011.** MEME-ChIP: motif analysis of large DNA datasets. *Bioinformatics* **27**(12): 1696-1697.
- Maeda H, Dudareva N. 2012.** The Shikimate Pathway and Aromatic Amino Acid Biosynthesis in Plants. *Annual Review of Plant Biology* **63**(1): 73-105.
- Mahboubi A, Niittylä T. 2018.** Sucrose transport and carbon fluxes during wood formation. *Physiol Plant* **164**(1): 67-81.
- Maher KA, Bajic M, Kajala K, Reynoso M, Pauluzzi G, West DA, Zumstein K, Woodhouse M, Bubb K, Dorrity MW, et al. 2018.** Profiling of Accessible Chromatin Regions across Multiple Plant Species and Cell Types Reveals Common Gene Regulatory Principles and New Control Modules. *Plant Cell* **30**(1): 15-36.
- Mäkelä A, Landsberg J, Ek AR, Burk TE, Ter-Mikaelian M, Ågren GI, Oliver CD, Puttonen P. 2000.** Process-based models for forest ecosystem management: current state of the art and challenges for practical implementation. *Tree Physiology* **20**(5-6): 289-298.
- Malinova I, Kunz HH, Alseikh S, Herbst K, Fernie AR, Gierth M, Fettke J. 2014.** Reduction of the cytosolic phosphoglucomutase in *Arabidopsis* reveals impact on plant growth, seed and root development, and carbohydrate partitioning. *PLoS One* **9**(11): e112468.
- Manjunath S, Kenneth Lee C-H, Winkle PV, Bailey-Serres J. 1998.** Molecular and biochemical characterization of cytosolic phosphoglucomutase in maize: expression during development and in response to oxygen deprivation. *Plant Physiology* **117**(3): 997-1006.

- Martínez-Vilalta J, Sala A, Asensio D, Galiano L, Hoch G, Palacio S, Piper FI, Lloret F. 2016.** Dynamics of non - structural carbohydrates in terrestrial plants: a global synthesis. *Ecological Monographs* **86**(4): 495-516.
- Mason TG, Maskell EJ. 1928.** Studies on the transport of carbohydrates in the cotton plant: II. The factors determining the rate and the direction of movement of sugars. *Annals of Botany* **42**(167): 66.
- McCarthy RL, Zhong R, Fowler S, Lyskowski D, Piyasena H, Carleton K, Spicer C, Ye ZH. 2010.** The poplar MYB transcription factors, PtrMYB3 and PtrMYB20, are involved in the regulation of secondary wall biosynthesis. *Plant Cell Physiol* **51**(6): 1084-1090.
- McCarthy RL, Zhong R, Ye ZH. 2009.** MYB83 is a direct target of SND1 and acts redundantly with MYB46 in the regulation of secondary cell wall biosynthesis in Arabidopsis. *Plant Cell Physiol* **50**(11): 1950-1964.
- McDougall G, Morrison I, Stewart D, Weyers J, Hillman J. 1993.** Plant fibres: botany, chemistry and processing for industrial use. *Journal of the Science of Food and Agriculture* **62**(1): 1-20.
- McFarlane HE, Doring A, Persson S. 2014.** The cell biology of cellulose synthesis. *Annu Rev Plant Biol* **65**: 69-94.
- Meinke DW, Cherry JM, Dean C, Rounsley SD, Koornneef M. 1998.** Arabidopsis thaliana: a model plant for genome analysis. *Science* **282**(5389): 662-682.
- Mellerowicz EJ, Baucher M, Sundberg B, Boerjan W. 2001.** Unraveling cell wall formation in the woody dicot stem. *Plant Molecular Biology* **47**(1/2): 239-274.
- Meng L-S, Bao Q-X, Mu X-R, Tong C, Cao X-Y, Huang J-J, Xue L-N, Liu C-Y, Fei Y, Loake GJ. 2021.** Glucose-and sucrose-signaling modules regulate the Arabidopsis juvenile-to-adult phase transition. *Cell Reports* **36**(2): 109348.
- Michael TP, VanBuren R. 2015.** Progress, challenges and the future of crop genomes. *Current Opinion in Plant Biology* **24**: 71-81.
- Mitsuda N, Iwase A, Yamamoto H, Yoshida M, Seki M, Shinozaki K, Ohme-Takagi M. 2007.** NAC transcription factors, NST1 and NST3, are key regulators of the formation of secondary walls in woody tissues of Arabidopsis. *Plant Cell* **19**(1): 270-280.
- Mitsuda N, Ohme-Takagi M. 2008.** NAC transcription factors NST1 and NST3 regulate pod shattering in a partially redundant manner by promoting secondary wall formation after the establishment of tissue identity. *The Plant Journal* **56**(5): 768-778.
- Mitsuda N, Seki M, Shinozaki K, Ohme-Takagi M. 2005.** The NAC transcription factors NST1 and NST2 of Arabidopsis regulate secondary wall thickenings and are required for anther dehiscence. *Plant Cell* **17**(11): 2993-3006.

- Monteith JL. 1977.** Climate and the efficiency of crop production in Britain. *Philosophical Transactions of the Royal Society of London. B, Biological Sciences* **281**(980): 277-294.
- Mooney HA, Hays RI. 1973.** Carbohydrate Storage Cycles in Two Californian Mediterranean-Climate Trees. *Flora* **162**(3): 295-304.
- Moore B, Zhou L, Rolland F, Hall Q, Cheng W-H, Liu Y-X, Hwang I, Jones T, Sheen J. 2003.** Role of the Arabidopsis glucose sensor HXK1 in nutrient, light, and hormonal signaling. *Science* **300**(5617): 332-336.
- Morell M, Copeland L. 1985.** Sucrose synthase of soybean nodules. *Plant Physiology* **78**(1): 149-154.
- Morreel K, Ralph J, Kim H, Lu F, Goeminne G, Ralph S, Messens E, Boerjan W. 2004.** Profiling of oligolignols reveals monolignol coupling conditions in lignifying poplar xylem. *Plant Physiol* **136**(3): 3537-3549.
- Mueller SC, Brown RM. 1980.** Evidence for an intramembrane component associated with a cellulose microfibril-synthesizing complex in higher plants. *Journal of Cell Biology* **84**(2): 315-326.
- Munoz FJ, Baroja-Fernandez E, Moran-Zorzano MT, Viale AM, Etxeberria E, Alonso-Casajus N, Pozueta-Romero J. 2005.** Sucrose synthase controls both intracellular ADP glucose levels and transitory starch biosynthesis in source leaves. *Plant Cell Physiol* **46**(8): 1366-1376.
- Murakami Y, Funada R, Sano Y, Ohtani J. 1999.** The differentiation of contact cells and isolation cells in the xylem ray parenchyma of *Populus maximowiczii*. *Annals of Botany* **84**(4): 429-435.
- Murata T, Sugiyama T, Minamikawa T, Akazawa T. 1966.** Enzymic mechanism of starch synthesis in ripening rice grains. *Archives of Biochemistry and Biophysics* **113**(1): 34-44.
- Naito K, Zhang F, Tsukiyama T, Saito H, Hancock CN, Richardson AO, Okumoto Y, Tanisaka T, Wessler SR. 2009.** Unexpected consequences of a sudden and massive transposon amplification on rice gene expression. *Nature* **461**(7267): 1130-1134.
- Nakaba S, Begum S, Yamagishi Y, Jin H-O, Kubo T, Funada R. 2011.** Differences in the timing of cell death, differentiation and function among three different types of ray parenchyma cells in the hardwood *Populus sieboldii* × *P. grandidentata*. *Trees* **26**(3): 743-750.
- Nguyen PV, Dickmann DI, Pregitzer KS, Hendrick R. 1990.** Late-season changes in allocation of starch and sugar to shoots, coarse roots, and fine roots in two hybrid poplar clones. *Tree Physiology* **7**(1-2-3-4): 95-105.
- Nilsson O, Aldén T, Sitbon F, Little CA, Chalupa V, Sandberg G, Olsson O. 1992.** Spatial pattern of cauliflower mosaic virus 35S promoter-luciferase expression in transgenic hybrid aspen trees monitored by enzymatic assay and non-destructive imaging. *Transgenic research* **1**(5): 209-220.
- Nishimura M, Beevers H. 1979.** Subcellular distribution of gluconeogenic enzymes in germinating castor bean endosperm. *Plant Physiology* **64**(1): 31-37.

- Nunez JGA, Kronenberger J, Wuillème S, Lepiniec L, Rochat C. 2008.** Study of AtSUS2 localization in seeds reveals a strong association with plastids. *Plant and Cell Physiology* **49**(10): 1621-1626.
- O'Malley RC, Huang SC, Song L, Lewsey MG, Bartlett A, Nery JR, Galli M, Gallavotti A, Ecker JR. 2016.** Cistrome and Epicistrome Features Shape the Regulatory DNA Landscape. *Cell* **165**(5): 1280-1292.
- Ohtani M, Nishikubo N, Xu B, Yamaguchi M, Mitsuda N, Goue N, Shi F, Ohme-Takagi M, Demura T. 2011.** A NAC domain protein family contributing to the regulation of wood formation in poplar. *Plant J* **67**(3): 499-512.
- Olsen JE, Junttila O, Nilsen J, Eriksson ME, Martinussen I, Olsson O, Sandberg G, Moritz T. 1997.** Ectopic expression of oat phytochrome A in hybrid aspen changes critical daylength for growth and prevents cold acclimatization. *The Plant Journal* **12**(6): 1339-1350.
- Palacio S, Hoch G, Sala A, Korner C, Millard P. 2014.** Does carbon storage limit tree growth? *New Phytol* **201**(4): 1096-1100.
- Paul MJ, Pellny TK. 2003.** Carbon metabolite feedback regulation of leaf photosynthesis and development. *Journal of Experimental Botany* **54**(382): 539-547.
- Payyavula RS, Tay KH, Tsai CJ, Harding SA. 2011.** The sucrose transporter family in *Populus*: the importance of a tonoplast PtaSUT4 to biomass and carbon partitioning. *Plant J* **65**(5): 757-770.
- Peltier DMP, Guo J, Nguyen P, Bangs M, Gear L, Wilson M, Jefferys S, Samuels-Crow K, Yocom LL, Liu Y, et al. 2021.** Temporal controls on crown nonstructural carbohydrates in southwestern US tree species. *Tree Physiol* **41**(3): 388-402.
- Pérez S, Bertoft E. 2010.** The molecular structures of starch components and their contribution to the architecture of starch granules: A comprehensive review. *Starch - Stärke* **62**(8): 389-420.
- Perkins M, Smith RA, Samuels L. 2019.** The transport of monomers during lignification in plants: anything goes but how? *Curr Opin Biotechnol* **56**: 69-74.
- Perrin R, Wilkerson C, Keegstra K. 2001.** Golgi enzymes that synthesize plant cell wall polysaccharides: finding and evaluating candidates in the genomic era. *Plant Cell Walls*: 115-130.
- Pesquet E, Korolev AV, Calder G, Lloyd CW. 2010.** The microtubule-associated protein AtMAP70-5 regulates secondary wall patterning in *Arabidopsis* wood cells. *Current Biology* **20**(8): 744-749.
- Pfister B, Zeeman SC. 2016.** Formation of starch in plant cells. *Cell Mol Life Sci* **73**(14): 2781-2807.
- Pires ND, Dolan L. 2012.** Morphological evolution in land plants: new designs with old genes. *Philosophical Transactions of the Royal Society B: Biological Sciences* **367**(1588): 508-518.

- Plavcová L, Jansen S 2015.** The Role of Xylem Parenchyma in the Storage and Utilization of Nonstructural Carbohydrates. *Functional and Ecological Xylem Anatomy*, 209-234.
- Plomion C, Leprovost Gg, Stokes A. 2001.** Wood Formation in Trees. *Plant Physiology* **127**(4): 1513-1523.
- Preston J, Wheeler J, Heazlewood J, Li SF, Parish RW. 2004.** AtMYB32 is required for normal pollen development in Arabidopsis thaliana. *The Plant Journal* **40**(6): 979-995.
- Pret'ová A, Obert B, Wetzstein H. 2001.** Leaf developmental stage and tissue location affect the detection of β -glucuronidase in transgenic tobacco plants. *Biotechnology letters* **23**(7): 555-558.
- Quentin AG, Pinkard EA, Ryan MG, Tissue DT, Baggett LS, Adams HD, Maillard P, Marchand J, Landhausser SM, Lacoite A, et al. 2015.** Non-structural carbohydrates in woody plants compared among laboratories. *Tree Physiol* **35**(11): 1146-1165.
- Quinlan AR, Hall IM. 2010.** BEDTools: a flexible suite of utilities for comparing genomic features. *Bioinformatics* **26**(6): 841-842.
- Raes J, Rohde A, Christensen JH, Van de Peer Y, Boerjan W. 2003.** Genome-wide characterization of the lignification toolbox in Arabidopsis. *Plant Physiol* **133**(3): 1051-1071.
- Ramos-Sánchez JM, Triozzi PM, Alique D, Geng F, Gao M, Jaeger KE, Wigge PA, Allona I, Perales M. 2019.** LHY2 integrates night-length information to determine timing of poplar photoperiodic growth. *Current Biology* **29**(14): 2402-2406. e2404.
- Recondo EF, Leloir LF. 1961.** Adenosine diphosphate glucose and starch synthesis.
- Regier N, Streb S, Zeeman SC, Frey B. 2010.** Seasonal changes in starch and sugar content of poplar (*Populus deltoides* x *nigra* cv. Dorskamp) and the impact of stem girdling on carbohydrate allocation to roots. *Tree Physiol* **30**(8): 979-987.
- Rende U, Wang W, Gandla ML, Jonsson LJ, Niittyla T. 2017.** Cytosolic invertase contributes to the supply of substrate for cellulose biosynthesis in developing wood. *New Phytol* **214**(2): 796-807.
- Rennie EA, Turgeon R. 2009.** A comprehensive picture of phloem loading strategies. *Proc Natl Acad Sci U S A* **106**(33): 14162-14167.
- Ricci WA, Lu Z, Ji L, Marand AP, Ethridge CL, Murphy NG, Noshay JM, Galli M, Mejia-Guerra MK, Colome-Tatche M, et al. 2019.** Widespread long-range cis-regulatory elements in the maize genome. *Nat Plants* **5**(12): 1237-1249.
- Richardson AD, Carbone MS, Huggett BA, Furze ME, Czimeczik CI, Walker JC, Xu X, Schaberg PG, Murakami P. 2015.** Distribution and mixing of old and new nonstructural carbon in two temperate trees. *New Phytol* **206**(2): 590-597.
- Richardson AD, Carbone MS, Keenan TF, Czimeczik CI, Hollinger DY, Murakami P, Schaberg PG, Xu X. 2013.** Seasonal dynamics and age of

- stemwood nonstructural carbohydrates in temperate forest trees. *New Phytol* **197**(3): 850-861.
- Riechmann JL, Heard J, Martin G, Reuber L, Jiang C-Z, Keddie J, Adam L, Pineda O, Ratcliffe O, Samaha R. 2000.** Arabidopsis transcription factors: genome-wide comparative analysis among eukaryotes. *Science* **290**(5499): 2105-2110.
- Roach M, Arrivault S, Mahboubi A, Krohn N, Sulpice R, Stitt M, Niittyla T. 2017.** Spatially resolved metabolic analysis reveals a central role for transcriptional control in carbon allocation to wood. *J Exp Bot* **68**(13): 3529-3539.
- Roach M, Arrivault S, Mahboubi A, Krohn N, Sulpice R, Stitt M, Niittyla T. 2018.** Corrigendum: Spatially resolved metabolic analysis reveals a central role for transcriptional control in carbon allocation to wood. *J Exp Bot* **69**(16): 4143-4144.
- Ross HA, Davies HV, Burch LR, Viola R, McRae D. 1994.** Developmental changes in carbohydrate content and sucrose degrading enzymes in tuberising stolons of potato (*Solanum tuberosum*). *Physiologia Plantarum* **90**(4): 748-756.
- Ruan YL. 2014.** Sucrose metabolism: gateway to diverse carbon use and sugar signaling. *Annu Rev Plant Biol* **65**: 33-67.
- Ruan YL, Jin Y, Yang YJ, Li GJ, Boyer JS. 2010.** Sugar input, metabolism, and signaling mediated by invertase: roles in development, yield potential, and response to drought and heat. *Mol Plant* **3**(6): 942-955.
- Ruan YL, Llewellyn DJ, Furbank RT. 2003.** Suppression of sucrose synthase gene expression represses cotton fiber cell initiation, elongation, and seed development. *Plant Cell* **15**(4): 952-964.
- Ruzicka K, Ursache R, Hejatko J, Helariutta Y. 2015.** Xylem development - from the cradle to the grave. *New Phytol* **207**(3): 519-535.
- Sala A, Hoch G. 2009.** Height - related growth declines in ponderosa pine are not due to carbon limitation. *Plant, Cell & Environment* **32**(1): 22-30.
- Sala A, Woodruff DR, Meinzer FC. 2012.** Carbon dynamics in trees: feast or famine? *Tree Physiol* **32**(6): 764-775.
- Sannigrahi P, Ragauskas AJ, Tuskan GA. 2010.** Poplar as a feedstock for biofuels: a review of compositional characteristics. *Biofuels, Bioproducts and Biorefining* **4**(2): 209-226.
- Sarkanen KV, Ludwig CH. 1971.** *Lignins. Occurrence, formation, structure, and reactions.*
- Sauter JJ, van Cleve B. 1994.** Storage, mobilization and interrelations of starch, sugars, protein and fat in the ray storage tissue of poplar trees. *Trees* **8**(6): 297-304.
- Scheller HV, Ulvskov P. 2010.** Hemicelluloses. *Annual Review of Plant Biology* **61**: 263-289.

- Schiestl-Aalto P, Kulmala L, Makinen H, Nikinmaa E, Makela A. 2015.** CASSIA--a dynamic model for predicting intra-annual sink demand and interannual growth variation in Scots pine. *New Phytol* **206**(2): 647-659.
- Schiestl-Aalto P, Ryhti K, Mäkelä A, Peltoniemi M, Bäck J, Kulmala L. 2019.** Analysis of the NSC Storage Dynamics in Tree Organs Reveals the Allocation to Belowground Symbionts in the Framework of Whole Tree Carbon Balance. *Frontiers in Forests and Global Change* **2**.
- Schiffthaler B, Delhomme N, Bernhardsson C, Jenkins J, Jansson S, Ingvarsson P, Schmutz J, Street N. 2019.** An improved genome assembly of the European aspen *Populus tremula*. *bioRxiv*: 805614.
- Schmolzer K, Gutmann A, Diricks M, Desmet T, Nidetzky B. 2016.** Sucrose synthase: A unique glycosyltransferase for biocatalytic glycosylation process development. *Biotechnol Adv* **34**(2): 88-111.
- Schneider TD, Stephens RM. 1990.** Sequence logos: a new way to display consensus sequences. *Nucleic acids research* **18**(20): 6097-6100.
- Schuetz M, Smith R, Ellis B. 2013.** Xylem tissue specification, patterning, and differentiation mechanisms. *J Exp Bot* **64**(1): 11-31.
- Schulze W, Schulze ED, Stadler J, Heilmeyer H, Stitt M, Mooney H. 1994.** Growth and reproduction of *Arabidopsis thaliana* in relation to storage of starch and nitrate in the wild - type and in starch - deficient and nitrate - uptake - deficient mutants. *Plant, Cell & Environment* **17**(7): 795-809.
- Sergeeva LI, Keurentjes JJ, Bentsink L, Vonk J, van der Plas LH, Koornneef M, Vreugdenhil D. 2006.** Vacuolar invertase regulates elongation of *Arabidopsis thaliana* roots as revealed by QTL and mutant analysis. *Proceedings of the National Academy of Sciences* **103**(8): 2994-2999.
- Seyfferth C, Wessels B, Jokipii-Lukkari S, Sundberg B, Delhomme N, Felten J, Tuominen H. 2018.** Ethylene-Related Gene Expression Networks in Wood Formation. *Front Plant Sci* **9**: 272.
- Sherson SM, Alford HL, Forbes SM, Wallace G, Smith SM. 2003.** Roles of cell - wall invertases and monosaccharide transporters in the growth and development of *Arabidopsis*. *Journal of Experimental Botany* **54**(382): 525-531.
- Shi R, Wang JP, Lin YC, Li Q, Sun YH, Chen H, Sederoff RR, Chiang VL. 2017.** Tissue and cell-type co-expression networks of transcription factors and wood component genes in *Populus trichocarpa*. *Planta* **245**(5): 927-938.
- Siegenthaler U, Stocker TF, Monnin E, Lüthi D, Schwander J, Stauffer B, Raynaud D, Barnola J-M, Fischer H, Masson-Delmotte V. 2005.** Stable carbon cycle-climate relationship during the late Pleistocene. *Science* **310**(5752): 1313-1317.
- Sitch S, Smith B, Prentice IC, Arneeth A, Bondeau A, Cramer W, Kaplan JO, Levis S, Lucht W, Sykes MT. 2003.** Evaluation of ecosystem dynamics,

- plant geography and terrestrial carbon cycling in the LPJ dynamic global vegetation model. *Global Change Biology* **9**(2): 161-185.
- Slattery M, Zhou T, Yang L, Dantas Machado AC, Gordan R, Rohs R. 2014.** Absence of a simple code: how transcription factors read the genome. *Trends Biochem Sci* **39**(9): 381-399.
- Smith AM, Stitt M. 2007.** Coordination of carbon supply and plant growth. *Plant Cell Environ* **30**(9): 1126-1149.
- Smith AM, Zeeman SC. 2020.** Starch: A Flexible, Adaptable Carbon Store Coupled to Plant Growth. *Annu Rev Plant Biol* **71**: 217-245.
- Smith RA, Schuetz M, Roach M, Mansfield SD, Ellis B, Samuels L. 2013.** Neighboring parenchyma cells contribute to Arabidopsis xylem lignification, while lignification of interfascicular fibers is cell autonomous. *The Plant Cell* **25**(10): 3988-3999.
- Somerville C, Bauer S, Brininstool G, Facette M, Hamann T, Milne J, Osborne E, Paredez A, Persson S, Raab T. 2004.** Toward a systems approach to understanding plant cell walls. *Science* **306**(5705): 2206-2211.
- Song D, Shen J, Li L. 2010.** Characterization of cellulose synthase complexes in Populus xylem differentiation. *New Phytologist* **187**(3): 777-790.
- Spicer R. 2014.** Symplasmic networks in secondary vascular tissues: parenchyma distribution and activity supporting long-distance transport. *Journal of Experimental Botany* **65**(7): 1829-1848.
- Sprugel D, Hinckley T, Schaap W. 1991.** The theory and practice of branch autonomy. *Annual Review of Ecology and Systematics* **22**(1): 309-334.
- Stein O, Granot D. 2019.** An Overview of Sucrose Synthases in Plants. *Front Plant Sci* **10**: 95.
- Stirbet A, Lazar D, Guo Y, Govindjee G. 2020.** Photosynthesis: basics, history and modelling. *Ann Bot* **126**(4): 511-537.
- Stormo GD. 2013.** Modeling the specificity of protein-DNA interactions. *Quant Biol* **1**(2): 115-130.
- Stormo GD, Schneider TD, Gold L, Ehrenfeucht A. 1982.** Use of the 'Perceptron' algorithm to distinguish translational initiation sites in E. coli. *Nucleic acids research* **10**(9): 2997-3011.
- Streb S, Egli B, Eicke S, Zeeman SC. 2009.** The debate on the pathway of starch synthesis: a closer look at low-starch mutants lacking plastidial phosphoglucomutase supports the chloroplast-localized pathway. *Plant Physiol* **151**(4): 1769-1772.
- Studer MH, DeMartini JD, Davis MF, Sykes RW, Davison B, Keller M, Tuskan GA, Wyman CE. 2011.** Lignin content in natural Populus variants affects sugar release. *Proceedings of the National Academy of Sciences* **108**(15): 6300-6305.
- Sturm A. 1999.** Invertases. Primary structures, functions, and roles in plant development and sucrose partitioning. *Plant Physiol* **121**(1): 1-8.

- Sturm A, Tang G-Q. 1999.** The sucrose-cleaving enzymes of plants are crucial for development, growth and carbon partitioning. *Trends in Plant Science* 4(10): 401-407.
- Stuttman J, Barthel K, Martin P, Ordon J, Erickson JL, Herr R, Ferik F, Kretschmer C, Berner T, Keilwagen J. 2021.** Highly efficient multiplex editing: one - shot generation of $8 \times$ *Nicotiana benthamiana* and $12 \times$ *Arabidopsis* mutants. *The Plant Journal* 106(1): 8-22.
- Sullivan AM, Arsovski AA, Lempe J, Bubb KL, Weirauch MT, Sabo PJ, Sandstrom R, Thurman RE, Neph S, Reynolds AP, et al. 2014.** Mapping and dynamics of regulatory DNA and transcription factor networks in *A. thaliana*. *Cell Rep* 8(6): 2015-2030.
- Sundell D, Mannapperuma C, Netotea S, Delhomme N, Lin YC, Sjödin A, Van de Peer Y, Jansson S, Hvidsten TR, Street NR. 2015.** The Plant genome integrative explorer resource: PlantGen IE. org. *New Phytologist* 208(4): 1149-1156.
- Sundell D, Street NR, Kumar M, Mellerowicz EJ, Kucukoglu M, Johnsson C, Kumar V, Mannapperuma C, Delhomme N, Nilsson O, et al. 2017.** AspWood: High-Spatial-Resolution Transcriptome Profiles Reveal Uncharacterized Modularity of Wood Formation in *Populus tremula*. *Plant Cell* 29(7): 1585-+.
- Takata N, Awano T, Nakata MT, Sano Y, Sakamoto S, Mitsuda N, Taniguchi T. 2019.** *Populus* NST/SND orthologs are key regulators of secondary cell wall formation in wood fibers, phloem fibers and xylem ray parenchyma cells. *Tree Physiol* 39(4): 514-525.
- Tarancón C, González-Grandío E, Oliveros JC, Nicolas M, Cubas P. 2017.** A conserved carbon starvation response underlies bud dormancy in woody and herbaceous species. *Frontiers in plant science* 8: 788.
- Tauberger E, Fernie AR, Emmermann M, Renz A, Kossmann J, Willmitzer L, Trethewey RN. 2000.** Antisense inhibition of plastidial phosphoglucomutase provides compelling evidence that potato tuber amyloplasts import carbon from the cytosol in the form of glucose - 6 - phosphate. *The Plant Journal* 23(1): 43-53.
- Taylor-Teeples M, Lin L, de Lucas M, Turco G, Toal TW, Gaudinier A, Young NF, Trabucco GM, Veling MT, Lamothe R, et al. 2015.** An *Arabidopsis* gene regulatory network for secondary cell wall synthesis. *Nature* 517(7536): 571-575.
- Taylor NG, Laurie S, Turner SR. 2000.** Multiple cellulose synthase catalytic subunits are required for cellulose synthesis in *Arabidopsis*. *Plant Cell* 12(12): 2529-2540.
- Tetlow IJ, Emes MJ. 2014.** A review of starch - branching enzymes and their role in amylopectin biosynthesis. *IUBMB life* 66(8): 546-558.
- The Arabidopsis Genome I. 2000.** Analysis of the genome sequence of the flowering plant *Arabidopsis thaliana*. *Nature* 408(6814): 796-815.

- Tian F, Yang DC, Meng YQ, Jin J, Gao G. 2020.** PlantRegMap: charting functional regulatory maps in plants. *Nucleic Acids Res* **48**(D1): D1104-D1113.
- Tixier A, Orozco J, Roxas AA, Earles JM, Zwieniecki MA. 2018.** Diurnal Variation in Nonstructural Carbohydrate Storage in Trees: Remobilization and Vertical Mixing. *Plant Physiology* **178**(4): 1602-1613.
- Trouillon J, Sentausa E, Ragno M, Robert-Genthon M, Lory S, Attrée I, Elsen S. 2020.** Species-specific recruitment of transcription factors dictates toxin expression. *Nucleic acids research* **48**(5): 2388-2400.
- Trumbore S, Czimczik CI, Sierra CA, Muhr J, Xu X. 2015.** Non-structural carbon dynamics and allocation relate to growth rate and leaf habit in California oaks. *Tree Physiol* **35**(11): 1206-1222.
- Tu X, Mejía-Guerra MK, Franco JAV, Tzeng D, Chu P-Y, Shen W, Wei Y, Dai X, Li P, Buckler ES. 2020.** Reconstructing the maize leaf regulatory network using ChIP-seq data of 104 transcription factors. *Nature communications* **11**(1): 1-13.
- Tuskan GA, Difazio S, Jansson S, Bohlmann J, Grigoriev I, Hellsten U, Putnam N, Ralph S, Rombauts S, Salamov A, et al. 2006.** The genome of black cottonwood, *Populus trichocarpa* (Torr. & Gray). *Science* **313**(5793): 1596-1604.
- Vanholme R, De Meester B, Ralph J, Boerjan W. 2019.** Lignin biosynthesis and its integration into metabolism. *Curr Opin Biotechnol* **56**: 230-239.
- Verbancic J, Lunn JE, Stitt M, Persson S. 2018.** Carbon Supply and the Regulation of Cell Wall Synthesis. *Mol Plant* **11**(1): 75-94.
- Wang H, Zhao Q, Chen F, Wang M, Dixon RA. 2011.** NAC domain function and transcriptional control of a secondary cell wall master switch. *The Plant Journal* **68**(6): 1104-1114.
- Wang JP, Matthews ML, Williams CM, Shi R, Yang C, Tunlaya-Anukit S, Chen HC, Li Q, Liu J, Lin CY, et al. 2018.** Improving wood properties for wood utilization through multi-omics integration in lignin biosynthesis. *Nat Commun* **9**(1): 1579.
- Wang L, Li XR, Lian H, Ni DA, He YK, Chen XY, Ruan YL. 2010.** Evidence that high activity of vacuolar invertase is required for cotton fiber and Arabidopsis root elongation through osmotic dependent and independent pathways, respectively. *Plant Physiol* **154**(2): 744-756.
- Wang W, Viljamaa S, Hodek O, Moritz T, Niittylä T. 2022.** Sucrose synthase activity is not required for cellulose biosynthesis in Arabidopsis. *The Plant Journal*.
- Wang Z, Mao Y, Guo Y, Gao J, Liu X, Li S, Lin YJ, Chen H, Wang JP, Chiang VL, et al. 2020.** MYB Transcription Factor161 Mediates Feedback Regulation of Secondary wall-associated NAC-Domain1 Family Genes for Wood Formation. *Plant Physiol* **184**(3): 1389-1406.
- Weber B, Zicola J, Oka R, Stam M. 2016.** Plant Enhancers: A Call for Discovery. *Trends Plant Sci* **21**(11): 974-987.

- Wei Z, Qu Z, Zhang L, Zhao S, Bi Z, Ji X, Wang X, Wei H. 2015.** Overexpression of poplar xylem sucrose synthase in tobacco leads to a thickened cell wall and increased height. *PLoS One* **10**(3): e0120669.
- Welham T, Pike J, Horst I, Flemetakis E, Katinakis P, Kaneko T, Sato S, Tabata S, Perry J, Parniske M, et al. 2009.** A cytosolic invertase is required for normal growth and cell development in the model legume, *Lotus japonicus*. *J Exp Bot* **60**(12): 3353-3365.
- Weston K. 1998.** Myb proteins in life, death and differentiation. *Current opinion in genetics & development* **8**(1): 76-81.
- White AC, Rogers A, Rees M, Osborne CP. 2016.** How can we make plants grow faster? A source–sink perspective on growth rate. *Journal of Experimental Botany* **67**(1): 31-45.
- Wiley E, Helliker B. 2012.** A re - evaluation of carbon storage in trees lends greater support for carbon limitation to growth. *New Phytologist* **195**(2): 285-289.
- Wiley E, Hoch G, Landhausser SM. 2017.** Dying piece by piece: carbohydrate dynamics in aspen (*Populus tremuloides*) seedlings under severe carbon stress. *J Exp Bot* **68**(18): 5221-5232.
- Wilkinson MD, Dumontier M, Aalbersberg IJ, Appleton G, Axton M, Baak A, Blomberg N, Boiten J-W, da Silva Santos LB, Bourne PE. 2016.** The FAIR Guiding Principles for scientific data management and stewardship. *Scientific data* **3**(1): 1-9.
- Wu L, Zhang M, Zhang R, Yu H, Wang H, Li J, Wang Y, Hu Z, Wang Y, Luo Z. 2021.** Down-regulation of OsMYB103L distinctively alters beta-1, 4-glucan polymerization and cellulose microfibrils assembly for enhanced biomass enzymatic saccharification in rice. *Biotechnology for biofuels* **14**(1): 1-15.
- Wu VW, Thieme N, Huberman LB, Dietschmann A, Kowbel DJ, Lee J, Calhoun S, Singan VR, Lipzen A, Xiong Y, et al. 2020.** The regulatory and transcriptional landscape associated with carbon utilization in a filamentous fungus. *Proc Natl Acad Sci U S A* **117**(11): 6003-6013.
- Würth MK, Pelaez-Riedl S, Wright SJ, Korner C. 2005.** Non-structural carbohydrate pools in a tropical forest. *Oecologia* **143**(1): 11-24.
- Yamaguchi M, Kubo M, Fukuda H, Demura T. 2008.** Vascular-related NAC-DOMAIN7 is involved in the differentiation of all types of xylem vessels in *Arabidopsis* roots and shoots. *Plant J* **55**(4): 652-664.
- Yamaguchi M, Mitsuda N, Ohtani M, Ohme-Takagi M, Kato K, Demura T. 2011.** VASCULAR-RELATED NAC-DOMAIN7 directly regulates the expression of a broad range of genes for xylem vessel formation. *Plant J* **66**(4): 579-590.
- Yamaguchi M, Ohtani M, Mitsuda N, Kubo M, Ohme-Takagi M, Fukuda H, Demura T. 2010.** VND-INTERACTING2, a NAC domain transcription factor, negatively regulates xylem vessel formation in *Arabidopsis*. *Plant Cell* **22**(4): 1249-1263.

- Yamasaki K, Kigawa T, Seki M, Shinozaki K, Yokoyama S. 2013.** DNA-binding domains of plant-specific transcription factors: structure, function, and evolution. *Trends in Plant Science* **18**(5): 267-276.
- Yang HW, Akagi T, Kawakatsu T, Tao R. 2019.** Gene networks orchestrated by MeGI: a single-factor mechanism underlying sex determination in persimmon. *Plant J* **98**(1): 97-111.
- Yang L, Xu M, Koo Y, He J, Poethig RS. 2013.** Sugar promotes vegetative phase change in *Arabidopsis thaliana* by repressing the expression of MIR156A and MIR156C. *Elife* **2**: e00260.
- Yang S-D, Seo PJ, Yoon H-K, Park C-M. 2011.** The *Arabidopsis* NAC transcription factor VNI2 integrates abscisic acid signals into leaf senescence via the COR/RD genes. *The Plant Cell* **23**(6): 2155-2168.
- Yao J, Shen Z, Zhang Y, Wu X, Wang J, Sa G, Zhang Y, Zhang H, Deng C, Liu J. 2020.** *Populus euphratica* WRKY1 binds the promoter of H⁺-ATPase gene to enhance gene expression and salt tolerance. *Journal of Experimental Botany* **71**(4): 1527-1539.
- Yazaki J, Galli M, Kim AY, Nito K, Aleman F, Chang KN, Carvunis A-R, Quan R, Nguyen H, Song L. 2016.** Mapping transcription factor interactome networks using HaloTag protein arrays. *Proceedings of the National Academy of Sciences* **113**(29): E4238-E4247.
- Yu SM, Lo SF, Ho TD. 2015.** Source-Sink Communication: Regulated by Hormone, Nutrient, and Stress Cross-Signaling. *Trends Plant Sci* **20**(12): 844-857.
- Zeeman SC, Smith SM, Smith AM. 2007.** The diurnal metabolism of leaf starch. *Biochem J* **401**(1): 13-28.
- Zhang J, Xie M, Tuskan GA, Muchero W, Chen JG. 2018.** Recent Advances in the Transcriptional Regulation of Secondary Cell Wall Biosynthesis in the Woody Plants. *Front Plant Sci* **9**: 1535.
- Zhang Y, Liu T, Meyer CA, Eeckhoutte J, Johnson DS, Bernstein BE, Nusbaum C, Myers RM, Brown M, Li W. 2008.** Model-based analysis of ChIP-Seq (MACS). *Genome biology* **9**(9): 1-9.
- Zhao Y, Li X, Xie J, Xu W, Chen S, Zhang X, Liu S, Wu J, El-Kassaby YA, Zhang D. 2022.** Transposable Elements: Distribution, Polymorphism, and Climate Adaptation in *Populus*. *Frontiers in plant science* **13**: 814718-814718.
- Zhao Y, Sun J, Xu P, Zhang R, Li L. 2014.** Intron-mediated alternative splicing of WOOD-ASSOCIATED NAC TRANSCRIPTION FACTOR1B regulates cell wall thickening during fiber development in *Populus* species. *Plant Physiol* **164**(2): 765-776.
- Zhong R, Demura T, Ye ZH. 2006.** SND1, a NAC domain transcription factor, is a key regulator of secondary wall synthesis in fibers of *Arabidopsis*. *Plant Cell* **18**(11): 3158-3170.

- Zhong R, Lee C, Ye ZH. 2010a.** Evolutionary conservation of the transcriptional network regulating secondary cell wall biosynthesis. *Trends Plant Sci* **15**(11): 625-632.
- Zhong R, Lee C, Ye ZH. 2010b.** Functional characterization of poplar wood-associated NAC domain transcription factors. *Plant Physiol* **152**(2): 1044-1055.
- Zhong R, Richardson EA, Ye ZH. 2007.** The MYB46 transcription factor is a direct target of SND1 and regulates secondary wall biosynthesis in Arabidopsis. *Plant Cell* **19**(9): 2776-2792.
- Zhong R, Ye ZH. 2010.** The poplar PtrWNDs are transcriptional activators of secondary cell wall biosynthesis. *Plant Signal Behav* **5**(4): 469-472.
- Zhong R, Ye ZH. 2012.** MYB46 and MYB83 bind to the SMRE sites and directly activate a suite of transcription factors and secondary wall biosynthetic genes. *Plant Cell Physiol* **53**(2): 368-380.
- Zhou J, Lee C, Zhong R, Ye Z-H. 2009.** MYB58 and MYB63 are transcriptional activators of the lignin biosynthetic pathway during secondary cell wall formation in Arabidopsis. *The Plant Cell* **21**(1): 248-266.
- Zhou J, Zhong R, Ye ZH. 2014.** Arabidopsis NAC domain proteins, VND1 to VND5, are transcriptional regulators of secondary wall biosynthesis in vessels. *PLoS One* **9**(8): e105726.

Popular science summary

Plants take up carbon dioxide from the atmosphere, acting as carbon sinks combatting climate change. The absorbed carbon is distributed to either growth or storage in the plant, and it is used both as a building material and for energy. In an aspen tree, a significant amount of carbon is put aside for long-term storage as starch, while most of the carbon used for growth is first distributed as sucrose and then used for wood formation.

The distribution of carbon inside the tree is described in the terms of source-sink dynamics, where photosynthetic tissues and organs such as leaves are the source while for example the developing wood is an important carbon sink. There is still much that is not known about how trees grow: how carbon is distributed between the two central processes of growth and storage, how sources and sinks communicate and regulate the flow of carbon, and which factors regulate the cell- and tissue-level processes in the sources and sinks themselves. For example, previous research has indicated that carbon allocation in developing wood is under regulation of proteins called transcription factors, but the regulatory mechanisms are mostly unknown.

In this PhD thesis I present results from four research projects related to different aspects of carbon allocation, tree growth and source-sink relationships. My results fill key knowledge gaps in the field and provide new starting points for future research projects on carbon allocation in trees.

Populärvetenskaplig sammanfattning

Växter fångar upp koldioxid från atmosfären, och är därmed viktiga kolsänkor som motarbetar klimatförändringen. Kol som absorberas distribueras antingen för att användas i tillväxt eller för att lagras, och det används i växten både som byggnadsmaterial och som energikälla. I ett aspträd lagras en stor del av kolet direkt som stärkelse, medan det mesta av kolet som används för tillväxt distribueras först som sukros och används sedan för att bygga upp vedämne.

Kolfördelningen i trädet beskrivs som ett samspel av källor och sänkor: fotosyntetiska vävnader och organ, såsom löv, är kolkällor medan till exempel vedbildning och ved under utveckling är viktiga kolsänkor. Det finns fortfarande mycket som vi inte vet om hur träd växer: hur kol fördelas mellan de två centrala processerna för tillväxt och lagring, hur källor och sänkor kommunicerar med varandra och reglerar kolflödet, samt vilka faktorer som reglerar processerna på cell- och vävnadsnivå i sänkor och källor. Tidigare forskning har till exempel visat att kolfördelningen i ved under utveckling regleras av en grupp proteiner som kallas för transkriptionsfaktorer, men själva regleringsmekanismerna är mestadels okända.

I denna doktorsavhandling presenterar jag resultat från fyra forskningsprojekt som är relaterade till olika aspekter av kolfördelning, trädutveckling, samt relation mellan kolkällor och kolsänkor. Mina resultat fyller viktiga kunskapsluckor inom fältet och erbjuder nya utgångspunkter för framtida forskningsprojekt kring kolfördelning i träd.

Suomenkielinen tiivistelmä

Yhteyttävät eli fotosyntetisoivat kasvit sitovat itseensä ilmakehän hiilidioksidia ja toimivat ilmastonmuutosta hidastavina hiilinieluinä. Sidottu hiili päätyy joko varastoon tai hyödynnettäväksi kasvussa, ja kasvit käyttävät sitä sekä rakennusmateriaalina että energianlähteenä. Esimerkiksi haapa varastoi merkittävän osan sitomastaan hiilestä tärkkelykseksi, jota voidaan säilyttää puussa pitkään, kun taas suurin osa kasvuun hyödynnettävästä hiilestä kuljetetaan puussa ensin sukroosina ja käytetään lopulta puuaineksen muodostamiseen.

Hiilen jakautumista puussa voidaan havainnollistaa lähde-nielu -dynamiikan avulla: yhteyttävät solukot ja kasvinosat kuten lehdet toimivat hiilen lähteinä kun taas esimerkiksi kehittyvä puuaines on tärkeä hiilinielu. Moni puiden kasvuun liittyvä yksityiskohta on vielä puutteellisesti tunnettu. Emme esimerkiksi tiedä kuinka hiili jaetaan eli allokoidaan kasvuun ja varastointiin, kuinka lähteiden ja nielujen väliset vuoro-vaikutukset vaikuttavat hiilen liikkeisiin puussa tai mitkä tekijät säätelevät solu- ja solukkotason tapahtumia hiilen lähteissä ja nieluissa. Aiemmissä tutkimuksissa on havaittu, että transkriptiotekijöiksi eli transkriptio-faktoreiksi kutsutut proteiinit ohjaavat hiilen allokaatiota kehittyvässä puussa, mutta niiden säätelymekanismeja ei vielä tunneta hyvin.

Väitöskirjassani esittelen tuloksia neljästä hiilen allokaatioon, puiden kasvuun sekä lähde-nielu -suhteisiin liittyvästä tutkimusprojektista. Tulokseni täyttävät tieteenalan tietoaaukkoja ja tarjoavat uusia lähtökohtia tuleville hiilen allokaatioon liittyville tutkimusprojekteille.

Acknowledgements

This PhD thesis would not have been completed without the help of the people listed here. Now that I'm heading toward new adventures, it's only right to thank you all.

First, I would like to thank my supervisor **Dr. Totte Niittylä** for giving me the opportunity to work on these interesting and challenging projects. I am grateful for your support, encouragement, guidance and patience during these years. Kiitos!

A special thanks goes to the current and previous members of my research group.

Anne, thank you for fikas and lunches, biking trips, gardening, cat-watching, running, and other activities; help with sampling and sectioning, discussions about science and life in general, and your friendship. Let's stay in touch!

Junko, it has been lovely to share an office with you and to lighten the working day with all our conversations. Thank you for your help with the cell wall lab analyses, and for letting me to assist in teaching. ありがとうございます！

Wei, thank you for all your help in the lab and many good suggestions during experiment planning. I have learned so much from working together with you.

Yohann, Pratibha, Huiling, Xin, Tanja, Loïc, Pieter, Tayebbeh, Sacha and Romain, thank you for your support and advice during the years of my PhD studies.

Teitur Ahlgren Kalman and Nicolas Delhomme, I cannot thank you enough for all your help and support with bioinformatics and data analysis.

I would like to thank the members of my reference group, **Nathaniel Street**, **Torgeir Hvidsten**, **László Bakó** and **Stephanie Robert**, for your feedback and helpful suggestions. Thank you especially Nat and Torgeir for your bioinformatics expertise.

I also would like to thank my opponent **Prof. Andrew D. Friend** as well as the members of the evaluation committee, **Prof. Torgny Näsholm**, **Prof. Leszek Kleczkowski** and **Dr. Kaisa Nieminen**, for taking the time to thoroughly evaluate my work.

Thanks to **the staff at the UPSC Poplar transformation facility** and the **Greenhouses** for taking good care of my trees.

A warm thank you to **all the colleagues at UPSC and SLU**. I am grateful for your help, advice and support. Thank you for making this a working place with a nice atmosphere! Special thanks to **the usual lunch crowd at the long table** for long and varied discussions about science, academia, life, and everything else.

Additional special thanks to everyone who is and has been involved in making UPSC an even better workplace through their involvement in the **UPSC Garden ☘**, **Greener UPSC** or the currently inactive **UPSC Wellness group**. It has been fun to organize all kinds of activities together with you!

Work is definitely not all that is important in life. Through the many, many clubs and organizations I am and have been involved with I have met **a lot of lovely people**, who have encouraged me during the PhD journey and brightened my days. You are too many to mention here by name, but you'll know who you are.

Ett stort tack till **SLI och byggruppen på lajvområdet i Tällberg** för allt lajvande, bygge, potatisbullar och myggiga sommandagar i världens kulaste lag och trevligaste sällskap.

Tack till allt gott folk i **medeltidsföreningen Uma**, speciellt ni som har varit med och dansat historiska danser.

Tack även **Umeå folkmusikföreningen** för både dans och trevligt musik.

Tack till **Björkstadens aikidoklubb**, ni har hjälpt mig bli starkare både fysiskt och mentalt. Nu har jag nått mitt mål och fått både de svarta, fina hakama-byxorna och den svarta, fina doktorshatten, vilket säkert betyder att nästa målet blir det svarta, fina bältet!

Kiitos kaikille **ystävilleni** lähellä ja kaukana. Erityiskiitokset **Oulun taikatytöporukalle** (∞+!) sekä **OIEI:n heimolle** mukavista hetkistä yhdessä, viime aikoina lähinnä etäyhteyden kautta. Toivottavasti nähdään pian ihan oikeasti!

Suurkiitokset **kotiväelle**. Kiitos monen monituisista postikorteista, puhelinsoitoista ja elämysristeilyistä. Kiitos tuesta, kannustuksesta ja kaikesta.

Aspen growth is not limited by starch reserves

Highlights

- Aspen trees employ a passive starch-storage mechanism during growth
- Carbon assimilation is not limiting growth of aspen trees under benign conditions
- Starch is not required for bud set and bud flush or its timing in aspen trees

Authors

Wei Wang, Loic Talide, Sonja Viljamaa, Totte Niittylä

Correspondence

totte.niittyla@slu.se

In brief

Wang et al. create low-starch aspen mutants and discover that aspen trees employ a passive investing strategy to save carbon for future needs and that tree growth is not carbon limited under benign conditions.



Report

Aspen growth is not limited by starch reserves

Wei Wang,¹ Loic Talide,¹ Sonja Viljamaa,¹ and Totte Niittylä^{1,2,*}¹Department of Forest Genetics and Plant Physiology, Swedish University of Agricultural Sciences, Umeå Plant Science Centre, Umeå S-901 83, Sweden²Lead contact*Correspondence: totte.niittyla@slu.se<https://doi.org/10.1016/j.cub.2022.06.056>

SUMMARY

All photosynthetic organisms balance CO₂ assimilation with growth and carbon storage. Stored carbon is used for growth at night and when demand exceeds assimilation. Gaining a mechanistic understanding of carbon partitioning between storage and growth in trees is important for biological studies and for estimating the potential of terrestrial photosynthesis to sequester anthropogenic CO₂ emissions.^{1,2} Starch represents the main carbon storage in plants.^{3,4} To examine the carbon storage mechanism and role of starch during tree growth, we generated and characterized low-starch hybrid aspen (*Populus tremula* × *tremuloides*) trees using CRISPR-Cas9-mediated gene editing of two *PHOSPHOGLUCOMUTASE* (*PGM*) genes coding for plastidial *PGM* isoforms essential for starch biosynthesis. We demonstrate that starch deficiency does not reduce tree growth even in short days, showing that starch is not a critical carbon reserve during diel growth of aspen. The low-starch trees assimilated up to ~30% less CO₂ compared to the wild type under a range of irradiance levels, but this did not reduce growth or wood density. This implies that aspen growth is not limited by carbon assimilation under benign growth conditions. Moreover, the timing of bud set and bud flush in the low-starch trees was not altered, implying that starch reserves are not critical for the seasonal growth-dormancy cycle. The findings are consistent with a passive starch storage mechanism that contrasts with the annual *Arabidopsis* and indicate that the capacity of the aspen to absorb CO₂ is limited by the rate of sink tissue growth.

RESULTS AND DISCUSSION

Our understanding of how the balance between tree growth and carbon storage is achieved is incomplete and often extrapolated from studies of annual herbs, like *Arabidopsis thaliana*. *Arabidopsis* utilizes an active storage mechanism whereby starch accumulation is adjusted to optimize growth and survival over the entire life cycle.⁵ The extent to which the *Arabidopsis*-based model is applicable to trees is unclear. Tree growth models have historically depicted starch reserves as buffers, accumulating excess carbon on a daily or seasonal basis, the so-called passive storage model.^{6,7} However, there is also experimental evidence indicating that trees actively store starch at the expense of growth.^{7–9}

Multiple studies have indicated a role for starch in providing carbon and energy when photosynthesis or sugar transport is limited, e.g., during dormancy, bud flush, or stress.^{8,10–14} A genetic link between seasonal starch content variation and stress has been observed for genomic variation connected to carbon storage in *Populus trichocarpa*. The storage carbohydrate variation in the outer stem and roots during dormancy was heritable and adapted to local climate, with greater starch reserves correlating with warmer and drier environments.¹⁵ The authors observed that genetic variation of stem starch content during dormancy did not correlate with genetic variation in stem diameter, suggesting that storage in the stem is independent of secondary growth in *Populus*.¹⁵ Thus, current results support a role

for starch in stress adaptation and during seasonal changes, but when tree growth is not limited by environmental factors its role remains less clear.^{7,8} Leaf starch content of growing almond (*Prunus dulcis*) trees increased during the day and decreased at night, supporting a role for leaf starch in maintaining growth and carbon balance during the diurnal cycle.¹⁶ However, despite many studies documenting tree starch levels, the relationship between starch and tree growth has been difficult to address. Progress has been hampered by the lack of mutant trees with defective starch metabolism. Starch is synthesized from ADP-glucose in the plastids, which in chloroplasts is derived from the reduction of CO₂ in the Calvin cycle.¹⁷ ADP-glucose biosynthesis in the plastids requires the activity of phosphoglucomutase (*PGM*), which facilitates the interconversion of glucose-6-phosphate and glucose-1-phosphate. Glucose-1-phosphate is the substrate of ADP-glucose pyrophosphorylase (*AGPase*), which catalyzes the synthesis of ADP-glucose. Consequently, *Arabidopsis pgm* and *adg1* mutants that lack plastidial *PGM* or *AGPase* contain only limited residual starch.^{18–20}

Low-starch aspen *pgm1pgm2* mutants

We identified two plastidial *PHOSPHOGLUCOMUTASE* genes (*PGM1* and *PGM2*) in the *Populus* genome, based on 89% amino acid sequence identity to *Arabidopsis PGM1* and the presence of a predicted plastid targeting sequence (Figure S1). CRISPR-Cas9-mediated gene editing was used to create mutations in *PGM1* and *PGM2*. Ten lines containing allelic homozygous



mutations were identified by PCR using gene-specific primers, then restriction enzyme digestion of the PCR products (Figure S1). Two lines—*pgm1pgm2* lines 1 and 2—were selected for detailed characterization. Sequencing the gene-edited loci revealed single base pair insertions causing premature stop codons in the second exon of both *PGM1* and *PGM2* (Figure 1A). Iodine staining indicated that both lines lacked starch in fully expanded source leaves harvested at the end of the light period, and in phloem tissues and root tips (Figures 1B–1D). The low-starch phenotype was confirmed by a quantitative assay, establishing that the double mutants contained no or only trace levels of leaf starch at the end of the photoperiod (Figure 1E).

Starch is not a critical carbon reserve during diurnal aspen growth

To assess the contribution of starch to tree growth, wild-type (WT) and *pgm1pgm2* trees were grown under 18-h/6-h day/night cycle in an automated phenotyping facility. No significant difference was observed in the height growth rate (Figure 2A) at the end of the growth period, stem thickness, wood density, and biomass of stems and leaves between WT and *pgm1pgm2* lines (Table S1). Root biomass obtained from a separate greenhouse experiment was also similar (Table S1). The only visible difference was a change in the petiole and leaf angle, resulting in slightly drooping leaves (Figure 2B). The leaf angle change caused a reduction in the canopy area of both lines when imaged from above, while in the side view only line 1 differed slightly from the WT (Figures 2C and 2D).

The normal growth of the *pgm1pgm2* trees is reminiscent of the *pgm* mutants of *Lotus japonicus* and *Pisum sativum*, which also grow well under a day/night cycle.^{21,22} Thus, the aspen phenotype is not unique in this regard. In contrast, Arabidopsis and tobacco *pgm* mutants exhibit carbon depletion at night and significantly reduced growth rates except under very long days or constant light.^{20,23} The fully expanded source leaves of WT aspen exhibited clear starch turnover during a diurnal cycle, with higher levels of starch at the end of the day than the end of the night (Figure 3A). These observations suggest that leaf starch supports growth and respiration during the diurnal cycle in aspen but does not play the critical role observed in Arabidopsis and tobacco. Investigation of the relationship between day length, growth, and starch levels in trees is complicated by tree species from the temperate zones of the world that have evolved to respond to day-length change to ensure correct timing of growth cessation and dormancy. In the aspen genotype used in this study, shortening of the day to approximately 15 h induces dormancy.^{24,25} However, the onset of dormancy takes several weeks and the growth rate is first reduced 3–4 weeks after the change from 18-h/6-h to 14-h/10-h or 8-h/16-h day/night cycle (Figure S2). These results show that the *pgm1pgm2* and WT trees grow at a similar rate under both 14-h/10-h and 8-h/16-h cycles.

Lack of starch does not affect soluble sugar pools in leaves or developing wood

To further investigate the carbohydrate status of the *pgm1pgm2* trees, we quantified sucrose, glucose, and fructose levels in the youngest fully expanded source leaves of trees grown under an 18-h/6-h day/night cycle. No significant difference between WT

and the mutants was observed (Figure 3B). In contrast, Arabidopsis *pgm* mutants accumulate significantly more sucrose, glucose, and fructose during the day compared to WT.²³ We noted that the fully expanded aspen source leaves contained 25–35 $\mu\text{mol g}^{-1} \text{FW}^{-1}$ sucrose, glucose, and fructose, approximately an order of magnitude more than the values reported for Arabidopsis rosette leaves.^{23,26} The relatively high soluble sugar pool in aspen leaves is thought to be associated with the passive symplasmic phloem loading mechanism.^{27,28} In the greenhouse-grown trees, the starch content in fully expanded WT source leaves at the end of the day was, on average, 100–150 $\mu\text{mol glucose equivalents g}^{-1} \text{FW}^{-1}$ (Figures 1 and 3), which is higher but broadly comparable with the 30–60 $\mu\text{mol g}^{-1} \text{FW}^{-1}$ typically reported for Arabidopsis.^{23,29} The ratio of glucose equivalents in starch and sucrose at the end of the photoperiod in the source leaves between the two different experiments reported in Figures 1 and 3 was similar: 1.7:1 and 1.6:1, respectively. Hence, aspen does not exhibit characteristics of a sucrose-storing species such as barley (*Hordeum vulgare*), which stores more sucrose than starch in leaves.³⁰ However, the sucrose pool in aspen leaves may be sufficient to maintain sugar homeostasis at night in the low-starch trees. Accordingly, we observed a reduction in the source leaf sucrose content between the end of the day and of the night in both WT and *pgm1pgm2* (Figure 3C). A similar decrease was also observed when comparing source leaves of trees transferred from 18-h/6-h to 8-h/16-h day/night (Figure 3D). To assess whether the source leaves of *pgm1pgm2* trees were experiencing carbon depletion, we analyzed the expression of carbon depletion marker genes at the end of the 16-h night. Quantitative real-time PCR analysis of the *Populus DARK INDUCIBLE 6 (DIN6)*, *DORMANCY-ASSOCIATED PROTEIN-LIKE 1 (DRM1)*, and *GIBBERELLIN-STIMULATED ARABIDOPSIS 6 (GASA6)* gene transcripts previously shown to respond to carbon depletion³¹ revealed no significant differences between WT and the mutants (Figure 3E). These results suggest that both starch and sucrose are utilized in aspen at night or when carbon demand exceeds assimilation, but that starch is not critical.

CO₂ assimilation is reduced in *pgm1pgm2* trees

If carbon was limiting tree growth and/or starch accumulation occurred at the expense of growth, the absence of starch biosynthesis in *pgm1pgm2* could be expected to free more carbon for growth. Since the blocked starch biosynthesis pathway did not cause obvious changes in tree growth, wood density, or soluble sugar levels, we investigated carbon assimilation rates in the WT and mutants. We measured CO₂ assimilation at different light intensities and leaf transpiration as a proxy for stomatal conductance. Under irradiance up to 100 $\mu\text{mol quanta m}^{-2} \text{s}^{-1}$, the *pgm1pgm2* lines did not differ from WT, but at higher irradiances the mutants showed reduced CO₂ uptake (Figure 4A). No significant difference occurred in leaf transpiration, showing that the reduction in CO₂ assimilation was not caused by reduced stomatal conductance (Figure 4B). To determine whether impaired absorption of light in *pgm1pgm2* source leaves contributed to the reduced CO₂ assimilation rate, we assayed chlorophyll content and the photosynthesis light-dependent reactions. The *pgm1pgm2* leaves had slightly increased chlorophyll content while all of the photosynthetic

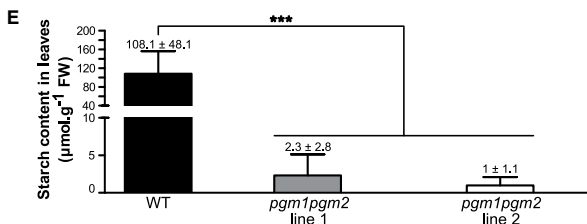
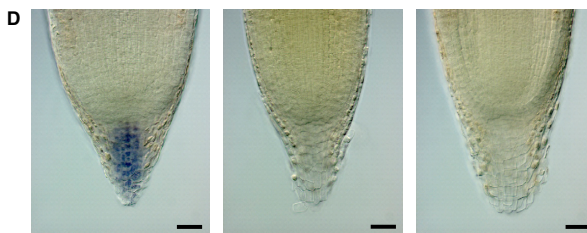
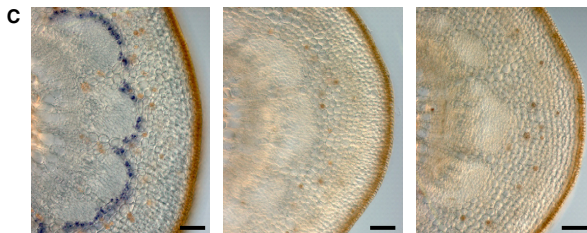
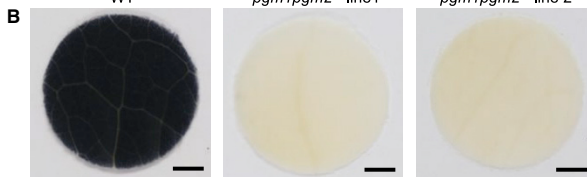
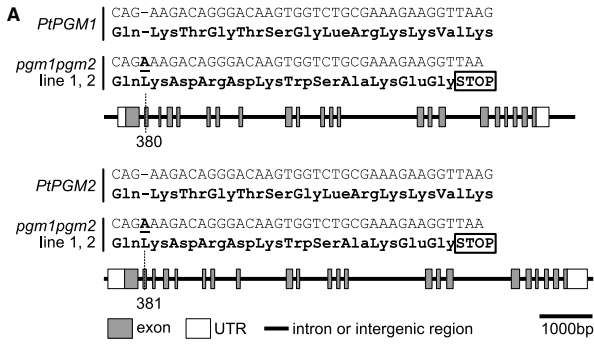


Figure 1. Mutation of the PHOSPHOGLUCOMUTASE1 and 2 genes in *Populus tremula* \times *tremuloides* and the low-starch phenotype of the *pgm1pgm2* mutants

(A) Schematic diagram showing the gene-edited mutations in the *PGM1* and *PGM2* genes and the resulting premature stop codons. See also Figure S1.

(B) Iodine-stained leaf discs from fully expanded source leaves of wild-type (WT) and *pgm1pgm2* line 1 and line 2 harvested at the end of the photoperiod.

(C and D) Iodine-stained stem cross-sections (C) and root tips of WT and *pgm1pgm2* line 1 and line 2 (D).

Scale bars, 3 mm (B), 40 μm (C), and 20 μm (D).

(E) Starch content in fully expanded source leaves of WT and *pgm1pgm2* line 1 and line 2. Note discontinuous y axis.

Data are mean \pm SD from 4, 5, and 5 biological replicates for WT, *pgm1pgm2* line 1, and line 2, respectively. *** $p < 0.001$ according to one-way ANOVA and Tukey post hoc test. See also Figure S4.

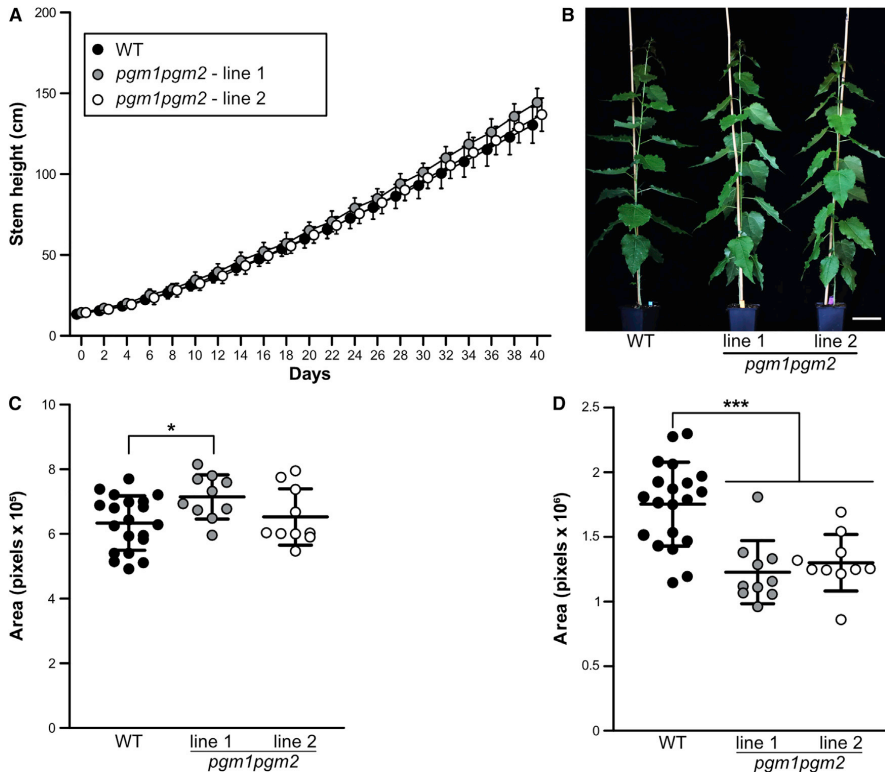


Figure 2. Morphology of *Populus tremula* × *tremuloides* WT and *pgm1pgm2* mutant trees

(A) Height growth rate of trees grown in an automated phenotyping facility for 40 days in an 18-h photoperiod. (B) Morphology of 1-month-old trees grown in an 18-h photoperiod. Scale bar, 10 cm.

(C and D) Canopy area imaged from the side (C) and from above (D).

Data are mean ± SD from 20, 10, and 10 biological replicates for WT, *pgm1pgm2* line 1, and line 2, respectively. *** $p < 0.001$ and ** $p < 0.05$ according to one-way ANOVA and Tukey post hoc test.

See also Figures S2 and S3 and Table S1.

parameters were comparable between the mutants and WT (Table S2). We conclude that impaired absorption of light in *pgm1pgm2* leaves does not explain the reduced CO_2 assimilation rate; a more likely explanation is a reduced flux through the photosynthetic carbon reduction cycle.

Control of carbon flux to starch in aspen leaves differs from Arabidopsis

In the automated growth phenotyping experiments, the photosynthetically active light intensity was 180–200 $\mu\text{mol quanta m}^{-2} \text{s}^{-1}$. It was possible that, at this level, the difference in the CO_2 assimilation rate between *pgm1pgm2* and WT is still too subtle to affect growth. To test this, the trees were grown under 500 $\mu\text{mol quanta m}^{-2} \text{s}^{-1}$ for 8 weeks. The mutants and WT again exhibited similar growth rate and wood density (Figure S2) while the CO_2 assimilation rate, but not stomatal conductance, was still reduced in the *pgm1pgm2* trees (Figures 4C and 4D).

Reduced photosynthesis in response to increasing light intensity has also been observed in the *pgm* and *adg* Arabidopsis mutants.^{20,32} However, one difference is that the photosynthesis is light saturated earlier in Arabidopsis *pgm* mutants compared to WT.³² In the *pgm1pgm2* and WT aspen leaves, the rate of CO_2 assimilation in response to increasing light begins to deviate after 100 $\mu\text{mol quanta m}^{-2} \text{s}^{-1}$ for both genotypes and does not become saturated until >1,500 (Figure 4).

We hypothesized that the lack of inhibition of CO_2 assimilation at $\leq 100 \mu\text{mol quanta m}^{-2} \text{s}^{-1}$ in *pgm1pgm2* aspens may reflect low carbon flux to the starch biosynthesis pathway in low light, and consequently lack of feedback inhibition of CO_2 assimilation when the pathway is blocked in the *pgm1pgm2*. To explore this, we compared the source leaf starch levels in WT trees grown in 18-h/6-h day/night cycles under irradiance of ~ 150 and $\sim 70 \mu\text{mol quanta m}^{-2} \text{s}^{-1}$. Even under the lower irradiance the trees continued to grow, suggesting growth adaptation to low

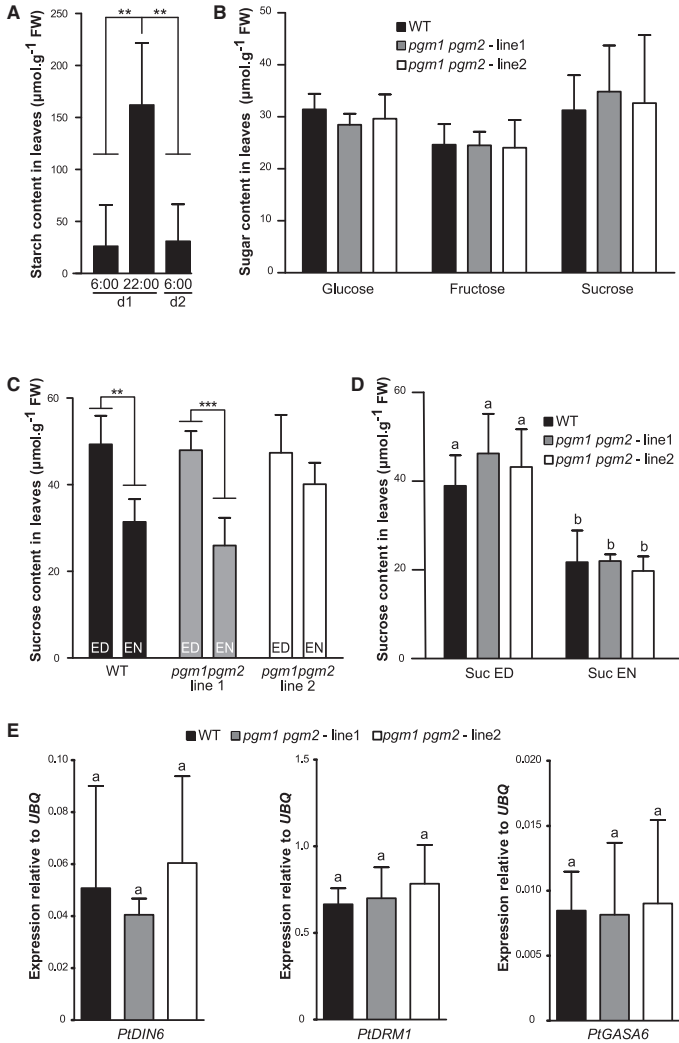


Figure 3. Starch, soluble sugar content, and carbon depletion marker gene expression in *Populus tremula* × *tremuloides* WT and *pgm1pgm2* leaves

(A) WT source leaf starch content at the onset of the photoperiod day 1 (06:00-d1), at the end of the photoperiod day 1 (22:00-d1), and at the onset of the photoperiod day 2 (06:00-d2). Data are mean ± SD from 5 biological replicates.

(B) Glucose, fructose, and sucrose levels in leaves from WT and *pgm1pgm2* grown in 18-h photoperiod in the middle of the photoperiod. Data are mean ± SD from 4, 5, and 5 biological replicates for WT, *pgm1pgm2* line 1, and line 2, respectively. (C) Source leaf sucrose content in WT and *pgm1pgm2* mutant trees grown in 18-h photoperiod. Samples were harvested at the end of day (ED) and at the end of night (EN). Data are mean ± SD from 5 biological replicates.

(A–C) *** $p < 0.001$ and ** $p < 0.01$ according to one-way ANOVA and Tukey post hoc test.

(D) Sucrose content in the source leaves of WT and *pgm1pgm2* trees after 10 days under 8-h short-day conditions. ED, end of the day; EN, end of the night.

(E) Relative transcript expression levels of carbon depletion genes in source leaves of WT and *pgm1pgm2* harvested at the end of the night after 10 days under 8-h short-day conditions. *PUBQ* is used as a reference.

(D and E) Values are means ± SD, $n = 5$ biological replicates. $p < 0.05$ according to one-way ANOVA and Tukey post hoc test. FW, fresh weight. See also Figure S2.

light and carbon supply (Figure S2). The trees growing in under $\sim 70 \mu\text{mol quanta m}^{-2} \text{ s}^{-1}$ contained only $\sim 10 \mu\text{mol g}^{-1} \text{FW}^{-1}$ starch at the end of the day while the trees under $\sim 150 \mu\text{mol quanta m}^{-2} \text{ s}^{-1}$ contained $\sim 74 \mu\text{mol g}^{-1} \text{FW}^{-1}$ (Figure S2) and $100\text{--}160 \mu\text{mol g}^{-1} \text{FW}^{-1}$ in the experiments with variable greenhouse light conditions of $150\text{--}200 \mu\text{mol quanta m}^{-2} \text{ s}^{-1}$ (Figures 1E and 3A). Thus, irradiance level correlates positively with source leaf starch content in aspen, and under limiting light, the rate of starch synthesis is drastically reduced while growth is proportionally less affected. There is also a correlation between leaf starch and irradiance levels in Arabidopsis.²⁹ However, the fact that Arabidopsis *pgm* mutants exhibit severe growth

defects²⁰ while the *pgm1pgm2* trees grow well shows that the control mechanism of carbon flux to leaf starch and its importance for growth differs between these species.

Wood composition is not altered in the *pgm1pgm2* trees

Carbon partitioning and whole-tree carbon balance are known to influence wood composition in aspen.^{33,34} Hence, wood was analyzed by pyrolysis-GC/MS, providing a comprehensive wood composition fingerprint by detecting

200–300 pyrolytic degradation products.³⁵ This analysis established that wood carbohydrate and lignin content, as well as carbohydrate:lignin ratio, did not differ significantly between WT and the *pgm1pgm2* lines (Figure S3). Neither did the evaluation of the entire MS spectra using principal component analysis reveal differences between WT and the mutants (Figure S3), further confirming that starch is not critical during aspen growth.

Bud set and bud flush are not altered in *pgm1pgm2* trees

Starch reserves in the roots, stem, and branches vary during the year in trees. In deciduous trees at the beginning of the growing

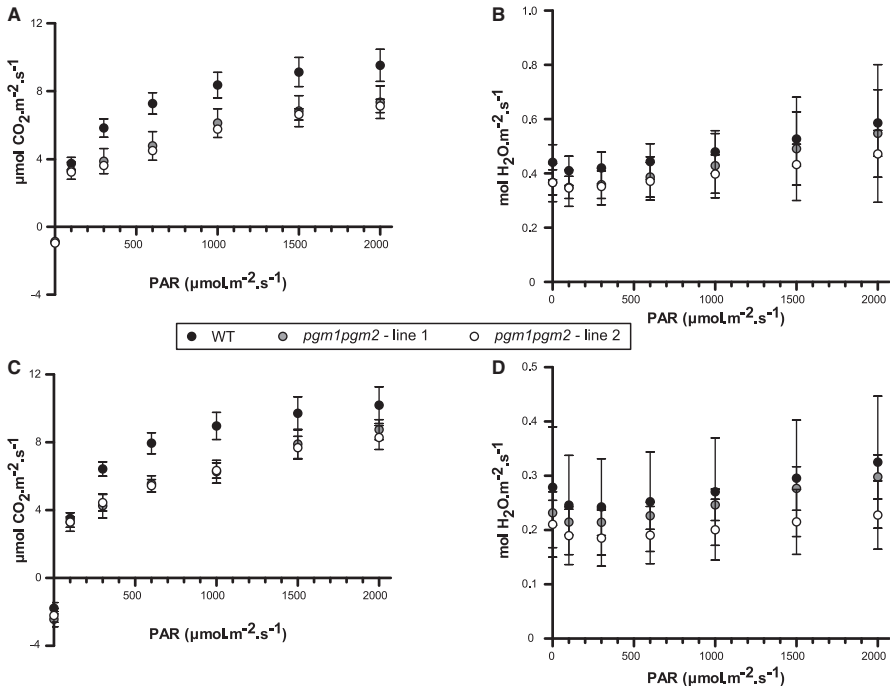


Figure 4. Effect of light intensity on the rate of CO₂ assimilation and stomatal conductance in the source leaves of *Populus tremula* × *tremuloides* WT and *pgm1pgm2* mutant trees

(A and B) CO₂ assimilation rate (A) and stomatal conductance (B) in source leaves of trees grown under 180–200 μmol quanta m⁻² s⁻¹. (C and D) CO₂ assimilation rate (C) and stomatal conductance (D) of source leaves in trees grown under 500 μmol quanta m⁻² s⁻¹. Photosynthetically active radiation (PAR). Data are mean ± SD from 4 biological replicates. See also Table S2.

season, starch reserves appear to be mobilized for the formation of new leaves.^{36–38} To examine the role of starch in this process, we compared the timing of bud flush in *pgm1pgm2* and WT trees. The trees were grown under 18-h light period for 6 weeks and then 14-h light period for 10 weeks to induce growth cessation, bud set, and dormancy. No difference between *pgm1pgm2* and WT trees was observed during the dormancy process (Figure S4). After dormancy induction the trees were exposed to 10 weeks of cold (4°C) followed by an 18-h light period at 22°C/18°C light/dark to induce bud flush. The bud flush process was monitored daily, but no difference between *pgm1pgm2* and WT trees was observed (Figure S4). These results confirm that starch synthesis is not required for dormancy onset and bud flush in aspen. The bud set and bud flush results combined with the lack of strong tree growth defects in the *pgm1pgm2* under different day lengths point to a passive starch storage mechanism, implying that aspen does not actively direct carbon to starch to ensure carbon supply for future growth and development.

Our observation that CO₂ assimilation was reduced in *pgm1pgm2* without obvious effects on the rate of tree

growth and biomass accumulation indicates that carbon availability does not limit tree growth. Growth was also probably not limited by water or mineral nutrients since trees were regularly watered and fertilized. This suggests processes downstream of CO₂ assimilation as limiting for tree growth under benign growing conditions. Accordingly, several ecophysiological studies of tree growth under diverse natural conditions have suggested that sink activity controlled by the environment and developmental cues restricts trees' capacity to assimilate to atmospheric CO₂.^{39,40} In conclusion, we suggest that aspen passively accumulates starch reserves that support growth and survival over a tree's lifespan. To elucidate the long-term consequences of low starch and reduced CO₂ assimilation, a comparison of whole-tree carbon budgets over multiple growth-dormancy cycles is needed. These are key issues when developing models of terrestrial carbon dynamics, building on understanding physiological processes underlying carbon dynamics in trees; indeed, there is both genetic and physiological evidence for the role of starch under adverse growth conditions and changing climate.^{8,10,15}

STAR★METHODS

Detailed methods are provided in the online version of this paper and include the following:

- **KEY RESOURCES TABLE**
- **RESOURCE AVAILABILITY**
 - Lead contact
 - Materials availability
- **EXPERIMENTAL MODEL AND SUBJECT DETAILS**
 - Plant material and growth conditions
- **METHOD DETAILS**
 - *PGM1PGM2* CRISPR vector construction, hybrid aspen transformation and genotyping
 - Phylogenetic analysis
 - Lugol staining
 - Sugar and starch measurement
 - RNA quantification and qPCR
 - Wood density measurement
 - Wood composition analysis using pyrolysis-GC/MS
 - Photosynthetic parameters
 - Bud set and bud break scoring
 - Bacteria species and strains
 - Accession numbers
- **QUANTIFICATION AND STATISTICAL ANALYSIS**
 - Statistical analysis
 - Data and code availability

SUPPLEMENTAL INFORMATION

Supplemental information can be found online at <https://doi.org/10.1016/j.cub.2022.06.056>.

ACKNOWLEDGMENTS

We thank Junko Takahashi-Schmidt and the UPSC Biopolymer Analytical Platform for help with the wood analysis and Edward Carlsson for help with starch measurements. This work was supported by the Swedish Research Council for Sustainable Development (Formas) (project grant 2016-01322), Bio4Energy (Swedish Programme for Renewable Energy), and the UPSC Centre for Forest Biotechnology funded by VINNOVA.

AUTHOR CONTRIBUTIONS

W.W., S.V., and L.T. conducted the experiments; W.W., S.V., L.T., and T.N. designed the experiments; and T.N. conceived the study and wrote the paper with contributions from all authors.

DECLARATION OF INTERESTS

The authors declare no competing interests.

Received: February 8, 2022

Revised: April 13, 2022

Accepted: June 16, 2022

Published: July 11, 2022

REFERENCES

1. Bastin, J.F., Finegold, Y., Garcia, C., Mollicone, D., Rezende, M., Routh, D., Zohner, C.M., and Crowther, T.W. (2019). The global tree restoration potential. *Science* 365, 76–79. <https://doi.org/10.1126/science.aax0848>.
2. IPCC (2018). Intergovernmental Panel on Climate Change (IPCC), An IPCC Special Report on the Impacts of Global Warming of 1.5°C Above Pre-Industrial Levels. <https://www.ipcc.ch/sr15/download/#chapter>.
3. Stitt, M., and Zeeman, S.C. (2012). Starch turnover: pathways, regulation and role in growth. *Curr. Opin. Plant Biol.* 15, 282–292. <https://doi.org/10.1016/j.pbi.2012.03.016>.
4. Kozłowski, T.T. (1992). Carbohydrate sources and sinks in woody plants. *Bot. Rev.* 58, 107–222. <https://doi.org/10.1007/bf02858600>.
5. Smith, A.M., and Stitt, M. (2007). Coordination of carbon supply and plant growth. *Plant Cell Environ.* 30, 1126–1149. <https://doi.org/10.1111/j.1365-3040.2007.01708.x>.
6. Le Roux, X., Lacoine, A., Escobar-Gutierrez, A., and Le Dizes, S. (2001). Carbon-based models of individual tree growth: a critical appraisal. *Ann. For. Science* 58, 469–506. <https://doi.org/10.1051/forest:2001140>.
7. Sala, A., Woodruff, D.R., and Meinzer, F.C. (2012). Carbon dynamics in trees: feast or famine? *Tree Physiol.* 32, 764–775. <https://doi.org/10.1093/treephys/tp143>.
8. Dietze, M.C., Sala, A., Carbone, M.S., Czimczik, C.I., Mantooth, J.A., Richardson, A.D., and Vargas, R. (2014). Nonstructural carbon in woody plants. *Annu. Rev. Plant Biol.* 65, 667–687. <https://doi.org/10.1146/annurev-arplant-050213-040054>.
9. Huang, J., Hammerbacher, A., Gershenzon, J., van Dam, N.M., Sala, A., McDowell, N.G., Chowdhury, S., Gleixner, G., Trumbore, S., and Hartmann, H. (2021). Storage of carbon reserves in spruce trees is prioritized over growth in the face of carbon limitation. *Proc. Natl. Acad. Sci. USA* 118, e2023297118. <https://doi.org/10.1073/pnas.2023297118>.
10. Klein, T., and Hoch, G. (2015). Tree carbon allocation dynamics determined using a carbon mass balance approach. *New Phytol.* 205, 147–159. <https://doi.org/10.1111/nph.12993>.
11. Essiamah, S., and Eschrich, W. (1985). Changes of starch content in the storage tissues of deciduous trees during winter and spring. *IAWA Bulletin* 6, 97–106. <https://doi.org/10.1163/22941932-90000921>.
12. Sauter, J.J., and van Cleve, B. (1994). Storage, mobilization and interrelations of starch, sugars, protein and fat in the ray storage tissue of poplar trees. *Trees (Berl.)* 8, 297–304. <https://doi.org/10.1007/bf00202674>.
13. Noronha, H., Silva, A., Dai, Z., Gallucci, P., Rombolá, A.D., Delrot, S., and Gerós, H. (2018). A molecular perspective on starch metabolism in woody tissues. *Planta* 248, 559–568. <https://doi.org/10.1007/s00425-018-2954-2>.
14. Berrocal-Lobo, M., Ibañez, C., Acebo, P., Ramos, A., Perez-Solis, E., Collada, C., Casado, R., Aragoncillo, C., and Allona, I. (2011). Identification of a homolog of *Arabidopsis* DSP4 (SEX4) in chestnut: its induction and accumulation in stem amyloplasts during winter or in response to the cold. *Plant Cell Environ.* 34, 1693–1704. <https://doi.org/10.1111/j.1365-3040.2011.02365.x>.
15. Blumstein, M., Richardson, A., Weston, D., Zhang, J., Muchero, W., and Hopkins, R. (2020). A new perspective on ecological prediction reveals limits to climate adaptation in a temperate tree species. *Curr. Biol.* 30, 1447–1453.e4. <https://doi.org/10.1016/j.cub.2020.02.001>.
16. Tixier, A., Orozco, J., Roxas, A.A., Earles, J.M., and Zwieniecki, M.A. (2018). Diurnal variation in nonstructural carbohydrate storage in trees: remobilization and vertical mixing. *Plant Physiol.* 178, 1602–1613. <https://doi.org/10.1104/pp.18.00923>.
17. Smith, A.M., and Zeeman, S.C. (2020). Starch: a flexible, adaptable carbon store coupled to plant growth. *Annu. Rev. Plant Biol.* 71, 217–245. <https://doi.org/10.1146/annurev-arplant-050718-100241>.
18. Lin, T.-P., Caspar, T., Somerville, C., and Preiss, J. (1988). Isolation and characterization of a starchless mutant of *Arabidopsis thaliana* (L.) Heynh lacking ADPglucose pyrophosphorylase activity. *Plant Physiol.* 86, 1131–1135. <https://doi.org/10.1104/pp.86.4.1131>.
19. Lin, T.-P., Caspar, T., Somerville, C.R., and Preiss, J. (1988). A starch deficient mutant of *Arabidopsis thaliana* with low ADPglucose

- pyrophosphorylase activity lacks one of the two subunits of the enzyme. *Plant Physiol.* 88, 1175–1181. <https://doi.org/10.1104/pp.88.4.1175>.
20. Caspar, T., Huber, S.C., and Somerville, C. (1985). Alterations in growth, photosynthesis, and respiration in a starchless mutant of *Arabidopsis thaliana* (L.) deficient in chloroplast phosphoglucomutase activity. *Plant Physiol.* 79, 11–17. <https://doi.org/10.1104/pp.79.1.11>.
 21. Harrison, C.J., Hedley, C., and Wang, T.L. (1998). Evidence that the *rug3* locus of pea (*Pisum sativum* L.) encodes plastidial phosphoglucomutase confirms that the imported substrate for starch synthesis in pea amyloplasts is glucose-6-phosphate. *Plant J.* 13, 753–762.
 22. Vriet, C., Welham, T., Brachmann, A., Pike, M., Pike, J., Perry, J., Parniske, M., Sato, S., Tabata, S., Smith, A.M., and Wang, T.L. (2010). A suite of *Lotus japonicus* starch mutants reveals both conserved and novel features of starch metabolism. *Plant Physiol.* 154, 643–655. <https://doi.org/10.1104/pp.110.161844>.
 23. Gibon, Y., Blasing, O.E., Palacios-Rojas, N., Pankovic, D., Hendriks, J.H.M., Fisahn, J., Hohne, M., Gunther, M., and Stitt, M. (2004). Adjustment of diurnal starch turnover to short days: depletion of sugar during the night leads to a temporary inhibition of carbohydrate utilization, accumulation of sugars and post-translational activation of ADP-glucose pyrophosphorylase in the following light period. *Plant J.* 39, 847–862. <https://doi.org/10.1111/j.1365-313X.2004.02173.x>.
 24. Nilsson, O., Aldén, T., Sitbon, F., Little, C.H.A., Chalupa, V., Sandberg, G., and Olsson, O. (1992). Spatial pattern of cauliflower mosaic virus 35S promoter luciferase expression in transgenic hybrid aspen trees monitored by enzymatic assay and non-destructive imaging. *Transgenic Res.* 1, 209–220. <https://doi.org/10.1007/bf02524751>.
 25. Olsen, J.E., Junttila, O., Nilsen, J., Eriksson, M.E., Martinussen, I., Olsson, O., Sandberg, G., and Moritz, T. (1997). Ectopic expression of oat phytochrome A in hybrid aspen changes critical daylength for growth and prevents cold acclimatization. *Plant J.* 12, 1339–1350. <https://doi.org/10.1046/j.1365-313x.1997.12061339.x>.
 26. Blasing, O.E., Gibon, Y., Gunther, M., Hohne, M., Morcuende, R., Osuna, D., Thimm, O., Usadel, B., Scheible, W.R., and Stitt, M. (2005). Sugars and circadian regulation make major contributions to the global regulation of diurnal gene expression in *Arabidopsis*. *Plant Cell* 17, 3257–3281. <https://doi.org/10.1105/tpc.105.035261>.
 27. Rennie, E.A., and Turgeon, R. (2009). A comprehensive picture of phloem loading strategies. *Proc. Natl. Acad. Sci. USA* 106, 14162–14167. <https://doi.org/10.1073/pnas.0902279106>.
 28. Turgeon, R., and Medville, R. (1998). The absence of phloem loading in willow leaves. *Proc. Natl. Acad. Sci. USA* 95, 12055–12060. <https://doi.org/10.1073/pnas.95.20.12055>.
 29. Moraes, T.A., Mengin, V., Annunziata, M.G., Encke, B., Krohn, N., Höhne, M., and Stitt, M. (2019). Response of the circadian clock and diel starch turnover to one day of low light or low CO₂. *Plant Physiol.* 179, 1457–1478. <https://doi.org/10.1104/pp.18.01418>.
 30. Sicher, R.C., Kremer, D.F., and Harris, W.G. (1984). Diurnal carbohydrate metabolism of barley primary leaves. *Plant Physiol.* 76, 165–169. <https://doi.org/10.1104/pp.76.1.165>.
 31. Taracón, C., González-Grandío, E., Oliveros, J.C., Nicolas, M., and Cubas, P. (2017). A conserved carbon starvation response underlies bud dormancy in woody and herbaceous species. *Front. Plant Sci.* 8, 788. <https://doi.org/10.3389/fpls.2017.00788>.
 32. Ekkehard Neuhaus, H., and Stitt, M. (1990). Control analysis of photosynthate partitioning: impact of reduced activity of ADP-glucose pyrophosphorylase or plastid phosphoglucomutase on the fluxes to starch and sucrose in *Arabidopsis thaliana* (L.). *Heynh. Planta* 182, 445–454. <https://doi.org/10.1007/bf02411398>.
 33. Dominguez, P.G., Donev, E., Derba-Maceluch, M., Bünder, A., Hedenström, M., Tomášková, I., Mellerowicz, E.J., and Niittylä, T. (2021). Sucrose synthase determines carbon allocation in developing wood and alters carbon flow at the whole tree level in aspen. *New Phytol.* 229, 186–198. <https://doi.org/10.1111/nph.16721>.
 34. Gerber, L., Zhang, B., Roach, M., Rende, U., Gorzsás, A., Kumar, M., Burgert, I., Niittylä, T., and Sundberg, B. (2014). Deficient sucrose synthase activity in developing wood does not specifically affect cellulose biosynthesis, but causes an overall decrease in cell wall polymers. *New Phytol.* 203, 1220–1230. <https://doi.org/10.1111/nph.12888>.
 35. Gerber, L., Eliasson, M., Trygg, J., Moritz, T., and Sundberg, B. (2012). Multivariate curve resolution provides a high-throughput data processing pipeline for pyrolysis-gas chromatography/mass spectrometry. *J. Anal. Appl. Pyrol.* 95, 95–100. <https://doi.org/10.1016/j.jaap.2012.01.011>.
 36. Gough, C.M., Flower, C.E., Vogel, C.S., and Curtis, P.S. (2010). Phenological and temperature controls on the temporal non-structural carbohydrate dynamics of *Populus grandidentata* and *Quercus rubra*. *Forests* 1, 65–81. <https://doi.org/10.3390/f1010065>.
 37. Landhäusser, S.M., and Lieffers, V.J. (2003). Seasonal changes in carbohydrate reserves in mature northern *Populus tremuloides* clones. *Trees Struct. Funct.* 17, 471–476. <https://doi.org/10.1007/s00468-003-0263-1>.
 38. Regier, N., Streb, S., Zeeman, S.C., and Frey, B. (2010). Seasonal changes in starch and sugar content of poplar (*Populus deltoides* x *nigra* cv. Dorskamp) and the impact of stem girdling on carbohydrate allocation to roots. *Tree Physiol.* 30, 979–987. <https://doi.org/10.1093/treephys/tpq047>.
 39. Korner, C. (2003). Carbon limitation in trees. *J. Ecol.* 91, 4–17. <https://doi.org/10.1046/j.1365-2745.2003.00742.x>.
 40. Körner, C. (2015). Paradigm shift in plant growth control. *Curr. Opin. Plant Biol.* 25, 107–114. <https://doi.org/10.1016/j.cpb.2015.05.003>.
 41. Koncz, C., and Schell, J. (1986). The promoter of TL-DNA gene 5 controls the tissue-specific expression of chimaeric genes carried by a novel type of Agrobacterium binary vector. *Mol. Gen. Genet.* 204, 383–396. <https://doi.org/10.1007/bf00331014>.
 42. Xing, H.-L., Dong, L., Wang, Z.-P., Zhang, H.-Y., Han, C.-Y., Liu, B., Wang, X.-C., and Chen, Q.-J. (2014). A CRISPR/Cas9 toolkit for multiplex genome editing in plants. *BMC Plant Biol.* 14, 327. <https://doi.org/10.1186/s12870-014-0327-y>.
 43. Kumar, S., Stecher, G., and Tamura, K. (2016). MEGA7: molecular evolutionary genetics analysis version 7.0 for bigger datasets. *Mol. Biol. Evol.* 33, 1870–1874. <https://doi.org/10.1093/molbev/msw054>.
 44. Fahlgren, N., Feldman, M., Gehan, M.A., Wilson, M.S., Shyu, C., Bryant, D.W., Hill, S.T., McEntee, C.J., Warnasooriya, S.N., Kumar, I., et al. (2015). A versatile phenotyping system and analytics platform reveals diverse temporal responses to water availability in *Setaria*. *Mol. Plant* 8, 1520–1535. <https://doi.org/10.1016/j.molp.2015.06.005>.
 45. Schneider, C.A., Rasband, W.S., and Eliceiri, K.W. (2012). NIH Image to ImageJ: 25 years of image analysis. *Nat. Methods* 9, 671–675. <https://doi.org/10.1038/nmeth.2089>.
 46. Roach, M., Gerber, L., Sandquist, D., Gorzsás, A., Hedenström, M., Kumar, M., Steinhauser, M.C., Feil, R., Daniel, G., Stitt, M., et al. (2012). Fructokinase is required for carbon partitioning to cellulose in aspen wood. *Plant J.* 70, 967–977. <https://doi.org/10.1111/j.1365-313x.2012.04929.x>.
 47. Hendriks, J.H., Kolbe, A., Gibon, Y., Stitt, M., and Geigenberger, P. (2003). ADP-glucose pyrophosphorylase is activated by posttranslational redox-modification in response to light and to sugars in leaves of *Arabidopsis* and other plant species. *Plant Physiol.* 133, 838–849. <https://doi.org/10.1104/pp.103.024513>.
 48. Smith, A.M., and Zeeman, S.C. (2006). Quantification of starch in plant tissues. *Nat. Protoc.* 1, 1342–1345. <https://doi.org/10.1038/nprot.2006.232>.
 49. Xu, M., Zang, B., Yao, H.S., and Huang, M.R. (2009). Isolation of high-quality RNA and molecular manipulations with various tissues of *Populus*. *Russ. J. Plant Physiol.* 56, 716–719. <https://doi.org/10.1134/s1021443709050197>.
 50. Livak, K.J., and Schmittgen, T.D. (2001). Analysis of relative gene expression data using real-time quantitative PCR and the 2^{-ΔΔCT} method. *Methods* 25, 402–408. <https://doi.org/10.1006/meth.2001.1262>.

51. Fataftah, N., Bag, P., André, D., Lihavainen, J., Zhang, B., Ingvarsson, P.K., Nilsson, O., and Jansson, S. (2021). GIGANTEA influences leaf senescence in trees in two different ways. *Plant Physiol.* *187*, 2435–2450. <https://doi.org/10.1093/plphys/kiab439>.
52. Rohde, A., Stome, V., Jorge, V., Gaudet, M., Vitacolonna, N., Fabbrini, F., Ruttink, T., Zaina, G., Marron, N., Dillen, S., et al. (2011). Bud set in poplar - genetic dissection of a complex trait in natural and hybrid populations. *New Phytol.* *189*, 106–121. <https://doi.org/10.1111/j.1469-8137.2010.03469.x>.
53. Ibañez, C., Kozarewa, I., Johansson, M., Ogren, E., Rohde, A., and Eriksson, M.E. (2010). Circadian clock components regulate entry and affect exit of seasonal dormancy as well as winter hardiness in *Populus* trees. *Plant Physiol.* *153*, 1823–1833. <https://doi.org/10.1104/pp.110.158220>.

STAR METHODS

KEY RESOURCES TABLE

REAGENT or RESOURCE	SOURCE	IDENTIFIER
Bacterial and virus strains		
<i>Escherichia coli</i> OmniMAX 2	ThermoFisher Scientific	Cat. No. C854003
<i>Agrobacterium tumefaciens</i> GV3101	⁴¹	N/A
Chemicals, peptides, and recombinant proteins		
RNeasy Mini Kit	Qiagen	Cat. No. 74106
Maxima First Strand cDNA Synthesis Kit	ThermoFisher Scientific	Cat. No. K1672
iQ SYBR Green Supermix	Bio-Rad	Cat. No. 1708880
Lugol solution	Sigma	Cat. No. L6146
α -Amylase	Roche	Cat. No. 10102814001
α -Amyloglucosidase	Roche	Cat. No. 10102857001
Hexokinase	Roche	Cat. No. 11426362001
Glucose-6-Phosphate Dehydrogenase	Roche	Cat. No. 10737232001
Phosphoglucose Isomerase	Roche	Cat. No. 10128139001
Invertase	Sigma	Cat. No. I4504-5G
Phusion High-Fidelity DNA Polymerase	ThermoFisher Scientific	Cat. No. F530S
FastDigest Eco311	ThermoFisher Scientific	Cat. No. FD0293
T4 DNA Ligase	ThermoFisher Scientific	Cat. No. 15224041
Experimental models: Organisms/strains		
Poplar: <i>Populus tremula</i> x <i>tremuloides</i> T89	N/A	N/A
Poplar: <i>pgm1pgm2</i> – line1	This study	N/A
Poplar: <i>pgm1pgm2</i> – line2	This study	N/A
Oligonucleotides		
PtPGM1-CR-F: CGCTTAGCTCTTCTCTTCTGT	This study	N/A
PtPGM1-CR-R: TTCTCAGCATCCAACATCCAG	This study	N/A
PtPGM2-CR-F: TTAGTTCTTCCCTCTCTGTCA	This study	N/A
PtPGM2-CR-R: CTACTTCTCAGCAACCAACAG	This study	N/A
PtDIN6-F: TGTTATCGCCCATCTGTACGAG	This study	N/A
PtDIN6-R: GATGAAATCCACACGGACCCATC	This study	N/A
PtDRM1-F: CCTCTTAACATCAAAGATATTGAC	This study	N/A
PtDRM1-R: GCAAGGTGCTACCAGGGTGG	This study	N/A
PtGASA6-F: GTTGCTGTCTTCTCTTGGCTC	This study	N/A
PtGASA6-R: CACCTCCTCGTGATTGTGATG	This study	N/A
PtUBQ-F: GTTGATTTTTGCTGGGAAGC	This study	N/A
PtUBQ-R: GATCTTGGCCTTACGTTGT	This study	N/A
Recombinant DNA		
Plasmid: pHSE401	⁴²	Addgene Plasmid # 62201
Plasmid: pCBC-DT1T2	⁴²	Addgene Plasmid # 50590
Plasmid: pHSE401-PGM1PGM2	This study	N/A
Software and algorithms		
GraphPad Prism	GraphPad Software	https://www.graphpad.com/scientific-software/prism/
Affinity Designer	Serif (Europe)	https://affinity.serif.com/en-us/designer/
MEGA7	⁴³	https://www.megasoftware.net/

(Continued on next page)

Continued

REAGENT or RESOURCE	SOURCE	IDENTIFIER
SIMCA 16	Sartorius AG	https://www.sartorius.com/en/products/process-analytical-technology/data-analytics-software/mvda-software/simca
PlantCV	Donald Danforth Plant Science Center ⁴⁴	https://plantcv.readthedocs.io/en/stable/
ImageJ	⁴⁵	https://imagej.nih.gov/ij/

RESOURCE AVAILABILITY

Lead contact

Further information and requests for resources and reagents should be directed to and will be fulfilled by the lead contact, Totte Niittyylä (totte.niittyyla@slu.se).

Materials availability

All unique/stable reagents generated in this study are available from the **Lead Contact** with a completed Materials Transfer Agreement.

Data and code availability

- All data reported in this paper will be shared by the **lead contact** upon request.
- This paper does not report original code.
- Any additional information required to reanalyze the data reported in this paper is available from the **lead contact** upon request.

EXPERIMENTAL MODEL AND SUBJECT DETAILS

Populus tremula x tremuloides clone T89 was used as the experimental model.

Plant material and growth conditions

Hybrid aspens (*Populus tremula x tremuloides*) were micropropagated from cuttings, grown *in vitro* for four weeks as described in Nilsson et al.²⁴ and then transferred to soil. The trees were grown in the greenhouse, controlled growth rooms or an automated phenotyping facility in a commercial soil/sand/fertilizer mixture (Yrkes Plantjord; Weibulls Horto, <http://www.weibullshorto.se>). In the greenhouse and growth rooms the trees were fertilized using approximately 200 ml of 1% Rika-S (N/P/K 7:1:5; Weibulls Horto) once a week after 3 weeks of planting. The temperature was at 20/18 °C (light/dark).

In the automated phenotyping platform experiment two *pgm1pgm2* mutant lines (10 replicate trees per line) and WT (20 replicate trees) were grown in an equal volume of commercial soil (K-jord; Hasselforsgården), watered two times a day, fertilized every 2 days with 50 ml 0.6% Rika-S (Weibulls Horto) and treated with Nemasys C on week 4 and 7 after potting. Photoperiod was 18-h light / 6-h dark, and temperature 22°C / 18°C light/dark and relative humidity 60%. Light irradiance was between 150-200 μmol m⁻² s⁻¹. The experiment was performed in the tree phenotyping platform (WIWAM Conveyor, SMO, Eeklo, Belgium) described in <https://www.upsc.se/plant-growth-facilities-at-upsc-and-slu-umea/325-upsc-tree-phenotyping-platform.html>. In the facility the trees move on a WIWAM Conveyor belt (SMO, Eeklo, Belgium) and pass every day through an automated watering and weighing station followed by a light curtain which measures tree height. After the height measurement the trees are photographed by three Imperx B4820 RGB-cameras from the side, from above and a focus on the lower part of the stem. The images and the height measurement data in .csv format are recorded on the WIWAM computer and visualized using the PIPPA web interface (<https://pippa.psb.ugent.be/>). Stem widths were measured from the focused stem images using ImageJ.⁴⁵ Tree canopy area was determined from the pictures taken from the side and from above using the RGB image workflow of the PlantCV software.⁴⁴ After 8 weeks the trees were harvested, and the total fresh weight of stem and leaves including petioles determined using an analytical balance (Sartorius Entris BCE32021-1S, precision 0.01 g). The root biomass of WT and *pgm1pgm2* mutants was measured in a separate greenhouse experiment (18-h/6-h light/dark) after roots were carefully separated from soil.

METHOD DETAILS

PGM1PGM2 CRISPR vector construction, hybrid aspen transformation and genotyping

pgm1pgm2 mutants were generated by gene editing of the *PGM1* and *PGM2* genes in the *Populus tremula x tremuloides* T89 background by using CRISPR-Cas9 and a pair of guide RNAs (gRNAs) targeting both *PGM1* and *PGM2*: GCTGAACCTGAAGGCATCA

and CAATTGAGGGTCAGAAGAC. The CRISPR-Cas9 and gRNA sequences were cloned into the pHSE401 vector as described in Xing et al.⁴² The construct was introduced into trees by Agrobacterium-mediated plant transformation of stem segments as described in Nilsson et al.²⁴ Independent transgenic lines were screened by PCR and restriction enzyme digestion to identify lines that were homozygous for gene-edited mutant alleles of both *PGM1* and *PGM2* (Figure S1). Mutations in the *PGM1* gene were identified by PCR using primers PtPGM1-CR-F: CGCTTAGCTCTTCTCTTTCTGT and PtPGM1-CR-R: TTCTCAGCATCCAACATCCAG and digested with Bpil (Thermo Fisher Scientific). Mutations in the *PGM2* gene were identified by PCR using primers PtPGM2-CR-F: TTAGTTCTCCCTCTCTGTCA and PtPGM2-CR-R: CTACTTTCTCAGCAACCAACAG and digested with Bpil (Thermo Fisher Scientific).

Phylogenetic analysis

The phylogenetic analysis was performed by Maximum Likelihood method in MEGA7.⁴³ The evolutionary history was deduced by the JTT matrix-based model. The tree with the highest log likelihood was selected. The initial tree for the heuristic search was obtained by applying BioNJ algorithms and Neighbor-Join to a matrix of pairwise distances with a JTT model and the topology with superior log likelihood value. The phylogenetic tree was drawn to scale and the branch lengths were measured in the number of substitutions per site. The analysis utilised seven PGM amino acid sequences from *Arabidopsis thaliana* and *Populus trichocarpa*.

Lugol staining

Leaf discs were harvested and incubated in fixation solution containing 80% ethanol (v/v), 5% formic acid (v/v) and 15% H₂O (v/v) at 80 °C for 10 min. The fixation solution was then replaced with 80% ethanol (v/v) and samples were incubated at 80 °C for 5 min. Ethanol was removed and leaf discs were stained in Lugol solution (Sigma, L6146) at room temperature for 3 min. Lugol solution was removed by rinsing leaf discs with distilled H₂O and incubated in fresh H₂O at 80 °C for 15 min and then at 4 °C for 15 min. For root tips and stem sections, WT and *pgm1pgm2* samples were incubated in 80% ethanol (v/v) for 10 min and then submerged in Lugol solution for 1 min. The samples were rinsed twice with distilled water and then mounted onto microscopy slides using clearing solution (80 g chloralhydrate, 30 mL glycerol and 10 mL water) as the mounting medium. The roots and stem sections were visualized with a Zeiss Axioplan 2 microscope equipped with differential interference contrast optics.

Sugar and starch measurement

Glucose, fructose and sucrose were extracted and measured as previously described in Roach et al.⁴⁶ The ethanol extraction pellet was used as starting material for starch determination, which was performed combining methods described by Hendriks et al.⁴⁷ and Smith and Zeeman.⁴⁸ Starch was gelatinized by resuspending the pellet into 0.1 M NaOH and incubating at 95 °C for 30 min, after which the samples were acidified by adding a mixture of 0.1 M sodium acetate/NaOH (pH 4.9) and 0.5 M HCl. Three technical replicates were prepared, and 50 mM sodium acetate/NaOH buffer, α -amylase and α -amylglucosidase was added to each of the sub-samples for starch degradation. Starch derived glucose was released by three overnight digestions at +37 °C under rotation, removing the supernatant for later analysis and adding new starch digestions mix each day. The amount of released glucose was quantified using an enzymatic assay as described in Roach et al.⁴⁶

RNA quantification and qPCR

WT and *pgm1pgm2* trees were first grown for 4 weeks in 18-h/6-h day/night cycle and then transferred to an 8-h/16-h day/night cycle for 10 days. Total RNA was extracted from the top most fully expanded source leaf using the CTAB-LiCl method.⁴⁹ RNA concentration was determined by NanoDrop 2000 (ThermoFisher Scientific). 1 μ g of total RNA from each sample was used for cDNA synthesis using the Maxima First Strand cDNA Synthesis Kit (ThermoFisher Scientific) according to the manufacturer's instructions. Quantitative real-time PCR was performed with a Bio-Rad CFX384 Touch Real-Time PCR Detection System, and the numerical values of transcript levels obtained using the relative quantification method.⁵⁰ 20 μ L of 1x iQ SYBR Green Supermix (Bio-Rad) was used for the reaction and the final concentration of each primer was 250 nM. Primers were designed with GC content between 40 to 60% and melting temperature between 50 and 60 °C. The specificity of the primers was checked by BLAST against the *Populus tremula x tremuloides* T89 genome sequence at <https://plantgenie.org>. The amplification specificity of each primer pair was verified by a melting curve (55 °C to 95 °C) exhibiting a single peak. The transcript levels of the carbon depletion genes were normalized to the expression level of *POLYUBIQUITIN 4* (*PtUBQ*).⁵¹ The primer sequences were: PtDIN6-F: TGTTATCGCCCATCTGTACGAG and PtDIN6-R: GATGAAATCCACACGACCCATC. PtDRM1-F: CCTCTTAACATCAAAGATATTGAC and PtDRM1-R: GCAAGGTTGC TACCAGGTTGG. PtGASA6-F: GTTGCTGTCTTCTCTTGGCTC and PtGASA6-R: CACCTCCTCGTGCATTGTGATG. PtUBQ-F: GTTGATTTTTGCTGGGAAGC and PtUBQ-R: GATCTTGGCCCTCACGTTGT.

Wood density measurement

A 2 cm stem segment harvested 10 cm above the soil was used for wood density analysis. Wood density was measured on a dry weight per wet volume basis. Wood pieces were placed in water on an XA105 analytical balance with precision of 0.01 mg (Mettler Toledo; <https://www.mt.com/>) and submerged to determine the sample volume based on displaced water weight. Samples were then oven dried at 102 °C for 24 h and weighed again to obtain the dry mass weight. The wood density was calculated from the dry weight-to-wet volume ratio.

Wood composition analysis using pyrolysis-GC/MS

Stems from automated phenotyping facility grown trees were debarked and the developing wood removed by scraping. The stem samples were freeze-dried for 72-h, and then filed to fine wood powder. 60 μg aliquots of the wood powder were weighed using a high-precision microbalance (Mettler Toledo XP6), with three technical replicates of each biological sample. These samples were applied to a pyrolyzer equipped with an auto sampler (PY-2020iD and AS-1020E, Frontier Lab, Japan) connected to a GC/MS (7890A/5975C; Agilent Technologies AB, Sweden). The pyrolysate was separated and analyzed according to the method described by Gerber et al.³⁵ Data analysis by principal component analysis was performed using the SIMCA 16 software (version 16.0.1.7928, Umetrics AB, Sweden).

Photosynthetic parameters

Light-response curve of photosynthesis rate and H_2O gas exchange rates were measured for top most fully expanded source leaf at mid-day at different photon irradiances (0, 50, 100, 300, 700, 1200, 1500 and 1800 $\text{mmol s}^{-1} \text{m}^{-2}$) using Licor portable gas exchange system (LI-COR 6400XT, <http://www.licor.com>). Leaf pigment and photosynthetic parameters were measured using a SPEEDZEN 200 (JBEAMBio) imaging system as described in Fataftah et al.⁵¹ The leaves for the pigment and photosynthetic parameter determination were detached from the tree at mid-day and equilibrated in the dark prior to the measurements. The nonphotochemical chlorophyll fluorescence quenching (NPQ) was determined as in Fataftah et al.⁵¹ using 1800 μmol actinic light for 3.5 min with 5400 μmol saturating pulses at 30 sec intervals.

Bud set and bud break scoring

WT and *pgm1pgm2* trees were grown under 18-h/6-h day/night cycle for 6 weeks and then transferred to 14-h/10-h day/night cycle for 10 weeks. Height, number of leaves formed after initiation of SD treatment and bud set stages were scored weekly as described previously.⁵² Dormant trees were then placed in a cold room at 4 °C for 10 weeks and then bud break was induced by transferring the trees to normal long day conditions (18-h/6-h light/dark, 21 °C). Bud-break stages of the apical buds were scored daily.⁵³

Bacteria species and strains

Escherichia coli OmniMAX 2 strain (ThermoFisher Scientific, Waltham, Massachusetts, United States) was used for CRISPR-Cas9 construct cloning and *Agrobacterium tumefaciens* strain GV3101 was used for aspen transformation.

Accession numbers

Sequence data from this article can be found in Phytozome *Populus trichocarpa* genome sequence version 10.1 or TAIR website under the following numbers: PtPGM1: POTRI.015G134700. PtPGM2: POTRI.012G132500. PtPGM3: POTRI.010G109500. PtPGM4: POTRI.008G132500. AtPGM: AT5G51820. AtPGM2: AT1G70730. AtPGM3: AT1G23190. PtDIN6: POTRI.009G072900. PtDRM1: POTRI.004G047100. PtGASA6: POTRI.017G083000. PtUBQ: POTRI.001G418500.

QUANTIFICATION AND STATISTICAL ANALYSIS

Statistical analysis

For multiple data sets comparisons, one-way ANOVA and Tukey post hoc test was performed. p values < 0.05 were considered as statistically significant differences.

Data and code availability

GraphPad Prism software was used for statistical analyses and graph construction. Affinity Designer software was used to prepare the figures and tables. MEGA7 software⁴³ was used for the phylogenetic analysis. SIMCA 16 software was used for principal component analysis. ImageJ software⁴⁵ was used to measure the stem width. The PlantCV software⁴⁴ was used to determine the tree canopy area.

Current Biology, Volume 32

Supplemental Information

Aspen growth is not limited by starch reserves

Wei Wang, Loic Talide, Sonja Viljamaa, and Totte Niittyä

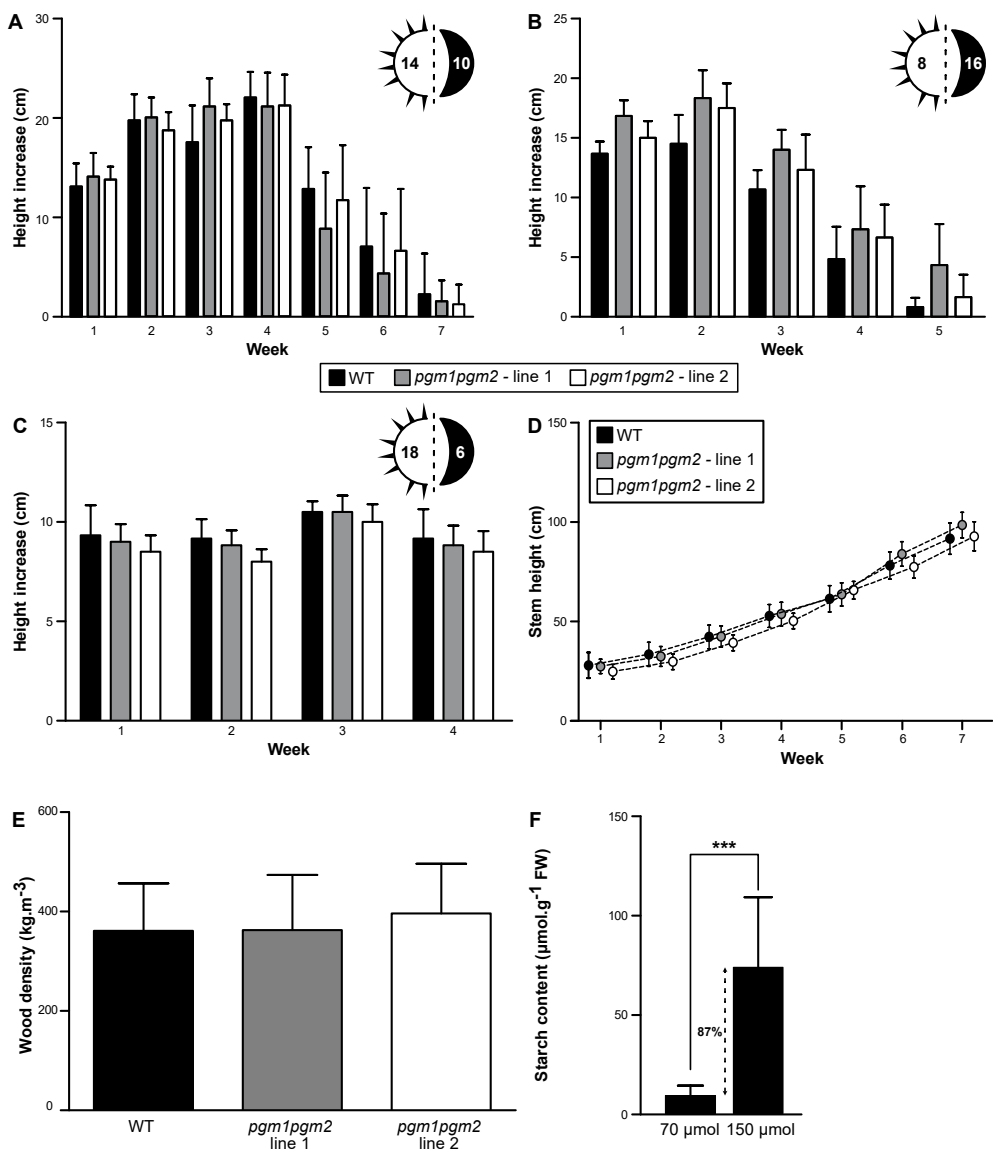


Figure S2. Stem height increase, wood density and leaf starch content in *Populus tremula x tremuloides* wild type (WT) and *pgm1pgm2* lines under different growth conditions. Related to Figure 2 and Figure 3.

(A) Stem height increase over a 7-week period after trees were moved from an 18-hour to a 14-hour photoperiod. $n = 10$ biological replicates. (B) Stem height increase over a 5-week period after trees were moved from an 18-hour to an 8-hour photoperiod. $n = 6$ biological replicates. (C) Stem height increase of trees grown in 18-hour photoperiod under $\sim 70 \mu\text{mol quanta m}^{-2} \text{ s}^{-1}$. (D) Rate of stem height growth over a 7-week period under $500 \mu\text{mol quanta m}^{-2} \text{ s}^{-1}$ irradiance. (E) Stem wood density of trees grown under $500 \mu\text{mol quanta m}^{-2} \text{ s}^{-1}$ for 8 weeks. $n = 12$ biological replicates. (F) Starch content of WT source leaves at the end of the photoperiod under $\sim 70 \mu\text{mol quanta m}^{-2} \text{ s}^{-1}$ and $\sim 150 \mu\text{mol quanta m}^{-2} \text{ s}^{-1}$. Data are mean \pm S.D. of 6 biological replicates. *** indicates statistically significant difference ($P < 0.001$). Fresh weight (FW).

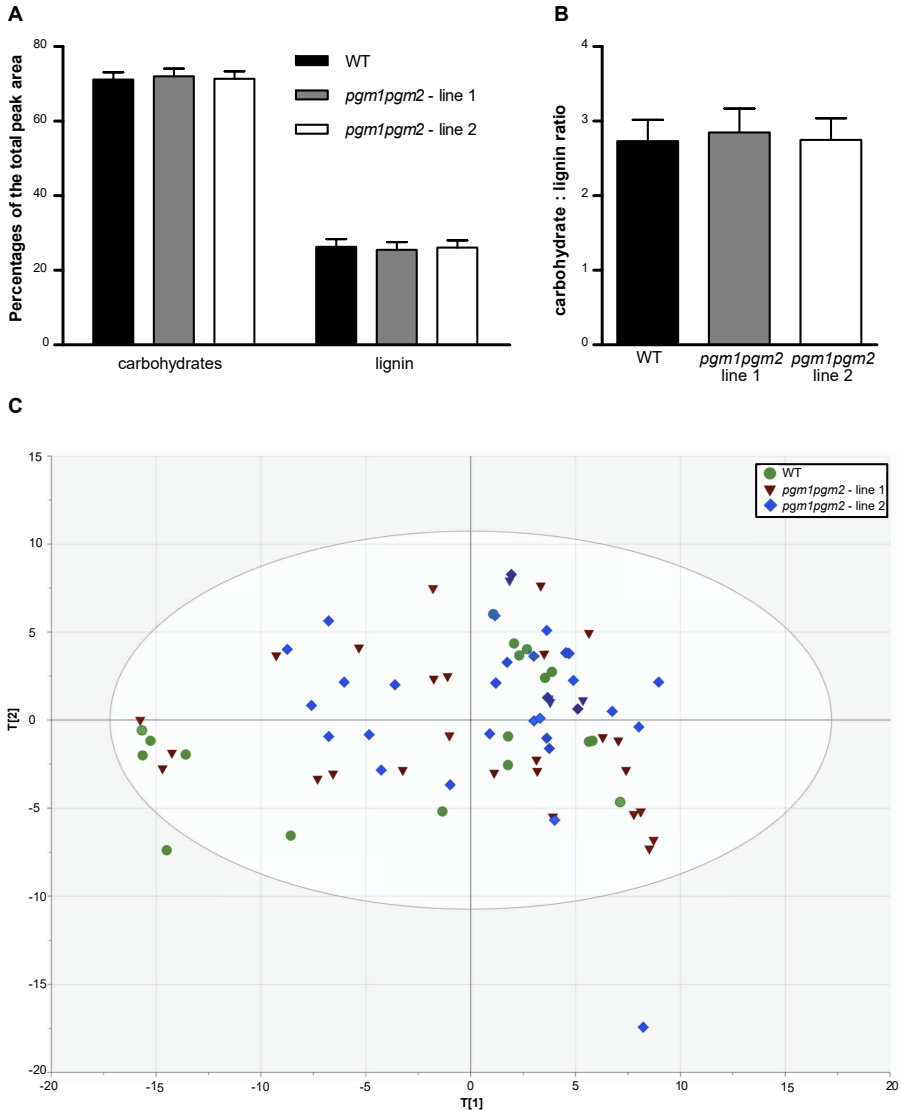


Figure S3. Wood total carbohydrates and lignin in wild type *Populus tremula x tremuloides* (WT) and *pgm1pgm2* mutant trees analyzed using pyrolysis-GC/MS. Related to Figure 2.

(A) Percentages of the total peak area of peaks attributable to carbohydrates and lignin. Peak annotation according to previous study^{S1}. Mean \pm SD, $n = 6$ biological replicates for WT. $n = 10$ biological replicates for *pgm1pgm2* - line 1 and line 2. (B) Carbohydrate : lignin ratio. (C) Principal component analysis (PCA) of the mature wood pyrolysis components of WT and *pgm1pgm2* as detected by pyrolysis-GC/MS. $n = 6$ biological replicates for WT and $n = 10$ biological replicates for *pgm1pgm2* - line 1 and line 2. Statistical values for PCA-X: R2X[1] (cumulative) 0.308, R2X[2] (cumulative) 0.12, Q2 (cumulative) score 0.491. Ellipse: Hotelling's T2 (95%).

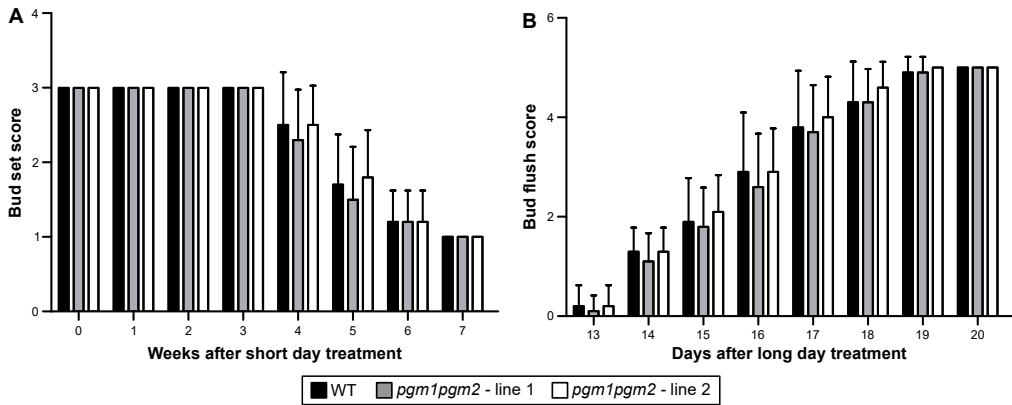


Figure S4. Comparison of bud set and bud flush in *Populus tremula x tremuloides* wild type (WT) and *pgm1pgm2* mutant trees. Related to Figure 1.

(A) Bud set scores of wild-type and *pgm1pgm2* trees after transfer from 18-h/6-h day night cycle to 14-h/10-h day/night cycle. (B) Bud flush score of wild-type and *pgm1pgm2* plants after transfer from 4 °C cold room to 18-h/6-h day/night cycle. Values are means \pm S.D. $n = 10$ biological replicates. One-way ANOVA, post-hoc Tukey HSD test. No statistically significant differences were observed between different genotypes.

	WT	<i>pgm1pgm2</i> - line 1	<i>pgm1pgm2</i> - line 2
Stem width (Pixels)	190.70 ± 14.73 (n = 20)	193.60 ± 11.35 (n = 10)	181.22 ± 11.92 (n = 9)
Wood density (kg.m ⁻³)	320.22 ± 22.23 (n = 6)	327.59 ± 27.23 (n = 10)	319.70 ± 21.90 (n = 10)
Leaf biomass (g FW)	97.61 ± 12.80 (n = 6)	101.34 ± 12.95 (n = 10)	95.08 ± 11.96 (n = 10)
Stem biomass (g FW)	75.69 ± 9.90 (n = 6)	83.04 ± 10.63 (n = 10)	75.26 ± 8.65 (n = 10)
Root biomass (g FW) ^a	27.17 ± 4.61 (n = 7)	21.99 ± 5.63 (n = 7)	23.65 ± 5.93 (n = 6)

Table S1. Growth parameters of 40-day-old *Populus tremula x tremuloides* wild type (WT) and *pgm1pgm2* mutant trees grown in 18-h photoperiod in an automated phenotyping facility. Related to Figure 2. ^a, root biomass is from greenhouse grown trees. Data are mean ± S.D. Number of biological replicates (n). Fresh weight (FW). No statistically significant differences according to one-way ANOVA and Tukey post hoc test.

	WT	<i>pgm1pgm2</i> - line 1	<i>pgm1pgm2</i> - line 2
F0	73.57 ± 3.00	74.90 ± 2.16	74.33 ± 2.94
Fm	356.57 ± 24.16	368.72 ± 23.35	368.45 ± 12.58
Fv/Fm	0.79 ± 0.01	0.80 ± 0.01	0.80 ± 0.00
NPQ	1.51 ± 0.03	1.31 ± 0.34	1.39 ± 0.34
Chlorophyll	19.79 ± 1.05	23.15 ± 2.38***	21.93 ± 1.35**

Table S2. Source leaf chlorophyll content and photosynthetic parameters in *Populus tremula x tremuloides* wild type (WT) and *pgm1pgm2* mutant trees. Related to Figure 4. For the photosynthetic parameters n = 4, and for chlorophyll n = 6, values are mean ± S.D. *** and ** indicate statistically significant difference (P < 0.001 and P < 0.01, respectively) according to one-way ANOVA and Tukey post hoc test.

Supplemental Reference

- S1. Gerber, L., Eliasson, M., Trygg, J., Moritz, T., and Sundberg, B. (2012). Multivariate curve resolution provides a high-throughput data processing pipeline for pyrolysis-gas chromatography/mass spectrometry. *J. Anal. Appl. Pyrolysis* 95, 95-100.

IV

Sucrose synthase activity is not required for cellulose biosynthesis in *Arabidopsis*

Wei Wang¹, Sonja Viljamaa¹, Ondrej Hodek¹, Thomas Moritz^{1,2} and Totte Niittylä^{1,*} 

¹Department of Forest Genetics and Plant Physiology, Umeå Plant Science Centre, Swedish University of Agricultural Sciences, SE 901 83, Umeå, Sweden, and

²Faculty of Health and Medical Sciences, Novo Nordisk Foundation Center for Basic Metabolic Research, University of Copenhagen, Copenhagen, Denmark

Received 21 February 2022; accepted 22 March 2022.

*For correspondence (e-mail totte.niittyla@slu.se).

SUMMARY

Biosynthesis of plant cell walls requires UDP-glucose as the substrate for cellulose biosynthesis, and as an intermediate for the synthesis of other matrix polysaccharides. The sucrose cleaving enzyme sucrose synthase (SUS) is thought to have a central role in UDP-glucose biosynthesis, and a long-held and much debated hypothesis postulates that SUS is required to supply UDP-glucose to cellulose biosynthesis. To investigate the role of SUS in cellulose biosynthesis of *Arabidopsis thaliana* we characterized mutants in which four or all six *Arabidopsis* SUS genes were disrupted. These *sus* mutants showed no growth phenotypes, vascular tissue cell wall defects, or changes in cellulose content. Moreover, the UDP-glucose content of rosette leaves of the sextuple *sus* mutants was increased by approximately 20% compared with wild type. It can thus be concluded that cellulose biosynthesis is able to employ alternative UDP-glucose biosynthesis pathway(s), and thereby the model of SUS requirements for cellulose biosynthesis in *Arabidopsis* can be refuted.

Keywords: UDP-glucose, cellulose, sucrose synthase, *Arabidopsis thaliana*.

INTRODUCTION

Cellulose, the main component of plant cell walls, is synthesized at the plasma membrane by the heteromeric cellulose synthase (cesA) rosette complex, which uses UDP-glucose as a substrate (McFarlane et al., 2014). Early evidence from cotton fibers pointed to an important role for sucrose synthase (SUS) in sucrose cleavage and UDP-glucose supply to cellulose biosynthesis. Significant proportion of SUS in the cotton fibers was associated with the membrane fraction, and *in situ* immunolocalization suggested SUS to be localized in the plasma membrane along the orientation of cellulose microfibrils (Amor et al., 1995; Haigler et al., 2001). These observations gave rise to a popular model, which depicts SUS in association with the cesA complexes channeling UDP-glucose for cellulose biosynthesis, albeit sometimes SUS is drawn with an associated question mark to indicate uncertainty about the direct association (Endler & Persson, 2011; Guerriero et al., 2010; Haigler et al., 2001; McFarlane et al. 2014; Stein & Granot, 2019).

Observations in different plant species have supported the association of SUS and cesA complexes. A SUS

antibody labeled reconstituted azuki bean (*Vigna angularis*) cesA complexes in an immunogold labeling assay, and it was reported that this SUS association with the rosette-like structures was required for *in vitro* cellulose biosynthesis activity (Fujii et al., 2010). Cotton plants with suppressed SUS activity exhibited reduced initiation and elongation of the cellulose-rich seed fibers, also supporting a SUS function in cellulose biosynthesis (Ruan et al., 2003). Immunoprecipitation of cesA complexes from developing wood of *Populus deltoides* × *canadensis* hybrid identified two SUS isoforms further suggesting a direct interaction between cesAs and SUS also in this species (Song et al., 2010).

Arabidopsis genome contains six SUS genes. Evidence challenging the role of SUS in cellulose biosynthesis was obtained by Barratt et al. (2009), who showed that the cellulose content in stems of quadruple *Arabidopsis sus1-sus2sus3sus4* (*sus^{quad}*) mutants did not differ from the wild type. However, this conclusion was later questioned by Baroja-Fernandez et al. (2012) who maintained that the quadruple *Arabidopsis sus* mutant contained sufficient SUS activity from the remaining two SUS isoforms SUS5 and SUS6 to support cellulose biosynthesis. Thus, the

importance of SUS in providing UDP-glucose to the CesA complexes is yet to be tested unequivocally. To settle the debate about SUS activity in the quadruple *sus* mutant we recently generated lines where all six Arabidopsis SUS genes were disrupted (Fünfgeld et al., 2022). The Fünfgeld et al. (2022) study focused on addressing the role of SUS in ADP-glucose and starch biosynthesis, while here we have used the same *sus* mutants to assess SUS function in UDP-glucose and cellulose biosynthesis.

RESULTS AND DISCUSSION

To address the role of SUS activity in cellulose biosynthesis in Arabidopsis we made use of the previously generated quadruple and sextuple Arabidopsis *sus* mutants (Barratt et al., 2009; Fünfgeld et al., 2022). Readers are referred to Fünfgeld et al. (2022) for detailed description of the genotypes and the results showing that the two allelic *sus^{sext-1}* and *sus^{sext-2}* mutants contain no measurable SUS activity. Here, wild-type, *sus^{quad}* and the *sus^{sext-1}* and *sus^{sext-2}* were grown on soil in a 16-h light period under controlled climate conditions. Under these conditions no visible growth differences were observed between *sus* mutants and wild type (Figure 1a). Compromised secondary cell wall biosynthesis leads to thinner and weaker cell walls, often evident as collapsed xylem vessels (Taylor et al., 2000). Therefore, transverse sections of inflorescence stems were prepared to investigate possible cell wall defects in the vascular bundles and the adjacent interfascicular fibers. Light microscopy of the toluidine blue-stained

cross-sections revealed no anatomical defects in the *sus* mutants (Figure 1b). Deficient primary wall cellulose synthesis interferes with cell expansion visible as reduced hypocotyl elongation in etiolated seedlings (Fagard et al., 2000). To inspect possible defects in primary cell wall biosynthesis we compared the hypocotyl length in etiolated 3-day-old wild-type, *sus^{quad}*, *sus^{sext-1}*, and *sus^{sext-2}* seedlings, but also in these experiments no differences between the *sus* mutants and wild type was observed (Figure 1c,d).

It is possible that lack of SUS activity leads to more subtle effects on cellulose biosynthesis, which would not manifest as anatomical and growth defects. However, quantification of cellulose content in the stems and rosette leaves of *sus^{quad}*, *sus^{sext-1}*, and *sus^{sext-2}* revealed no changes (Figure 2a,b). To elucidate the reason for the lack of growth phenotypes and cellulose defects further we quantified the UDP-glucose pool in rosette leaves of wild type, *sus^{quad}*, *sus^{sext-1}*, and *sus^{sext-2}*. Reliable quantification of UDP-glucose from plant extracts requires rapid quenching of metabolism, extraction, and precise liquid chromatography–tandem mass spectrometry (LC-MS/MS) analysis. UDP-glucose analysis is difficult to perform with success on traditional reversed phase chromatography due to the polarity of the compound. Here we developed a new method combining hydrophilic interaction chromatography (HILIC) with the addition of medronic acid in the mobile phase, which was previously proposed to improve peak shapes of phosphate-containing compounds (Hsiao

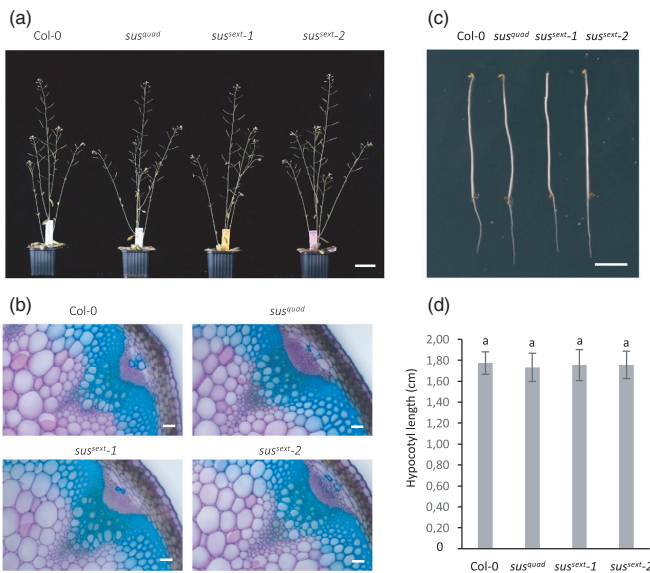


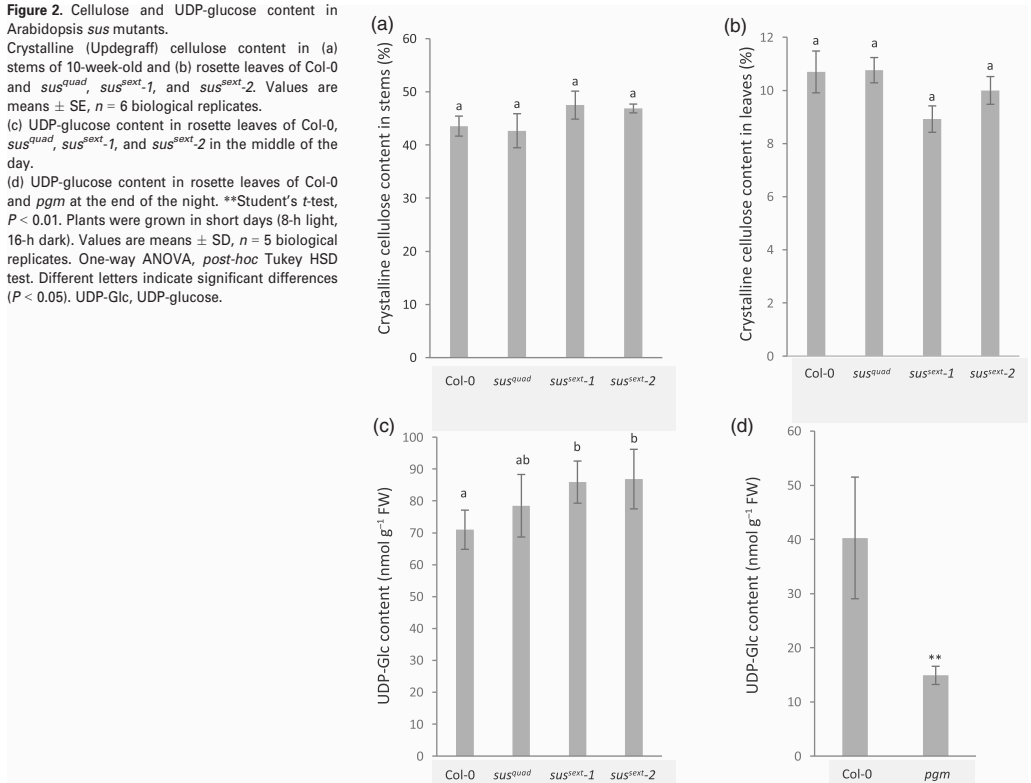
Figure 1. Phenotype of Arabidopsis *sus* mutants. (a) Eight-week-old wild type (Col-0) and *sus^{quad}*, *sus^{sext-1}*, and *sus^{sext-2}* grown in long days (16-h light, 8-h dark). (b) Stem cross-sections of Col-0 and *sus^{quad}*, *sus^{sext-1}*, and *sus^{sext-2}* stained with 0.1% toluidine blue. Scale bars = 50 μ m. (c) Etiolated Col-0 and *sus^{quad}*, *sus^{sext-1}*, and *sus^{sext-2}* seedlings grown for 5 days in the dark. Scale bar = 0.5 cm. (d) Hypocotyl length of Col-0 and *sus^{quad}*, *sus^{sext-1}*, and *sus^{sext-2}* seedlings grown for 5 days in the dark. Values are means \pm SE, $n = 25$ biological replicates. One-way ANOVA, *post-hoc* Tukey HSD test. Letters indicate no significant differences ($P < 0.05$).

Figure 2. Cellulose and UDP-glucose content in *Arabidopsis sus* mutants.

Crystalline (Updegraff) cellulose content in (a) stems of 10-week-old and (b) rosette leaves of Col-0 and *sus^{quad}*, *sus^{sext-1}*, and *sus^{sext-2}*. Values are means \pm SE, $n = 6$ biological replicates.

(c) UDP-glucose content in rosette leaves of Col-0, *sus^{quad}*, *sus^{sext-1}*, and *sus^{sext-2}* in the middle of the day.

(d) UDP-glucose content in rosette leaves of Col-0 and *pgm* at the end of the night. **Student's *t*-test, $P < 0.01$. Plants were grown in short days (8-h light, 16-h dark). Values are means \pm SD, $n = 5$ biological replicates. One-way ANOVA, *post-hoc* Tukey HSD test. Different letters indicate significant differences ($P < 0.05$). UDP-Glc, UDP-glucose.



et al., 2018). A combination of polymer-based HILIC column with medronic acid in the mobile phase resulted in improved peak symmetry (Figure S1). Thus, together with MS/MS including carbon-13 labeled UDP-glucose as an internal standard the method provides an alternative for accurate determination of UDP-glucose levels. This analysis revealed that the size of the UDP-glucose pool in the rosette leaves of *sus^{quad}* was in fact increased by 10.6% and by 21.0% and 22.4% in *sus^{sext-1}* and *sus^{sext-2}*, respectively (Figure 2c). These counter-intuitive results indicated that alternative UDP-glucose synthesis pathway(s) were upregulated and compensated for the missing SUS activity. As an additional control, we analyzed rosette leaf extracts of the starchless *Arabidopsis pgm* mutant, which exhibits reduced UDP-glucose levels compared with wild type at the end of the dark period (Gibon et al., 2006). In line with the previously published results, the UDP-glucose levels were reduced in *pgm* corroborating the LC-MS/MS analysis (Figure 2d).

Based on these observations, it can thus be concluded that SUS activity is not required for cellulose biosynthesis

in *Arabidopsis* resolving the long-standing debate about the role of SUS in cellulose biosynthesis. Sucrose cleavage by invertases followed by hexose phosphorylation by hexokinases and fructokinases, and UDP-glucose biosynthesis by UGPase activity provide a possible alternative pathway (Barnes & Anderson, 2018; Barratt et al., 2009; Rende et al., 2017). It should be noted, however, that *Arabidopsis sus1sus4* mutants exhibit growth defects under hypoxia pointing to the importance of the SUS pathway under stress conditions (Bieniawska et al., 2007). A role for SUS in plant stress tolerance was recently also supported by the growth defects observed in hybrid aspen *SUSRNAi* lines grown under natural conditions for 5 years (Dominguez et al., 2021).

EXPERIMENTAL PROCEDURES

Plant material and growth conditions

The *Arabidopsis thaliana* ecotype Columbia-0 (Col-0) was used as the wild-type control. The quadruple *sus1234* (*sus^{quad}*) mutant was described in Barratt et al. (2009). The sextuple mutants

sus12345⁶ (*sus^{sext1}*) and *sus12345⁶* (*sus^{sext2}*) were generated by CRISPR/Cas9 as described in Fünfgeld et al. (2022). The starchless *pgm* mutant (germplasm CS3092) characterized by Caspar et al. (1985) was obtained from the ABRC (<https://abrc.osu.edu/>). For the hypocotyl elongation assay, seeds were surface sterilized with 70% ethanol and 0.1% Tween-20 and sowed on half-strength Murashige and Skoog plates with 1% sucrose and 0.8% plant agar. Then plates were kept at 4°C for 3 days in the dark followed by light treatment at 22°C for 6 h to ensure uniform germination. After this, the plates were wrapped in aluminum foil and placed vertically at 22°C for 5 days. Images of etiolated seedlings were taken by a Canon EOS 650D camera and analyzed by ImageJ (<http://www.imagej.nih.gov/ij/>). For the other experiments, plants were grown in soil at 22°C with a photoperiod of 16 h light and 8 h dark (long day) or 8 h light and 16 h dark (short day) and 65% relative humidity. Valoya NS12 LED tubes were used and the light intensity is 150 $\mu\text{mol m}^{-2} \text{sec}^{-1}$.

Anatomy

Sections of the stems from the bottom part of 10-week-old wild-type and mutant plants were stained in 0.1% (w/v) Toluidine blue and rinsed with water for three times. The sections were mounted in water and observed under a Zeiss Axioplan 2 microscope equipped with a Zeiss AxioCam HRC camera. Images were processed and analyzed using ZEN 2 blue edition (Zeiss, Jena, Germany).

Cellulose analysis

The bottom 5 cm part of stems from 10-week-old plants grown in long day conditions were used for cellulose analysis. The freeze-dried samples were ground in liquid nitrogen with mortar and pestle, and alcohol insoluble residues were extracted by sequentially heating the samples in 80% and 70% ethanol at 95°C for 30 min, followed by treatment with chloroform/methanol (1:1) and washing with 100% acetone. The samples were resuspended in 0.1 M potassium phosphate buffer (pH 7.0) containing 0.01% sodium azide, and starch was removed by digesting the samples twice overnight with α -amylase (10102814001; 10 U μl^{-1} ; Roche, Basel, Switzerland) at +37°C, under gentle rotation. Cellulose content was measured using the Updegraff method (Updegraff, 1969) followed by an anthrone assay (Scott & Melvin, 1953) to quantify the released glucose.

LC-MS/MS analysis of UDP-glucose

Rosette leaves of 4-week-old wild-type and *sus* mutants grown in short days were harvested and homogenized in liquid nitrogen. Ten milligrams of each sample was placed into a 1.5 ml Eppendorf tube together with 250 μl of ice-cold extraction medium (chloroform/methanol, 3:7) and incubated at -20°C for 2 h. After this, 10 μl 50 μM UDP- α -D-[UL- $^{13}\text{C}_6$]glucose (Omicron Biochemicals, Inc., South Bend, IN, USA) was added to each sample as an internal standard. Samples were then extracted twice with 200 μl of ice-cold water, the aqueous layers were combined and dried in a freeze-dryer. The dried samples were dissolved in 50 μl of 50% methanol and diluted 10-fold before the analysis by LC-MS/MS. The separation of metabolites was achieved by injecting 3 μl of a sample to a HILIC column (iHILIC-(P) Classic, PEEK, 150 \times 2.1 mm, 5 μm ; HILICON, Umeå, Sweden) and mobile phase composed of (A) 10 mM ammonium acetate in water pH 9.4, and (B) 10 mM ammonium acetate in 90% acetonitrile pH 9.4 at a flow rate of 0.2 ml min^{-1} . Ammonium hydroxide was used to adjust pH of the mobile phase and mobile phase was supplemented by 5 μM medronic acid. The gradient elution program was set as follows: 0.0 min (95% B), 15 min (30% B), 18 min (30% B), 19 min (95% B),

and 27 min (95% B). The LC-MS/MS system consisted of an Agilent 1290 UPLC connected to an Agilent 6490 triple quadrupole (Agilent, Santa Clara, CA, USA). Analytes were ionized in electrospray source operated in the negative mode. The source and gas parameters were set as follows: ion spray voltage -3.5 kV , gas temperature 150°C , drying gas flow 11 L min^{-1} , nebulizer pressure 20 psi, sheath gas temperature 350°C , sheath gas flow 12 L min^{-1} , and fragmentor 380 V. Multiple reaction monitoring transitions of UDP-glucose and UDP-glucose- $^{13}\text{C}_6$ were optimized by using flow injection analysis (Table S1). Quantification of UDP-glucose was conducted based on calibration curve using UDP-glucose- $^{13}\text{C}_6$ as an internal standard. Linearity of the method was determined through a 10-point and weighted (1/x) calibration, which covered the range from 15 nM to 10 μM with the coefficient of determination $R^2 = 0.9958$. The limit of detection and limit of quantification were determined as a peak height of UDP-glucose that is 3- and 10-fold the signal-to-noise ratio, respectively. Accuracy was evaluated by spiking the real samples with the standard solution of UDP-glucose ($n = 3$) at three concentration levels (0.1, 1.5, and 5 μM); accuracy was in an acceptable range of $100 \pm 15\%$. Precision was calculated as RSD of repeated measurements ($n = 6$) of the spiked samples at three concentration levels; precision did not exceed 15%. All validation parameters are listed in Table S2.

ACKNOWLEDGEMENTS

We thank Junko Takahashi-Schmidt and the biopolymer analytical facility at UPSC for help with cellulose analysis. This work was supported by Bio4Energy (Swedish Programme for Renewable Energy), the Umeå Plant Science Centre, Berzelii Centre for Forest Biotechnology funded by VINNOVA, and the Swedish Research Council for Sustainable Development (Formas).

AUTHOR CONTRIBUTIONS

WW and SV carried out experiments and analyzed data, OH and TM developed and performed the UDP-glucose quantification assay, WW and TN conceived the project, and TN wrote the article with contributions from all the authors.

CONFLICT OF INTERESTS

The authors declare that they have no competing interests.

DATA AVAILABILITY STATEMENT

All relevant data can be found within the manuscript and its supporting materials.

SUPPORTING INFORMATION

Additional Supporting Information may be found in the online version of this article.

Table S1. LC-MS/MS reaction monitoring parameters.

Table S2. Validation parameters for quantification of UDP-glucose in plant extracts.

Figure S1. Example of UDP-glucose chromatograms.

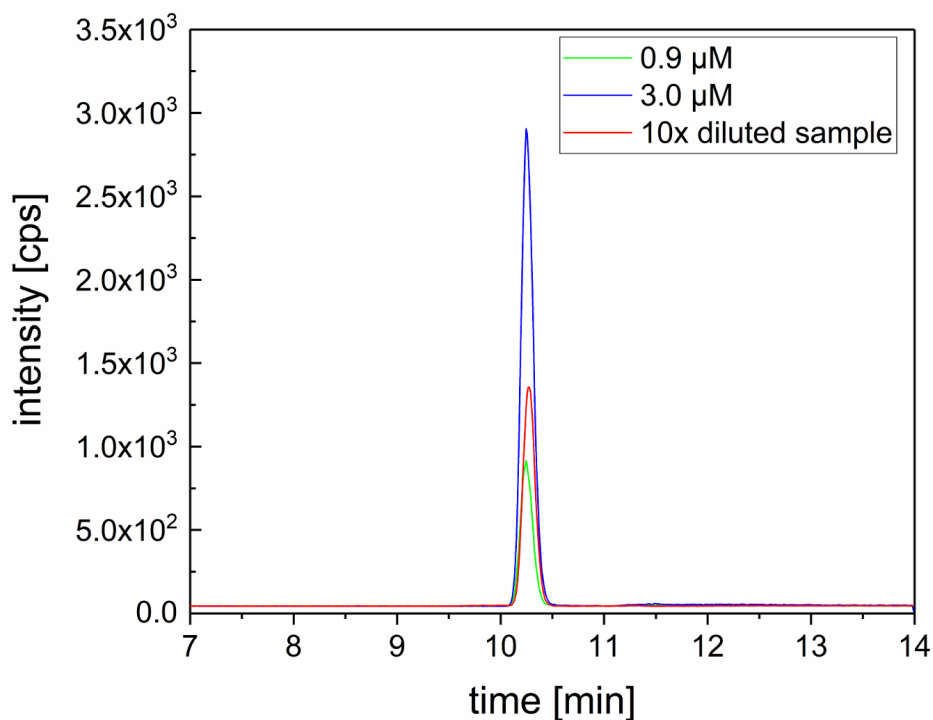
REFERENCES

- Amor, Y., Haigler, C.H., Johnson, S., Wainscott, M. & Delmer, D.P. (1995) A membrane-associated form of sucrose synthase and its potential role in synthesis of cellulose and callose in plants. *Proceedings of the National Academy of Sciences of the United States of America*, **92**(20), 9353–9357.

- Barnes, W.J. & Anderson, C.T. (2018) Cytosolic invertases contribute to cellulose biosynthesis and influence carbon partitioning in seedlings of *Arabidopsis thaliana*. *The Plant Journal*, **94**(6), 956–974.
- Baroja-Fernandez, E., Munoz, F.J., Li, J., Bahaji, A., Almagro, G., Montero, M. *et al.* (2012) Sucrose synthase activity in the *sus1/sus2/sus3/sus4* *Arabidopsis* mutant is sufficient to support normal cellulose and starch production. *Proceedings of the National Academy of Sciences of the United States of America*, **109**(1), 321–326.
- Barratt, D.H., Derbyshire, P., Findlay, K., Pike, M., Wellner, N., Lunn, J. *et al.* (2009) Normal growth of *Arabidopsis* requires cytosolic invertase but not sucrose synthase. *Proceedings of the National Academy of Sciences of the United States of America*, **106**(31), 13124–13129.
- Bieniawska, Z., Paul Barratt, D.H., Garlick, A.P., Thole, V., Kruger, N.J., Martin, C. *et al.* (2007) Analysis of the sucrose synthase gene family in *Arabidopsis*. *The Plant Journal*, **49**(5), 810–828.
- Caspar, T., Huber, S.C. & Somerville, C. (1985) Alterations in growth, photosynthesis, and respiration in a starchless mutant of *Arabidopsis thaliana* (L.) deficient in chloroplast phosphoglucomutase activity. *Plant Physiology*, **79**, 11–17.
- Dominguez, P.G., Donev, E., Derba-Maceluch, M., Bunder, A., Hedenstrom, M., Tomaskova, I. *et al.* (2021) Sucrose synthase determines carbon allocation in developing wood and alters carbon flow at the whole tree level in aspen. *The New Phytologist*, **229**(1), 186–198.
- Endler, A. & Persson, S. (2011) Cellulose synthases and synthesis in *Arabidopsis*. *Molecular Plant*, **4**(2), 199–211.
- Fagard, M., Desnos, T., Desprez, T., Goubet, F., Refregier, G., Mouille, G. *et al.* (2000) PROCUSTE1 encodes a cellulose synthase required for normal cell elongation specifically in roots and dark-grown hypocotyls of *Arabidopsis*. *Plant Cell*, **12**(12), 2409–2424.
- Fujii, S., Hayashi, T. & Mizuno, K. (2010) Sucrose synthase is an integral component of the cellulose synthesis machinery. *Plant & Cell Physiology*, **51**(2), 294–301.
- Fünfgeld, M.M.F.F., Wang, W., Ishihara, H., Arrivault, S., Feil, R., Smith, A.M. *et al.* (2022) Sucrose synthases are not involved in starch synthesis in *Arabidopsis* leaves. *Nature Plants*. <https://doi.org/10.1038/s41477-022-01140-y>.
- Gibon, Y., Usadel, B., Blaesing, O.E., Kamlage, B., Hoehne, M., Trethewey, R. *et al.* (2006) Integration of metabolite with transcript and enzyme activity profiling during diurnal cycles in *Arabidopsis* rosettes. *Genome Biology*, **7**, R76. Available from: <https://doi.org/10.1186/gb-2006-7-8-r76>
- Guerriero, G., Fugelstad, J. & Bulone, V. (2010) What do we really know about cellulose biosynthesis in higher plants? *Journal of Intergrative Plant Biology*, **52**(2), 161–175.
- Haigler, C.H., Ivanova-Datcheva, M., Hogan, P.S., Salnikov, V.V., Hwang, S., Martin, K. *et al.* (2001) Carbon partitioning to cellulose synthesis. *Plant Molecular Biology*, **47**(1/2), 29–51.
- Hsiao, J.J., Potter, O.G., Chu, T.W. & Yin, H. (2018) Improved LC/MS methods for the analysis of metal-sensitive analytes using Medronic acid as a Mobile phase additive. *Analytical Chemistry*, **90**(15), 9457–9464.
- McFarlane, H.E., Doring, A. & Persson, S. (2014) The cell biology of cellulose synthesis. *Annual Review of Plant Biology*, **65**, 69–94.
- Rende, U., Wang, W., Gandla, M.L., Jonsson, L.J. & Niittyla, T. (2017) Cytosolic invertase contributes to the supply of substrate for cellulose biosynthesis in developing wood. *The New Phytologist*, **214**(2), 796–807.
- Ruan, Y.L., Llewellyn, D.J. & Furbank, R.T. (2003) Suppression of sucrose synthase gene expression represses cotton fiber cell initiation, elongation, and seed development. *Plant Cell*, **15**(4), 952–964.
- Scott, T.A. & Melvin, E.H. (1953) Determination of dextran with Anthrone. *Analytical Chemistry*, **25**(11), 1656–1661.
- Song, D., Shen, J. & Li, L. (2010) Characterization of cellulose synthase complexes in *Populus* xylem differentiation. *The New Phytologist*, **187**(3), 777–790.
- Stein, O. & Granot, D. (2019) An overview of sucrose synthases in plants. *Frontiers in Plant Science*, **10**, 95.
- Taylor, N.G., Laurie, S. & Turner, S.R. (2000) Multiple cellulose synthase catalytic subunits are required for cellulose synthesis in *Arabidopsis*. *Plant Cell*, **12**(12), 2529–2540.
- Updegraff, D.M. (1969) Semimicro determination of cellulose in biological materials. *Analytical Biochemistry*, **32**(3), 420–424.

Table S1. Multiple reaction monitoring parameters.

Analyte	Precursor	Product	Collision	Dwell time	Type of transition
	ion	ion	energy [V]	[ms]	
UDP-Glc	565.0	322.9	25	150	quantifier
		78.8	77	150	qualifier
UDP-Glc- ¹³ C ₆	571.0	322.8	21	150	quantifier
		78.9	77	150	qualifier

**Figure S1.** Extracted and overlaid chromatograms of UDP-Glucose (MRM transition: 565.0 > 322.9) from calibration solutions and from 10× diluted sample. Chromatographic conditions as described in *LC-MS/MS* analysis section.**Table S2.** Validation parameters for quantification of UDP-glucose in plant extracts.

Analyte	LOD [nM]	LOQ [nM]	<i>R</i> ²	Precision [%]			Accuracy [%]		
				Low	Medium	High	Low	Medium	High
UDP-Glc	5	15	0.9958	1.1	12.6	1.1	88.8	88.6	87.6

